

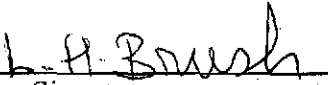
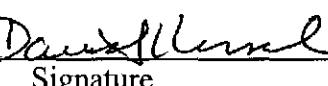
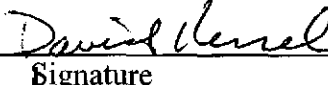
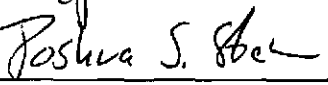
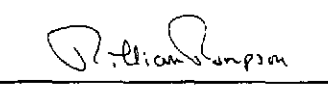
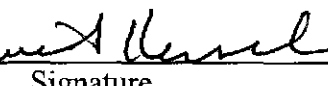
532445

**Sandia National Laboratories  
Carlsbad Programs Group**

**Waste Isolation Pilot Plant**

**Effects of Supercompacted Waste and Heterogeneous Waste Emplacement  
on Repository Performance**

**Revision 1**

Author:	Clifford W. Hansen (6821)		October 17, 2003
	Print	Signature	Date
Author:	Larry H. Brush (6822)		October 17, 2003
	Print	Signature	Date
For Author:	Michael B. Gross (CTAC)		October 17, 2003
	Print	Signature	Date
For Author:	Francis D. Hansen (6820)		October 17, 2003
	Print	Signature	Date
Author:	Byoung Yoon Park (6821)		October 17, 2003
	Print	Signature	Date
Author:	Joshua S. Stein (6821)		October 17, 2003
	Print	Signature	Date
Author:	T. William Thompson (CTAC)		October 17, 2003
	Print	Signature	Date
For Technical Review:	James Mewhinney		October 17, 2003
	Print	Signature	Date
Management Review:	David S. Kessel (6821)		October 17, 2003
	Print	Signature	Date
QA Review:	Mario J. Chavez (6820)		October 17, 2003
	Print	Signature	Date

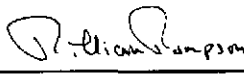
**Information Only**

**Sandia National Laboratories  
Carlsbad Programs Group**

**Waste Isolation Pilot Plant**

**Effects of Supercompacted Waste and Heterogeneous Waste Emplacement  
on Repository Performance**

**Revision 1**

Author:	Clifford W. Hansen (6821)	October 17, 2003
Print	Signature	Date
Author:	Larry H. Brush (6822)	October 17, 2003
Print	Signature	Date
Author:	Michael B. Gross (CTAC)	October 17, 2003
Print	Signature	Date
Author:	Francis D. Hansen (6820)	October 17, 2003
Print	Signature	Date
Author:	Byoung Yoon Park (6821)	October 17, 2003
Print	Signature	Date
Author:	Joshua S. Stein (6821)	October 17, 2003
Print	Signature	Date
Author:	T. William Thompson (CTAC)	October 17, 2003
Print	 Signature	Date
Technical Review:	James Mewhinney	October 17, 2003
Print	Signature	Date
Management Review:	David S. Kessel (6821)	October 17, 2003
Print	Signature	Date
QA Review:	Mario J. Chavez (6820)	October 17, 2003
Print	Signature	Date

Information Only

## EXECUTIVE SUMMARY

During the development of the performance assessment for the Compliance Certification Application (CCA), the U.S. Department of Energy (DOE) choose to assume random placement of transuranic waste in the Waste Isolation Pilot Plant (WIPP), and developed conceptual and numerical models accordingly. The U.S. Environmental Protection Agency (EPA) reviewed these models and their results, and determined that DOE had modeled accurately random placement of waste in the disposal system.

However, since that time the Idaho National Engineering and Environmental Laboratory has developed the Advanced Mixed Waste Treatment Project to treat contact-handled transuranic debris waste by supercompaction. Emplacement of supercompacted waste was not represented in the performance assessment for the CCA. For this reason, DOE submitted to EPA an evaluation of the effects of supercompacted waste on the long-term performance of the WIPP repository. After review of DOE's evaluation, EPA requested additional information regarding the effects of supercompacted waste, and also raised similar concerns about other waste types and associated packaging, such as pipe overpacks from the Rocky Flats Environmental Technology Site.

To respond to EPA's concerns, DOE has conducted a new performance assessment that considered these waste types and associated packaging. The performance assessment also evaluated the significance of assumptions about waste representation. Based on this new performance assessment, DOE concludes that:

- With supercompacted wastes in the repository, total normalized releases from the repository remain below the regulatory limits.
- Explicit representation of the specific features of supercompacted waste, such as structural rigidity, is not warranted in modeling since performance assessment results are relatively insensitive to the effects of such features.
- Performance assessment results are not affected significantly by the assumption of random waste emplacement and the representation of waste as a homogeneous material.

DOE's response to EPA required a systematic re-evaluation of key aspects of its performance assessment. First, DOE assessed the baseline features, events and processes (FEPs) to identify specific components of performance assessment that could be affected by supercompacted waste. DOE found that no changes to the waste-related FEPs were warranted in the new performance assessment.

DOE determined whether, and to what extent, these waste packages and waste heterogeneity required representation in the performance assessment. Analysis of creep closure of waste filled rooms indicated that a wider range of long-term porosities could occur relative to that established in the CCA, given the uncertainties about the structural integrity of waste

packages and spatial arrangement of the packages. For this reason, the new performance assessment treated creep closure as an uncertain variable. The sensitivity analysis showed that the uncertainty introduced by variable creep closure is not significant to the results of performance assessment.

Chemical conditions were re-examined under a range of possible arrangements of waste, and DOE found that MgO backfill remained sufficient to maintain desired chemical conditions. In addition, DOE found that the constituents of supercompacted waste would not alter the reactions that determine chemical equilibrium and, consequently, no changes to actinide solubilities or to the gas generation models were warranted.

Supercompacted waste contains elevated amounts of cellulose, plastics and rubbers (CPR) relative to other waste streams, and the future arrangement of this waste in the WIPP is uncertain. Thus, the new performance assessment treated the spatial distribution of CPR as uncertain. The sensitivity analysis demonstrated that uncertainty in the spatial distribution of CPR has little effect on performance assessment results.

DOE examined the representation of the properties of the waste and determined that no changes to permeability, shear strength or tensile strength were warranted. Based on this evaluation, DOE concluded that no changes to the models for direct releases were necessary. Moreover, DOE examined the significance of heterogeneity in waste radioactivity and in waste emplacement, and concluded that direct releases are relatively insensitive to these heterogeneities.

## TABLE OF CONTENTS

1	Introduction.....	8
1.1	Analysis Approach.....	10
1.2	Outline of Report .....	12
2	Background.....	14
2.1	Waste Representation in the CCA and PAVT .....	14
2.2	Advance Mixed Waste Treatment Project .....	15
2.3	AMWTP Debris (Supercompacted) Waste.....	15
2.4	AMWTP Uncompacted (Non-Debris) Waste .....	17
2.5	Waste Emplacement in Panel 1.....	18
3	Waste Representation in the Performance Assessment .....	20
3.1	Creep Closure and Waste Porosity .....	20
3.1.1	Waste Packages in the Structural Analysis.....	20
3.1.2	Response Models for Waste Packages.....	23
3.1.3	Waste Package Configurations .....	24
3.1.4	Initial Room Porosity.....	27
3.1.5	Base Gas Potential and Production Rate.....	27
3.1.6	Porosity Surface for Various Waste Types .....	28
3.1.7	Implementation in New Performance Assessment .....	34
3.2	Chemical Conditions in the Repository .....	37
3.2.1	Actinide Solubilities.....	37
3.2.2	Anoxic Corrosion.....	41
3.2.3	Radiolysis.....	41
3.3	Implementation of Gas Generation.....	42
3.3.1	Heterogeneity in CPR Concentration.....	43
3.3.2	Heterogeneity in Iron Concentration .....	44
3.4	Waste Permeability .....	45
3.4.1	Waste Permeability in the CCA and PAVT.....	45
3.4.2	Waste Permeability of the New Waste Forms .....	45
3.4.3	Effect of Waste Permeability on Direct Releases .....	46
3.5	Shear and Tensile Strength .....	49
3.5.1	Shear Strength.....	49
3.5.2	Tensile Strength .....	50
3.6	Cuttings and Cavings Releases .....	50
3.7	Spallings Releases.....	51
3.8	Stuck Pipe and Gas Erosion.....	52
3.9	Direct Brine Releases.....	54
3.10	Summary of Model and Parameter Changes .....	55
4	Results of Performance Assessment .....	56
4.1	Execution of the Performance Assessment.....	56
4.2	Results for Two-Phase Flow in and near the Repository.....	57
4.2.1	Undisturbed Model Results (S1 Scenario).....	57
4.2.2	Disturbed Model Results (S2 Scenario).....	59
4.3	Results for Repository Performance .....	62
4.3.1	Comparison of Component Releases .....	65

4.3.2	Analysis of Direct Brine Releases .....	67
5	Sensitivity Analysis .....	71
5.1	Sensitivity to Fraction of AMWTP Waste in a Single Waste Panel.....	71
5.2	Sensitivity to Porosity Surface.....	72
5.3	Sensitivity of Cuttings and Cavings to Random Placement of Waste .....	75
5.4	Sensitivity of Spallings to Waste Heterogeneity and Random Placement of Waste	
	76	
6	Summary and Conclusions .....	78
7	References.....	81

## LIST OF TABLES

Table 1.	Crosswalk of EPA issues for AMWTP waste with DOE responses.....	9
Table 1 (cont).	Crosswalk of EPA issues for AMWTP waste with DOE responses.....	10
Table 2.	Screened-in FEPs requiring further investigation.....	11
Table 3.	Initial room porosity for various waste configurations.....	27
Table 4.	Total gas potential and gas production rates for each waste configuration. ....	28
Table 5.	Distribution of WAS_AMW/CLOSMOD1. ....	35
Table 6.	Distribution of WAS_AMW/CLOSMOD2.....	36
Table 7.	Waste volumes in the repository and in the realistic and conservative cases.....	38
Table 8.	MgO safety factors and other parameters.....	39
Table 9.	Ligand concentrations in WIPP brines (M). ....	40
Table 10.	Comparison of $\text{Log}(f_{\text{CO}_2})$ , pH, and solubilities (M). ....	41
Table 11.	Radionuclide loadings ( $\text{Ci}/\text{m}^3$ ).....	42
Table 12.	Densities of cellulosic, plastic, and rubber materials in CH-TRU waste. ....	43
Table 13.	Description of waste properties for the layered model.....	46
Table 14.	Properties for random waste material types.....	47
Table 15.	Representation of supercompacted waste and waste heterogeneity. ....	55
Table 16.	Code versions and CMS libraries for this performance assessment.....	56

## TABLE OF FIGURES

Figure 1. AMWTP pucks produced by supercompaction of 55-gallon drums of debris waste. ....	15
Figure 2. Six 100-gallon drum payload assembly (DOE 2000, Figure 2.1-7).....	16
Figure 3. Illustration of waste containers and waste configuration. ....	17
Figure 4. Photograph of a 12-inch-diameter pipe overpack and schematic diagram of the loading scheme for a 6-inch-diameter pipe overpack. ....	19
Figure 5. Illustrations of structural differences in waste containers. ....	22
Figure 6. Computational mesh and boundary conditions for standard and pipe overpack waste. ....	25
Figure 7. Computational mesh and boundary conditions for combined and supercompacted waste configurations. ....	26
Figure 8. Deformed grids around the disposal room containing various waste types at 10,000 years for $f=0$ , no gas generation.....	29
Figure 9. Porosity histories for various waste types, $f=0$ .....	30
Figure 10. Porosity histories for various waste types, $f=0.4$ .....	31
Figure 11. Porosity histories for various waste types, $f=1.0$ .....	31
Figure 12. Porosity histories for various waste types, $f=2.0$ .....	32
Figure 13. Porosity histories for a room containing the 12-inch POP waste.....	32
Figure 14. Porosity histories for a room containing 2/3 supercompacted and 1/3 standard waste. ....	33
Figure 15. Porosity histories for a room containing only supercompacted waste. ....	33
Figure 16. BRAGFLO grid used in the performance assessment.....	34
Figure 17. Schematic of the layered model (Figure 4-25, Hansen et al., 1997). ....	47
Figure 18. Schematic of the random model for waste permeability (Figure 4-26, Hansen et al., 1997). ....	48
Figure 19. Pressure in the waste panel for the AMW (left) and CRA1 (right) analyses, S1 scenario. ....	58
Figure 20. Comparison of pressure in the waste panel, S1 scenario.....	58
Figure 21. Brine saturation in the waste panel for the AMW (left) and CRA1 (right) analyses, S1 scenario. ....	59
Figure 22. Porosity in the waste panel for the AMW (left) and CRA1 (right) analyses, S1 scenario. ....	59
Figure 23. Pressure in the waste panel for the AMW (left) and CRA1 (right) analyses, S2 scenario. ....	60
Figure 24. Comparison of pressure in the waste panel, S2 scenario.....	60
Figure 25. Brine saturation in the waste panel for the AMW (left) and CRA1 (right) analyses, S2 scenario. ....	61
Figure 26. Porosity in the waste panel for the AMW (left) and CRA1 (right) analyses, S2 scenario. ....	61
Figure 27. Brine flow to the Culebra for the AMW (left) and CRA1 (right) analyses, S2 scenario. ....	62
Figure 28. Total normalized releases, AMW calculation. ....	63
Figure 29. Total normalized releases, CRA1 calculation. ....	63

Figure 30. Comparison of total normalized releases. ....	64
Figure 31. Cuttings releases for the AMW calculation.....	65
Figure 32. Mean CCDFs for component releases, AMW calculation. ....	66
Figure 33. Mean CCDFs for component releases, CRA1 calculation. ....	66
Figure 34. DBR releases in the AMW calculation. ....	67
Figure 35. DBR releases in the CRA1 calculation. ....	68
Figure 36. DBR volumes before 1,500 years for a second intrusion into the lower waste panel (S4 and S5 scenarios.) .....	69
Figure 37. Pressure and brine saturation in the waste panel for Vector 22 in the AMW (left) and CRA1 (right) calculations. ....	70
Figure 38. Mobilized concentrations in Salado brine (Scenarios S4 and S5).....	70
Figure 39. Sensitivity of pressure to FRACAMW, S1 scenario. ....	72
Figure 40. Sensitivity of pressure in the waste panel to CLOSMOD1 (AMW calculation.).....	73
Figure 41. Pressure in the waste panel for vectors where the Standard Waste Model applies to the rest of repository (AMW calculation.).....	73
Figure 42. Pressure in the waste panel for vectors where the Combined Waste Model applies to the rest of repository (AMW calculation.).....	74
Figure 43. Pressure vs. porosity in the waste panel at 1,000 years (left) and at 10,000 years (right) for the S1 scenario (AMW calculation.) .....	75
Figure 44. Sensitivity of cuttings and cavings releases to random placement of waste. ....	76
Figure 45. Sensitivity of spillings releases to assumptions about waste placement. ....	77

# 1 Introduction

In 1996, the U.S. Department of Energy (DOE) completed a performance assessment for the Waste Isolation Pilot Plant (WIPP). The performance assessment was part of the Compliance Certification Application (CCA) (DOE, 1996) submitted to the U.S. Environmental Protection Agency (EPA) to demonstrate compliance with the long-term disposal regulations in 40 CFR 191 (Subparts B and C) and the compliance criteria in 40 CFR 194. In 1997, EPA required a verification of the calculations performed for the CCA, termed the Performance Assessment Verification Test (PAVT).

During the development of the performance assessment for the CCA, DOE had the option under the EPA regulations (40 CFR 194.24(d)) of specifying a waste loading scheme for the repository or assuming random placement of the waste in the disposal system. DOE chose to assume random placement of the waste, and developed conceptual and numerical models consistent with this assumption. EPA reviewed this approach and determined that DOE accurately modeled random placement of waste in the disposal system. (EPA, 1998a, 27391)

Since certification, the Idaho National Engineering and Environmental Laboratory (INEEL) has developed the Advanced Mixed Waste Treatment Project (AMWTP) to process 55-gallon drums of contact-handled transuranic (CH-TRU) debris waste prior to shipment to the WIPP. The AMWTP will involve retrieval, characterization, repackaging, and compacting 55-gallon drums of debris waste and placing the compacted drums into 100-gallon drums prior to shipment. Emplacement of this “supercompacted” waste in the WIPP was not considered in the inventories for the CCA or PAVT (SNL 1997a; SNL 1997b) and was not represented in predictions of long-term repository performance.

In December 2002, DOE submitted to EPA an evaluation of the effects of supercompacted waste from the AMWTP on the long-term performance of the WIPP repository (DOE, 2002). After review of DOE’s evaluation, EPA requested additional information and raised concerns regarding potential effects of AMWTP waste on the long-term performance of the repository (EPA, 2003a). Several of EPA’s concerns involved the assumption that waste would be randomly placed in the repository. During ensuing discussions, EPA raised similar concerns regarding other waste types and associated packaging, such as pipe overpacks (WIPP PA, 2003a)<sup>1</sup>.

This report responds to the issues identified by EPA. Table 1 summarizes these concerns and identifies the sections within this report where these concerns are addressed.

---

<sup>1</sup> Pipe overpacks are thick-walled cylinders containing CH-TRU waste that are placed within protective packing and then placed within a 55-gallon drum. See Section 2.5 for details.

**Table 1. Crosswalk of EPA issues for AMWTP waste with DOE responses.**

General Issue	Pertinent Section(s) of this Report	
	Specific Issue	Section(s)
Review of FEPs may be incomplete (Attachment, first paragraph)	FEPs screening	1.1
	Creep closure accounting for various waste forms	3.1
PA assumptions for AMWTP waste should be reviewed, specifically assumptions related to homogeneity of emplaced waste (Attachment, second and third paragraphs)	Potential effects of heterogeneity on creep closure	3.1
	Potential effects of heterogeneity on chemical processes	3.2 and 3.3
	Potential effects of heterogeneity on waste properties such as permeability, shear strength, and tensile strength	3.4 and 3.5
	Potential effects of heterogeneity in the densities of cellulosic, plastic, and rubber materials on repository performance	3.3.1
Perform a thorough analysis of the radionuclides released by a borehole intrusion (Attachment, fourth paragraph)	Potential effects from waste heterogeneity on direct release mechanisms	3.6, 3.7, and 3.9
	The stuck pipe and gas erosion mechanisms for spalling	3.8
	Sensitivity of direct releases to the presence of supercompacted wastes	4.3, 5.3 and 5.4
What is the total inventory from INEEL, including waste that is already emplaced? (Attachment, fifth paragraph)	The total inventory for this performance assessment includes the emplaced waste from all sites, including INEEL	2.2 and 5.1
What are the effects from increased densities of cellulosic, plastic, and rubber materials in supercompacted waste? (Attachment, sixth paragraph)	Potential effects from increased density of cellulosic, plastic, and rubber materials on gas generation	3.3 and 5.1
Analyses should include the latest models, including those for the Option D panel closures and for the new conceptual model for spalling. (Attachment, seventh paragraph)	PA methodology for this analysis is described in Section 1.2.	1.2
	The performance assessment includes the final inventory for the CRA	4.1
	The BRAGFLO model includes the Option D panel closures	4.1
	The new conceptual model for spalling has not been approved by the Spallings Peer Review Panel and is not fully implemented in WIPP PA; therefore this analysis uses the PAVT model for spallings.	Not Addressed

**Table 2 (cont). Crosswalk of EPA issues for AMWTP waste with DOE responses.**

Computer codes and the PA System Database (Attachment, eighth paragraph)	All software Quality Assurance activities and documentation have been completed for the computer codes in this analysis, as required by the EPA (EPA, 2003b).	4.1
	The PA Parameters Database was approved by the EPA on 15 May 2003 (EPA, 2003c).	4.1
What is the effect of the porosity and permeability of supercompacted AMWTP waste on “stuck pipe” and “gas erosion” mechanisms for spalling. (Attachment, ninth paragraph)	The porosity and permeability of supercompacted waste	3.1 and 3.4
	Impact of these material properties on the stuck pipe and gas erosion mechanisms for spalling	3.9
The assumption of homogeneity for the nonradioactive inventory components needs to be reevaluated, given that they are not present in similar proportions in the compacted and uncompacted waste streams. (Attachment, tenth paragraph)	Potential effects of heterogeneity on room closure	3.1
	Potential effects of heterogeneity on chemical processes	3.2 and 3.3
	Potential effects of heterogeneity on waste permeability, shear strength, and tensile strength	3.4
	Potential effects of heterogeneity in the densities of cellulosic, plastic, and rubber materials on repository performance	3.3 and 5.1
Density, shear strength, permeability, and porosity of supercompacted AMWTP waste should be clearly defined and justified. (Attachment, eleventh paragraph)	Density and porosity of supercompacted waste	3.1
	Shear strength and permeability of supercompacted waste	3.4
The presence of supercompacted AMWTP waste could alter the creep closure process, resulting in new ranges for waste properties (Attachment, twelfth paragraph)	Creep closure process for rooms with supercompacted waste	3.1
	Effect of creep closure on waste properties	3.1 and 3.4

## **1.1 Analysis Approach**

To address EPA’s concerns within a consistent analysis framework, DOE elected to conduct a new performance assessment. To guide the formulation of the performance assessment, DOE summarized EPA’s issues as two general questions:

1. What is the expected repository performance when supercompacted waste is explicitly represented in the performance assessment?
2. What is the significance to performance assessment of the representation of supercompacted waste and of waste heterogeneity in general?

Prior to conducting the new performance assessment, DOE examined the FEPs baseline to determine whether the FEPs included in the performance assessment (i.e., screened in) would

account for the supercompacted waste (WIPP PA, 2002). The assessment concluded that the FEPs screened in were adequate to represent supercompacted waste, and that none of the FEPs that had been screened out should be implemented in the new performance assessment. Thus, no new FEPs were added to the new performance assessment to accommodate the supercompacted waste in the inventory. However, the examination identified a set of screened in FEPs for which implementation should be investigated (Table 2).

**Table 3. Screened-in FEPs requiring further investigation.**

<b>ID No.</b>	<b>FEP</b>	<b>FEP Base Assumption</b>	<b>Possible Implementation Issue(s)</b>	<b>Pertinent Section(s)</b>
W2	Waste Inventory	The quantity and type of radionuclides emplaced in the repository will dictate performance requirements	Supercompacted waste may increase the fissile mass in localized areas within the repository.	3.2.3
W3	Heterogeneity of waste forms	The distribution of radionuclides within the different waste types could affect release patterns	Loading schemes and disposal schedules may present inconsistencies with random emplacement assumption.	2.5
W5	Container material inventory	Steel and other materials will corrode and affect the amount of gas generated	Supercompacted waste will increase the corrodible metals content over previous estimates.	3.3.2
W32	Consolidation of waste	Salt creep and room closure will change waste properties	Initial waste properties (densities) are different than those previously assumed.	3.1
W44	Degradation of organic material	Microbial breakdown of cellulosic material in the waste will generate gas	Supercompacted waste may possess greater amounts of cellulosic material than previous estimates.	3.3.1
W49	Gases from metal corrosion	Anoxic corrosion of steel will produce hydrogen	Greater amounts of gas may be produced than those previously assumed.	3.2.2
W51	Chemical effects of corrosion	Corrosion reactions will lower the oxidation state of brines and affect gas generation rates	Current reaction rates may need revision.	3.2.2
W64	Effect of metal corrosion	Metal corrosion will have an effect on chemical conditions in the repository by absorbing oxygen	Greater amounts of metal may require revision of coupled chemical processes.	3.2, 3.3.2
W84	Cuttings	Waste material intersected by a drill bit could be transported to the ground surface	Intersection of a 100 gallon overpack with supercompacted waste may cause cuttings releases to increase.	3.6, 5.3
W85	Cavings	Waste material eroded from a borehole wall by drilling fluid could be transported to the ground surface	Supercompacted waste may change waste properties thereby changing cavings into borehole.	3.5
W86	Spallings	Waste material entering a borehole through repository depressurization could be transported to the ground surface	Supercompacted waste may have different shear strength/physical properties than those assumed in the CCA.	3.4, 5.4

The FEPs analysis concluded that the following models, parameters or numerical implementation of models may be affected by the inclusion of supercompacted waste, and merited further investigation:

- Creep closure of waste-filled regions.
- Chemical conditions in the repository assumed for calculation of actinide solubilities and of gas generation rates.
- Gas generation models.
- Implementation of gas generation models.
- Parameters representing hydrological and mechanical properties of the waste (permeability, shear strength and tensile strength).
- Waste heterogeneity in direct release models.
- Mechanisms used in the model for spallings (blowout, stuck pipe and gas erosion.)

Based on the results of the FEPs analysis, the performance assessment was conducted in three steps:

- (1) Preliminary analyses to determine how to represent supercompacted waste and waste heterogeneity in performance assessment models. These analysis address creep closure of rooms, chemical conditions in the waste, mechanical properties of the waste (e.g. permeability, shear strength and tensile strength), and the representation of waste heterogeneity in direct releases models.
- (2) Execution of the performance assessment and comparison of results with requirements of 40 CFR 191.
- (3) Sensitivity analyses to determine the significance to performance assessment results of these waste forms and of waste heterogeneity.

## **1.2 Outline of Report**

Section 2 first summarizes the representation of waste in the CCA and the PAVT. The salient properties of supercompacted waste are presented, indicating why these properties lead to questions about waste representation in performance assessment. Section 2 concludes by summarizing the actual emplacement of waste in Panel 1, and indicates why DOE chose to include pipe overpack wastes as part of the heterogeneous waste considered in this analysis.

Section 3 describes the representation of supercompacted waste and of waste heterogeneity in the performance assessment. The section first presents the results from modeling of room closure accounting for supercompacted waste, and describes the uncertain parameters added to performance assessment to determine sensitivity to variations in room closure. Next, Section 3 presents an analysis of the effects of supercompacted waste on assumptions about the chemical environment in the repository. Gas generation processes included in

performance assessment are discussed, and parameters are introduced to determine the possible effects of heterogeneity in the spatial distribution of supercompacted waste. The parameters that represent waste material properties, such as permeability and tensile strength, are examined and any changes to these parameters are explained.

Section 3 next investigates whether changes to the models for direct releases are required to account for waste heterogeneity in this analysis. The stuck pipe and gas erosion mechanisms for solid releases are discussed.

Section 4 outlines the execution of the performance assessment and presents the results of calculations. Section 5 presents a sensitivity analysis examining the significance of the uncertainty parameters included to represent the supercompacted waste, and the importance of the assumptions about waste placement and heterogeneity in the direct release models. The conclusions of this report are summarized in Section 6.

## 2 Background

This section summarizes the waste representation used in the CCA and the PAVT, and presents information about the waste to be shipped to WIPP from the AMWTP. The report includes a discussion of the waste already emplaced in Panel 1 of the WIPP that is relevant to the overall analytical framework.

### 2.1 Waste Representation in the CCA and PAVT

During the development of the performance assessment for the CCA, DOE had the option of specifying a waste loading scheme for the repository or assuming random placement of waste in the disposal system. The DOE chose to assume random placement of waste, and developed conceptual and numerical models for performance assessment consistent with this assumption. Analysis showed that the assumption of random waste placement had little effects on the conclusions of the PA (EPA, 1997). The EPA reviewed DOE's approach to random placement during the certification process and found (EPA 1998a, 27391):

*“Section 194.24(d) requires DOE either to include a waste loading scheme which conforms to the waste loading conditions used in the PA and in compliance assessments, or to assume random placement of waste in the disposal system. The DOE elected to assume that radioactive waste would be emplaced in the WIPP in a random fashion. The DOE examined the possible effects of waste loading configurations on repository performance (specifically, releases from human intrusion scenarios) and concluded that the waste loading scheme would not affect releases. The DOE incorporated the assumption of random waste loading in its performance and compliance assessments (pursuant to §194.32 and §194.54, respectively).*

*The EPA determined that, because the DOE had assumed random waste loading, a final waste loading plan was unnecessary. The EPA determined that, in the PA, DOE accurately modeled random placement of waste in the disposal system. Since EPA concurred with DOE that a final waste loading plan was unnecessary, DOE does not have to further comply with §194.24(f), requiring DOE to conform with the waste loading conditions, if any, used in the PA and compliance assessment. Therefore, EPA finds that DOE complies with §§194.24(d) and (f).”*

Random placement of waste means that the probability of finding a waste stream at a specific location in the repository is proportional to the emplaced volume of the waste stream. The assumption of random placement was implemented by treating the waste as a homogeneous material, with properties derived from the constituent waste streams. The analysis in this report is designed to determine whether performance assessment may continue to use the assumption of random placement and the representation of waste as a homogeneous material,

or whether the heterogeneities introduced by supercompacted waste should be represented in the performance assessment.

## **2.2 Advance Mixed Waste Treatment Project**

The AMWTP is designed to retrieve, characterize, prepare and store CH-TRU waste at the INEEL for shipment to the WIPP. The CH-TRU waste at INEEL consists of debris and non-debris wastes. The debris wastes will be processed through a sort, size, and volume reduction (supercompaction) process (i.e., treated AMWTP waste). The non-debris waste also will be retrieved, characterized, prepared and stored for shipment to WIPP, but will not be supercompacted. The DOE expects that the AMWTP will ship both supercompacted and uncompacted waste concurrently.

In this report the term supercompacted waste refers to the treated debris waste from the AMWTP. The term uncompacted refers to the untreated debris waste that is not compacted. The term AMWTP waste refers to both waste forms together.

## **2.3 AMWTP Debris (Supercompacted) Waste**

The AMWTP will compact 55-gallon drums of debris waste and place the compacted drums into 100-gallon drums before shipment to the WIPP. The compacted 55-gallon drums are referred to as “pucks” (see Figure 1) and the 100-gallon drums are referred to as 100-gallon containers, or simply containers. Each puck has a final volume of 15 to 35 gallons, and each 100-gallon container is anticipated to contain from 3 to 5 pucks, with an average of 4 pucks per container.



**Figure 1. AMWTP pucks produced by supercompaction of 55-gallon drums of debris waste.**

The 100-gallon container is made of steel. The outside height of the container (with lid) is 35 inches and its outside diameter is 32 inches (DOE 2000, Figure 2.1-6). The height of a

container is very similar to the height of a 55-gallon drum; however, its diameter is larger (32 inches versus 24 inches). The weight of an empty 100-gallon container is 95 pounds (43.1 kg) (DOE 2000, Table 2.1-20). The volume of the 100-gallon container is 0.379 m<sup>3</sup>.

The loading of pucks into 100-gallon containers will be managed to meet applicable transportation and waste acceptance criteria. The 100-gallon containers will then be loaded into a TRUPACT-II or a HalfPACT for shipment to the WIPP. Each TRUPACT-II can hold six 100-gallon containers in two layers of three each (see Figure 2) and each HalfPACT can hold three 100-gallon containers in a single layer. Assuming that a shipment consists of two TRUPACT-II packages and one HalfPACT package, each shipment of supercompacted waste from INEEL will have five three-packs of 100-gallon containers, or a total of 15 100-gallon containers containing on average 60 pucks.

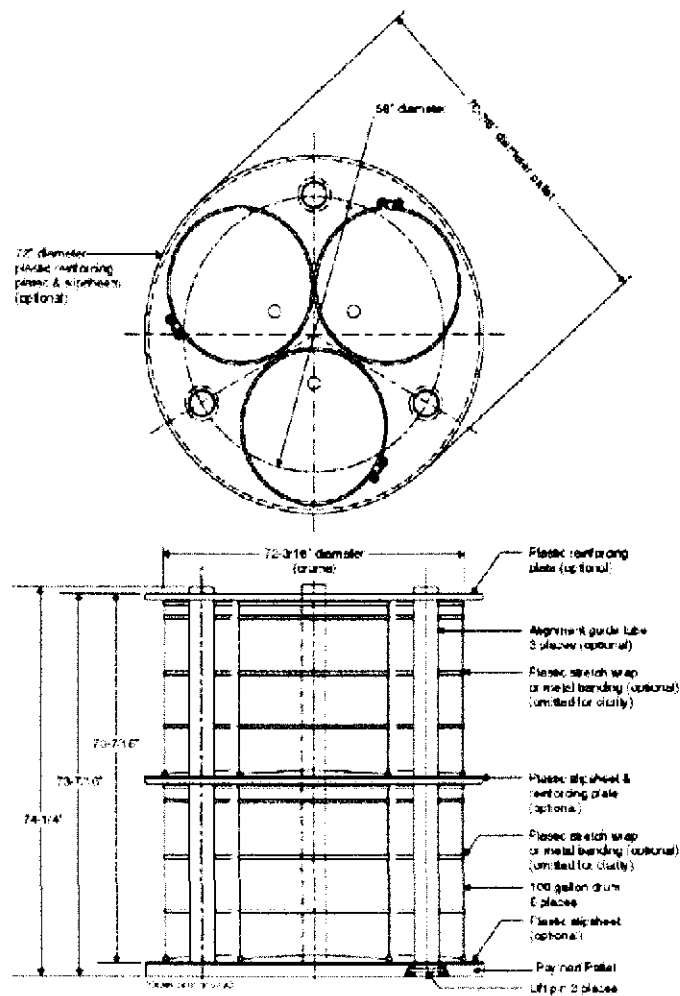
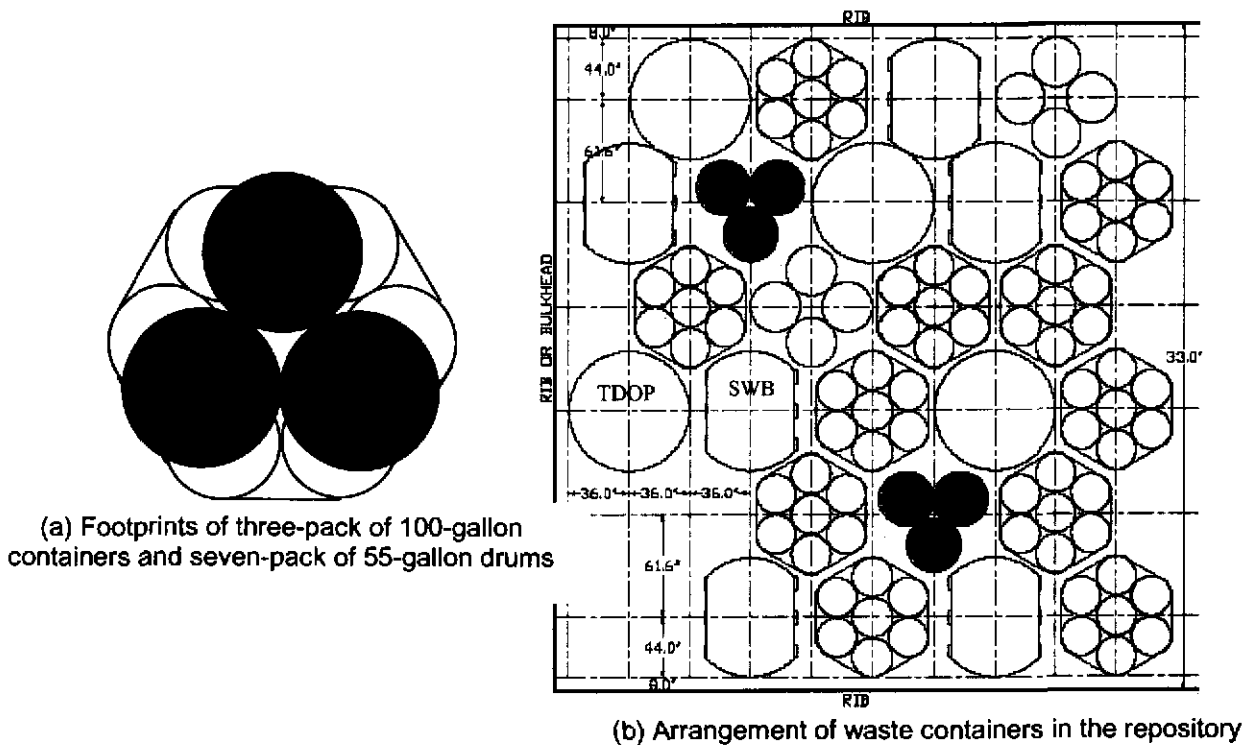


Figure 2. Six 100-gallon drum payload assembly (DOE 2000, Figure 2.1-7).

The estimated disposal inventory of supercompacted waste is based on a total of 52,440 100-gallon containers (Leigh and Lott, 2003a). The total emplaced volume of these containers is 19,875 m<sup>3</sup>, based on 0.379 m<sup>3</sup> per 100-gallon container. The total volume of the actual waste is somewhat less, due to void space within the 100-gallon containers.

The operational plan of the WIPP is to emplace waste as it arrives; consequently, supercompacted waste (in three packs of 100-gallon overpacks) will be intermingled with ten-drum overpacks (TDOPs), standard waste boxes (SWBs), four packs of 85-gallon drums, and 55-gallon drums from all sites. This approach is operationally efficient because a three-pack of 100-gallon containers fits within the footprint of a seven-pack of 55-gallon drums, as illustrated in Figure 3a. In addition, the outside height of the 55-gallon drum is similar to that of a 100-gallon container. It follows that a three-pack and a seven-pack are physically configured as a one-for-one replacement for the purpose of waste handling in the repository. The potential emplacement of a mix of seven-packs, three-packs, TDOPs, and SWBs is illustrated in Figure 3b.



**Figure 3. Illustration of waste containers and waste configuration.**

## **2.4 AMWTP Uncompacted (Non-Debris) Waste**

The AMWTP also will ship uncompacted waste to the WIPP. The AMWTP will process 55-gallon drums of non-debris waste and load these drums into TDOPs or SWBs for shipment. Processing for the non-debris waste streams consists solely of storage and load management to ensure that each TDOP or SWB meets the applicable transportation and waste acceptance

criteria for the WIPP. The TDOPs and SWBs will then be loaded into a TRUPACT-II or HalfPACT for shipment to the WIPP. Each TRUPACT-II can hold a single TDOP and two SWBs, and each HalfPACT can hold a single SWB.

The inventory for uncompacted AMWTP waste is based on a total of 7,138 TDOPs and 3,573 SWBs (Leigh and Lott, 2003b). The total emplaced volume of these containers is 40,944 m<sup>3</sup>, based on inner volumes of 4.79 m<sup>3</sup> per TDOP and 1.89 m<sup>3</sup> per SWB.<sup>2</sup>

The emplaced volume of uncompacted AMWTP waste is about twice as great as the emplaced volume of supercompacted AMWTP waste. The total volume of both AMWTP waste types is 60,819 m<sup>3</sup>, which will fill about 36 percent of the total available volume for CH-TRU waste<sup>3</sup>. By way of comparison, the total volume of CH-TRU waste from all INEEL waste streams in the inventory for the CCA and PAVT was about 28,607 m<sup>3</sup> (DOE 1996a Appendix BIR).

## **2.5 Waste Emplacement in Panel 1**

The WIPP began to receive waste in 1999, and after four years of waste emplacement in Panel 1, operations were terminated and the explosion wall portion of the panel closure system was constructed. Several rooms within Panel 1 do not contain waste; the effect of these of these empty rooms on repository performance was determined to be negligible, and is not discussed further in this report (EPA Docket A-98-49, Item II-B3-19). However, the large number of pipe overpack waste containers placed in Panel 1 is relevant to the structural analysis in this report. Approximately 43% of the containers in Panel 1 include a pipe overpack (Park and Hansen, 2003.)

Mixed oxide residues from the Rocky Flats Environmental Technology Site (RFETS) have been loaded into pipe overpacks prior to shipment to the WIPP (see Figure 4). The pipe overpacks are thick-walled cylinders that are more rigid than 55-gallon drums. The presence of pipe overpacks may alter the time-dependent creep closure of rooms, particularly in rooms with a concentration of pipe overpacks. The homogeneous waste model used in the CCA and PAVT does not include the possible effects of varying room closure. Thus, the pipe overpack containers are included in the room closure analysis presented in Section 3.1.

---

<sup>2</sup> (7,138 TDOPs)(4.79 m<sup>3</sup>/TDOP) + (3,573 SWBs)(1.89 m<sup>3</sup>/SWB) = 40,944 m<sup>3</sup>.

<sup>3</sup> (60,819 m<sup>3</sup>)/(168,485 m<sup>3</sup>) = 36%.



**Figure 4. Photograph of a 12-inch-diameter pipe overpack and schematic diagram of the loading scheme for a 6-inch-diameter pipe overpack.**

### **3 Waste Representation in the Performance Assessment**

This section presents the results of the preliminary analysis that determined how supercompacted waste and waste heterogeneity are represented in the performance assessment conducted for this report. Structural analysis of creep closure of repository rooms for different configurations of waste and waste packages concludes that uncertainty in room closure should be examined in the performance assessment. Chemical conditions assumed for calculation of actinide solubilities and gas generation rates are shown to be unaffected by the presence of supercompacted waste; MgO safety factors are shown to remain above the minimum for a variety of waste configurations. Examination of gas generation mechanisms concludes that the heterogeneity in CPR concentrations may be important and should be examined in the performance assessment. Analysis of waste permeability, shear strength, and tensile strength concludes that no changes to these parameters are warranted in the performance assessment.

Examination of the direct releases models for cuttings and cavings, spallings and direct brine releases recommends no change to these models. However, the analysis concludes that the sensitivity of the direct release models to the assumption of random waste placement should be evaluated.

#### **3.1 Creep Closure and Waste Porosity**

This section describes the structural analysis conducted to answer EPA's questions about creep closure (EPA, 2003a). The analysis follows the strategy outlined in the governing Analysis Plan (AP107) (WIPP PA, 2003a). Computations were completed with the finite element code SANTOS, which was used to compute creep closure for the CCA, and to assess the effects of raising the repository horizon to Clay Seam G (Park and Holland, 2003). SANTOS has been qualified to the software requirements of NP 19-1 (WIPP PA, 2003b). Park and Hansen (2003) present details and additional background for the SANTOS calculations for this analysis.

The structural analysis found that room closure may vary significantly depending on the waste and waste containers placed in the room. Thus, the analysis recommends that the performance assessment include variable room closure, and that the significance of the uncertainty in room closure in the performance assessment should be evaluated.

##### **3.1.1 Waste Packages in the Structural Analysis**

This analysis uses the term "waste package" to refer to both the waste container and its contents. The structural analysis for the CCA assumed that all waste is contained in 55-gallon drums. The mechanical stiffness of the waste was based on a weighted average of experimental data for various waste types (Butcher et al., 1991). Since the future state (in terms of structural integrity) of the waste is uncertain, it was assumed that the waste and waste containers would rapidly degrade to a structurally weak, composite material, and thus

the drums would not constitute a significant barrier to room closure. The structural analysis for the CCA did not account for variability in the stiffness of different waste packages.

In this structural analysis, the waste was characterized by its general structural form, which may depend on the type of container (Figure 5). The standard waste package is the 55-gallon drum (Figure 5A), which was the baseline waste unit considered in the CCA. Characteristics of this waste container, its contents and the degradation of both were used to quantify many of the parameters underpinning the CCA.

Figure 5B illustrates the pipe overpack (see Section 2.5 and Figure 4.) Approximately half of the drums in Panel 1 include a pipe overpack within the standard 55-gallon drum. There are several different types of pipe overpacks, however, this analysis only considered the two most prevalent types - the overpacks with pipes that are 12 inches and 6 inches in diameter.

The third waste container is the 100-gallon container filled with supercompacted waste. Supercompacted waste comprises 55-gallon drums that are compressed under a load of approximately 9000 psi. The resulting crushed drums, called pucks, are inserted into a 100-gallon container (Figure 5C).

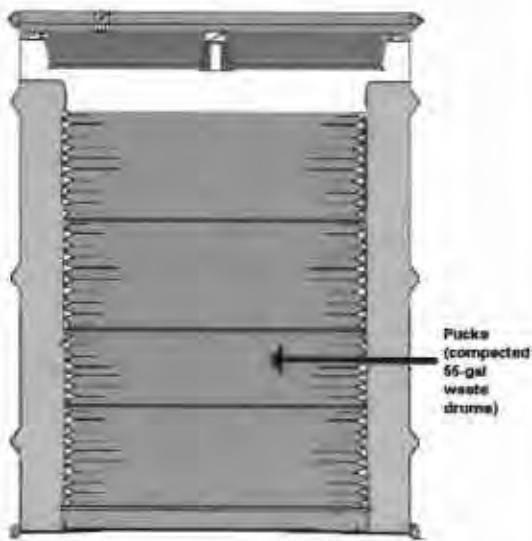
Another waste container is the TDOP (Figure 5D). The TDOP holds 10 55-gallon drums of waste.



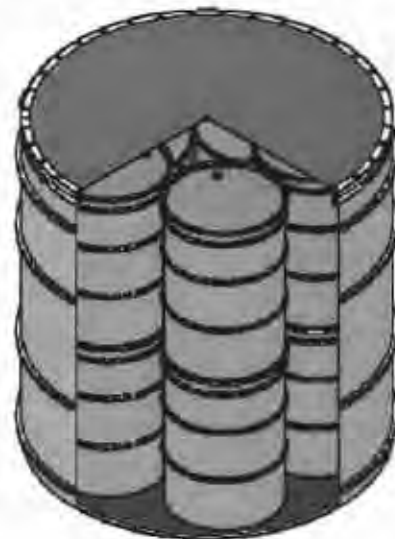
**A. 55-Gallon Drum**



**B. Pipe Overpack within a 55-Gallon Drum**



**C. AMWTP Compressed Pucks in 100-Gallon Drum**



**D. Ten Drum Overpack (TDOP)**

**Figure 5. Illustrations of structural differences in waste containers.**

Based on these types of waste packages, response models were developed that describe waste deformation. Next, potential configurations of waste packages in a representative room were identified. The calculation of creep closure required preliminary calculations to determine the initial porosity of each configuration and the parameters appropriate for the gas generation model applied during room closure. SANTOS calculations determined the closure of the room for each waste package configuration, and provided the time-dependent porosity of waste rooms for the performance assessment calculations.

### 3.1.2 Response Models for Waste Packages

The conceptual model for room closure describes salt creep into a disposal room. In the process of room closure the rock salt impinges on and compresses the waste until stress equilibrium is reached. The conceptual models for salt and other lithologies in proximity to the rooms are well understood and documented (NRC, 1996).

Response models describe the deformation of each type of waste package in response to the stresses and strains resulting from salt creep. The response model used in this analysis for waste in 55-gallon drums, referred to as the standard waste model, is the same as the volumetric plasticity model used in the calculations supporting the CCA (Stone, 1997). This model was developed from empirical stress-deformation test data.

Response models were developed both for 6-inch and 12-inch pipe overpacks by finite element modeling. The modeling, presented in Park and Hansen (2003), used numerical grids and material properties for the pipe overpacks that were developed during mechanical analyses completed to satisfy transportation requirements (Ludwigsen et al., 1998). The engineering dimensions and properties from these mechanical calculations were used to define models that simulated uniaxial, triaxial ( $\sigma_1 > \sigma_2 = \sigma_3$ ), and hydrostatic loading, and to determine parameters (e.g., volumetric plasticity coefficients) for the pipe overpack waste model. The uniaxial test simulation was used to compute the shear modulus and the bulk modulus. The triaxial test simulation defined the deviatoric yield surface. The hydrostatic test simulation was used to evaluate the pressure-volumetric strain data.

The response model for supercompacted waste (Park and Hansen, 2003) was developed from qualitative descriptions of the waste package. The supercompacted waste is assumed to be incompressible. The waste is compacted to stress levels greater than can occur in the underground at WIPP. The supercompaction process applies approximately 60 MPa (9,000 psi) to compress 55-gallon drums (BNFL, 2003); the maximal *in situ* stress at WIPP is about 15 MPa (2,150 psi). Therefore the supercompacted waste could not be further deformed by salt compaction.

No response model was developed for TDOPs or the SWBs. These containers are larger in diameter than and pipe overpacks and are constructed of thinner materials; therefore they are expected to be less stiff than the pipe overpacks. However, the TDOPs and SWBs may be more stiff than the standard 55-gallon drums. If these waste packages are structurally stiff, their effect on room closure is bounded by the results from the analyses of pipe overpacks and supercompacted waste. On the other hand, if the TDOPs and SWBs are structurally

compliant, then their effect on room closure is bounded by that of standard waste in 55-gallon drums. The uncertainty in the response model for TDOPs and SWBs is captured by treating the room closure model as uncertain, as described in Section 3.1.7.

### 3.1.3 Waste Package Configurations

The uncertainty in future placement of waste packages in disposal rooms and in waste package response models required structural calculations for a variety of waste package configurations. Waste package configurations were chosen to cover a range of combinations of porosity and waste package structural characteristics (rigidity). To ensure that these configurations covered the range of possibilities, intermediate cases representing combinations of standard and supercompacted waste packages in various ratios were also examined.

The following six configurations were examined in the analysis of room closure:

1. All standard waste (55-gallon drums)
2. All 6-inch pipe overpacks
3. All 12-inch pipe overpacks
4. A mix of 1/3 supercompacted waste and 2/3 standard waste
5. A mix of 2/3 supercompacted waste and 1/3 standard waste
6. All supercompacted waste

In the calculations of room closure, the computational grid components (elements, boundary conditions, tractions, etc.) shown in Figure 6 were kept identical for all computations. The response model for the waste, the initial porosity of the room, and the gas generation potential of the waste material were varied.

As shown in Figure 6, the standard waste response model was applied to the waste region to represent a room filled with structurally compliant waste in 55-gallon drums. The standard waste configuration (and model) also represents the configuration in which TDOPs are structurally compliant. The pipe overpack response models were applied to the waste regions to represent the combination of high waste porosity and high rigidity. The possibility that the TDOPs are structurally stiff is accounted for by the pipe overpack configurations.

As shown in Figure 7, combined cases included supercompacted waste in proportions of 1/3 and 2/3 with standard waste to represent intermediate conditions. The response models for each waste form were applied to the respective columns of waste in the computational grid. The analysis also considered a room of supercompacted waste to capture the case of low waste porosity and high rigidity.

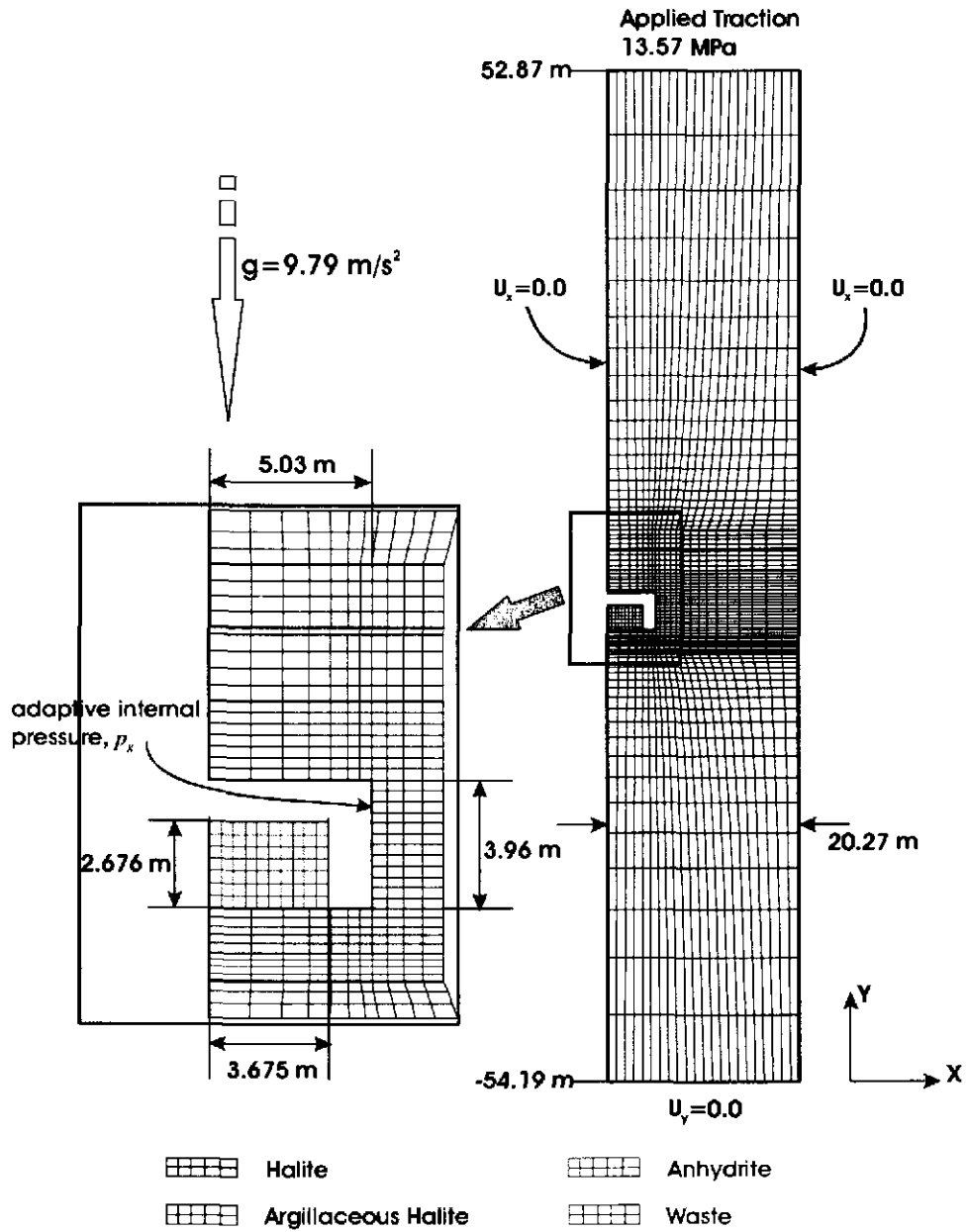


**Figure 6. Computational mesh and boundary conditions for standard and pipe overpack waste.**

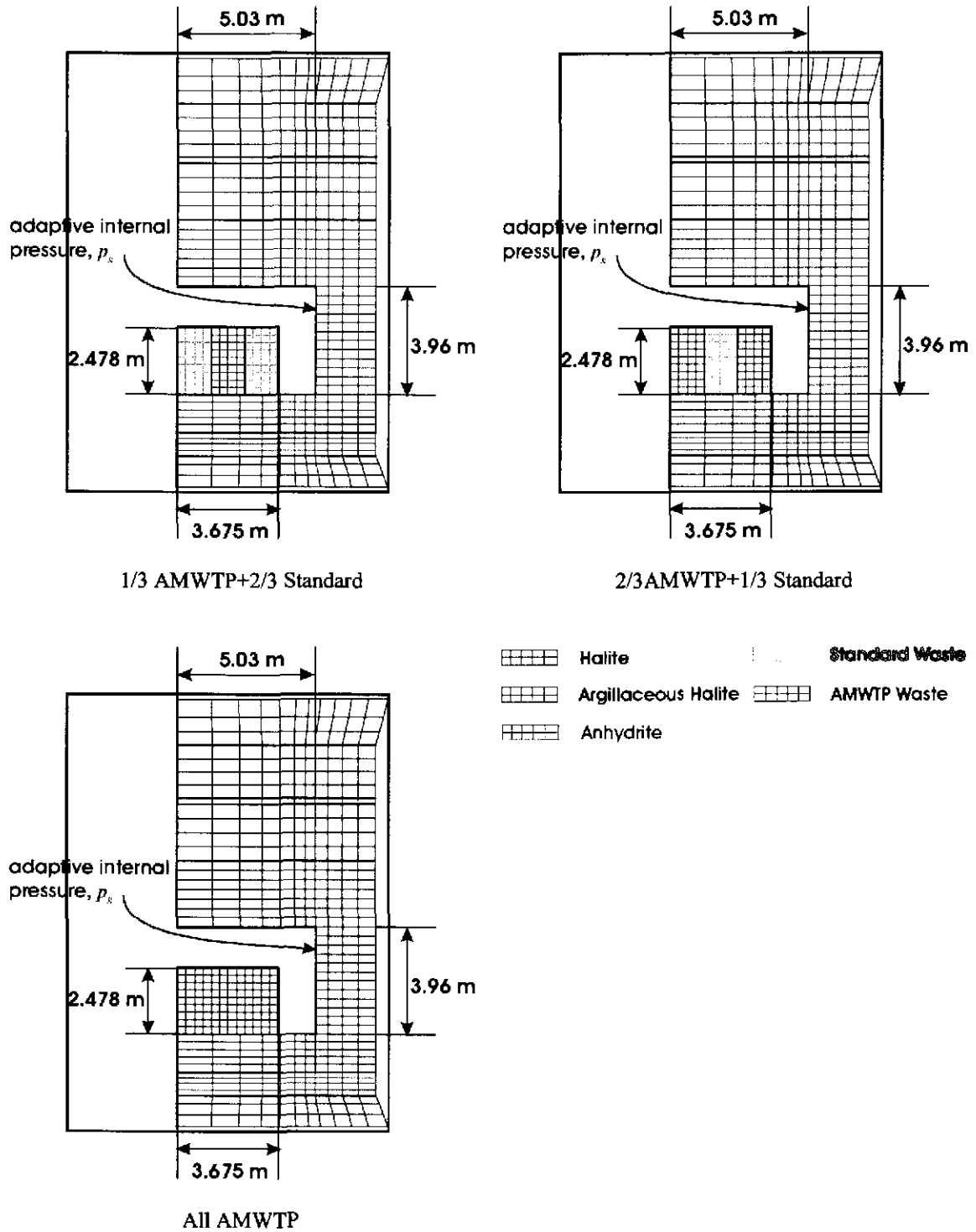


**Figure 7. Computational mesh and boundary conditions for combined and supercompacted waste configurations.**

### 3.1.4 Initial Room Porosity

Calculation of porosity requires a determination of the initial room porosity. The initial room porosity for each waste package configuration is given in Table 3 (see Park and Hansen, 2003 for details of the calculation). The standard waste configuration has the highest initial porosity and the all supercompacted waste configuration has the lowest. Thus, the six waste package configurations capture the range of possible initial porosity. The MgO backfill is considered in the calculation of the initial room porosity, but is not represented as a structural element.

**Table 4. Initial room porosity for various waste configurations.**

Standard	6" POP <sup>a</sup>	12" POP	1/3 AMWTP	2/3 AMWTP	All AMWTP
0.848	0.835	0.831	0.808	0.773	0.743

<sup>a</sup> POP = pipe overpack

### 3.1.5 Base Gas Potential and Production Rate

Gas production is a significant component of the room closure model and thus is considered separately for each waste package in the calculation of room closure.

A gas production potential and a base gas generation rate were estimated for each waste package. For the structural calculations the base gas generation rate was varied by factors ranging from 0.0 (no gas generation) to 2.0 (twice the base rate), to capture uncertainty in actual gas generation from the waste materials.

For the standard waste the base gas production potential from anoxic corrosion of iron-containing metals was estimated at 1,050 moles/drum, with a base production rate of 1 mole/drum/year (Stone, 1997.) The gas production potential from microbial activity was estimated to be 550 moles/drum, with a production rate of 1 mole/drum/year. Gas production ceases after 1050 years. The total amount of gas generated in a disposal room for the standard waste case was based on 6,804 waste drums per room (Stone, 1997). For this analysis, the base gas generation potential and gas production rate for the pipe overpack configuration are assumed to be the same as the standard waste package configuration in terms of gas generation potential.

The amount of gas generated from a single supercompacted puck is assumed to be same as the amount generated from an uncompacted 55-gallon drum. Additionally, the gas generation rate from a single puck is assumed to be equal to the gas generation rate for an uncompacted drum (1 mole/drum/year). Since an average of four pucks are placed in each 100-gallon container, and three 100-gallon containers fill the same space occupied by a seven-pack arrangement of 55-gallon drums, the supercompacted waste has a gas production

potential and base gas generation rate 12/7 larger than the potential and rate for the standard waste.

For the 1/3 supercompacted and 2/3 standard waste configuration, the total amount of gas generated in a disposal room is based on 3,888 pucks and 4,536 standard drums per room (Park and Hansen, 2003.) For the 2/3 supercompacted and 1/3 standard waste configuration, the total amount of gas generated in a disposal room is based on 7,776 pucks and 2,268 standard drums per room. In the all supercompacted waste package configuration, the total amount of gas generated in a disposal room is based on 11,664 waste pucks per room. Table 4 summarizes the total potential for gas production, in moles, and the gas production rates for the six waste loading schemes.

**Table 5. Total gas potential and gas production rates for each waste configuration.**

Parameter	Standard	6" POP	12" POP	1/3 AMWTP	2/3 AMWTP	All AMWTP
Total gas potential from 0 yr to 550 yrs (mol)	$7.5 \times 10^6$	$7.5 \times 10^6$	$7.5 \times 10^6$	$9.3 \times 10^6$	$1.1 \times 10^7$	$1.3 \times 10^7$
Total gas potential from 550 yrs to 1050 yrs (mol)	$3.4 \times 10^6$	$3.4 \times 10^6$	$3.4 \times 10^6$	$4.2 \times 10^6$	$5.0 \times 10^6$	$5.8 \times 10^6$
Gas production rate from 0 yr to 550 yrs (mol/s)	$4.3 \times 10^{-4}$	$4.3 \times 10^{-4}$	$4.3 \times 10^{-4}$	$5.3 \times 10^{-4}$	$6.4 \times 10^{-4}$	$7.4 \times 10^{-4}$
Gas production rate from 550 yrs to 1050 yrs (mol/s)	$2.2 \times 10^{-4}$	$2.2 \times 10^{-4}$	$2.2 \times 10^{-4}$	$2.7 \times 10^{-4}$	$3.2 \times 10^{-4}$	$3.7 \times 10^{-4}$

### 3.1.6 Porosity Surface for Various Waste Types

In performance assessment calculations, room closure initially proceeds as if the room were open. The free air space is eliminated early by creep closure without resistance from the waste package. Eventually the salt contacts the waste package stacks and deforms the waste package according to the relevant response model. At the same time, the conceptual models for corrosion and gas generation allow internal pressure to build within the room. Thus, the room closure owing to salt creep is modified by the structural response of the waste and by gas generation. These competing conditions (creep closure, waste package rigidity, gas generation) yield porosity histories for each waste package configuration that are compiled into a porosity surface for incorporation into performance assessment calculations.

The standard waste configuration was calculated as part of the assessment of the effects of raising the repository to Clay Seam G (Park and Holland, 2003). Calculations for the other five cases are reported by Park and Hansen (2003). For each waste package configuration, 13 separate calculations were conducted in which the gas generation rate was varied from the base rate by factors ( $f$ ) ranging from 0.0 (no gas generation) to 2.0 (twice the base rate listed in Table 4). Figure 8 illustrates final room closure and waste compression for the case of no gas generation. Generally speaking, the standard waste configuration is the most structurally compliant; this case initiates with the greatest porosity and closes down to the lowest porosity, because the waste offers the least resistance to deformation. In contrast, the case with all supercompacted waste package configuration has the lowest initial porosity but has a

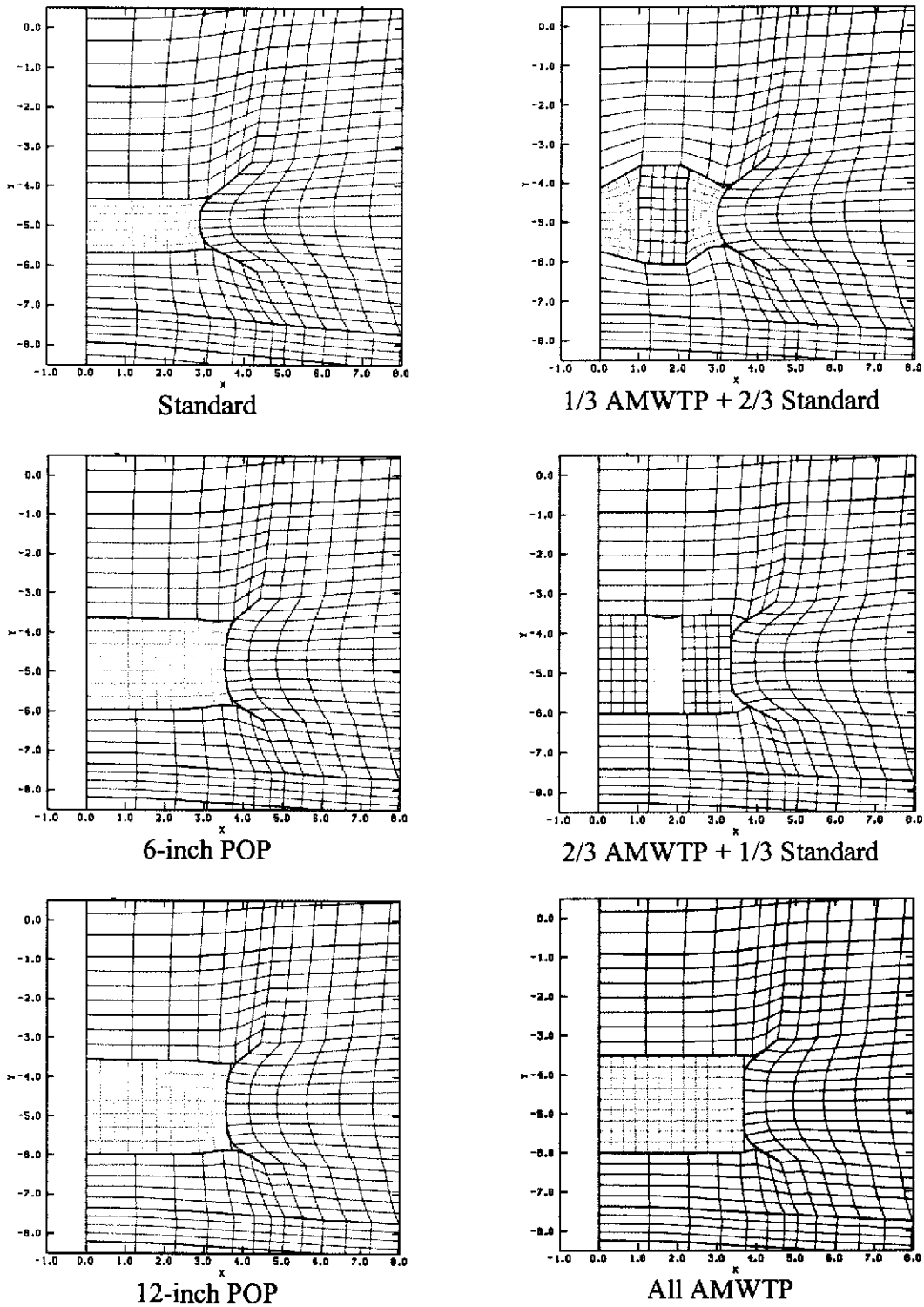


**Figure 8. Deformed grids around the disposal room containing various waste types at 10,000 years for  $f=0$ , no gas generation.**

higher long-term porosity than does the standard waste configuration; the rigidity of the supercompacted waste prevents room closure after the surrounding rock contacts the waste.

For a gas generation rate of zero, porosity histories for various waste package configurations are compared in Figure 9. The uppermost lines represent the room closure response of the pipe overpack configurations. Structural analysis of the 12-inch and 6-inch pipe overpacks indicated some degree of local buckling of the waste package, but that pipe overpacks would not yield at the maximal loads in the underground (~15 MPa), thus the pipe overpack waste configuration remains stable (Park and Hansen, 2003). Therefore, these room inventories start with a high porosity and retain relatively high porosity after salt creep closure has essentially ended. In contrast, the standard waste configuration begins with almost identical porosity to the pipe overpacks (0.85 versus 0.83 for overpacks). However, in the absence of gas generation, the standard waste 55-gallon drum compresses readily, achieving the lowest porosity (the lowest curve in Figure 9).

The porosity curves for the mixed standard and supercompacted waste configurations and the all supercompacted waste configuration lie between the two extremes represented by the standard 55-gallon drum waste and the pipe overpack configurations. In the case of a room of supercompacted waste, the free space of the room diminishes rapidly until the creeping salt and deforming outer containers impinge on the pucks. The configurations with mixed standard and supercompacted waste show different porosities in the transient period while the room closes. However, the long-term porosity of these cases is similar to the all supercompacted waste configuration.

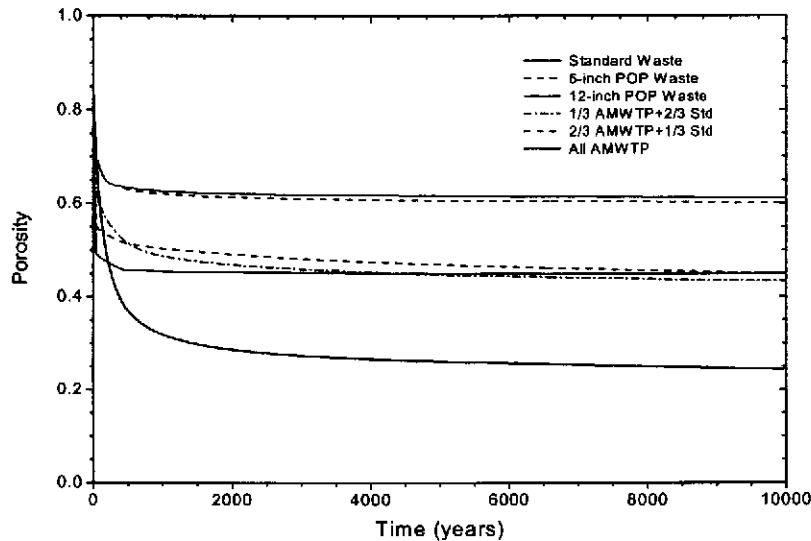


**Figure 9. Porosity histories for various waste types,  $f=0$ .**

Figures 10, 11 and 12 compare porosity histories for gas generation rates of 0.4, 1.0 and 2.0 times the base gas generation rate for each waste package configuration. Park and Hansen (2003) present porosity history results for all 13 gas generation rates (corresponding to the values of  $f$ ) used in the performance assessment calculations. As sufficient gas is generated, room closure reverses and porosity increases. As gas generation rates increase, all waste package configurations tend toward similar long-term porosities.

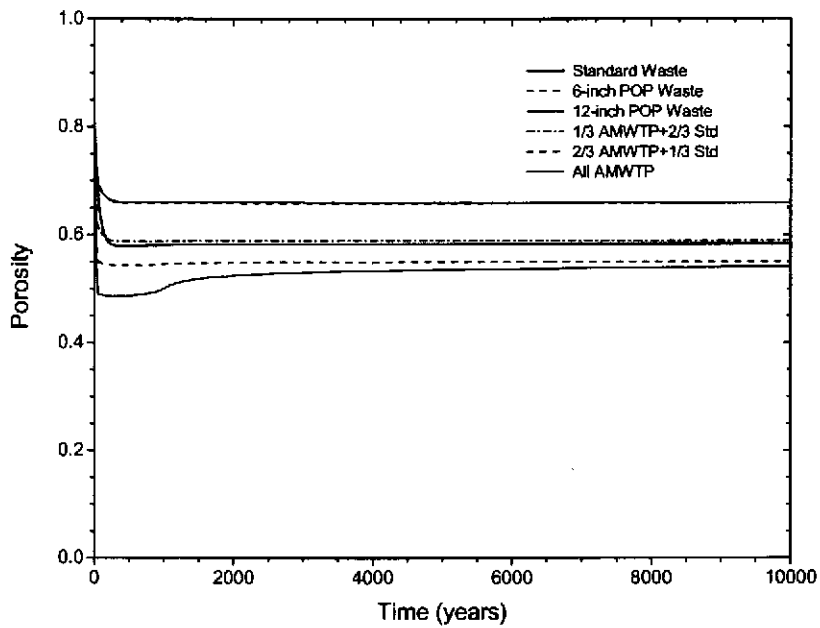


Figure 10. Porosity histories for various waste types,  $f=0.4$ .

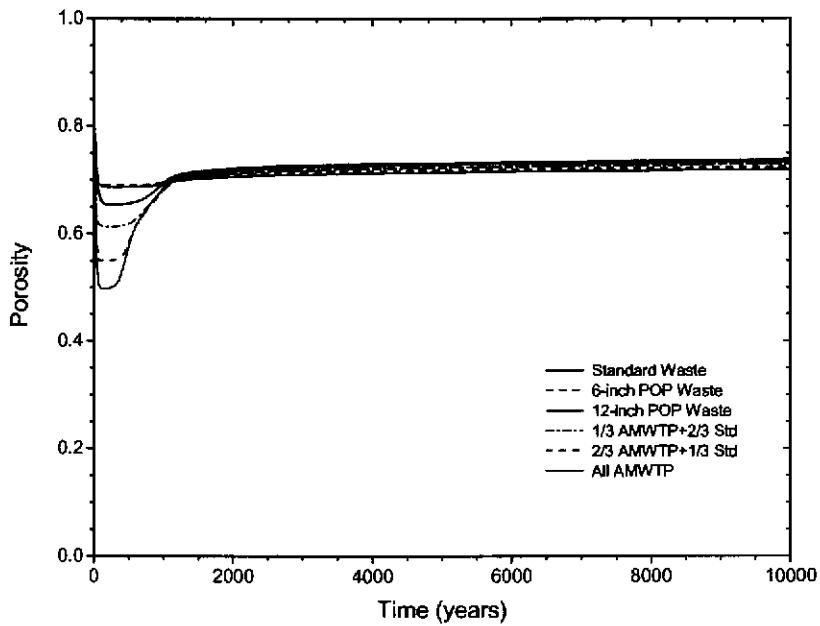
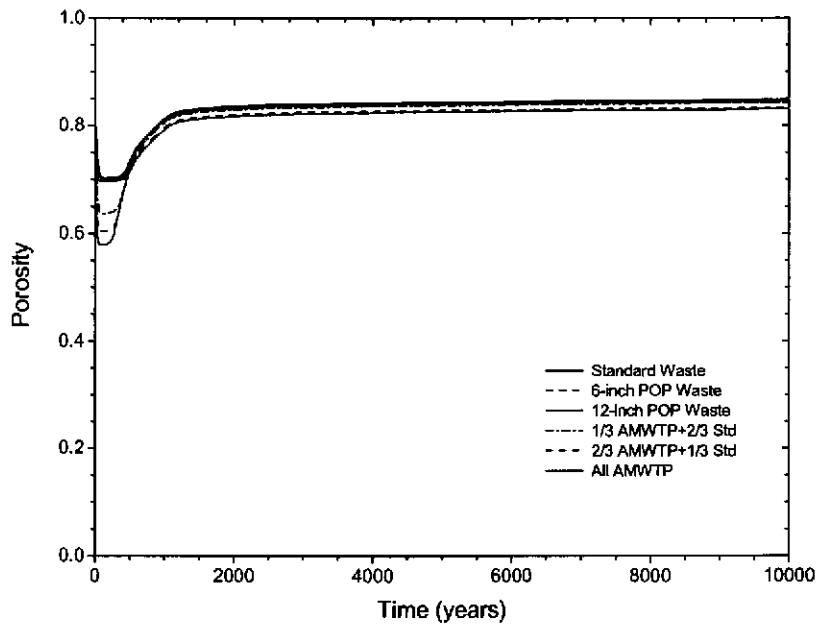
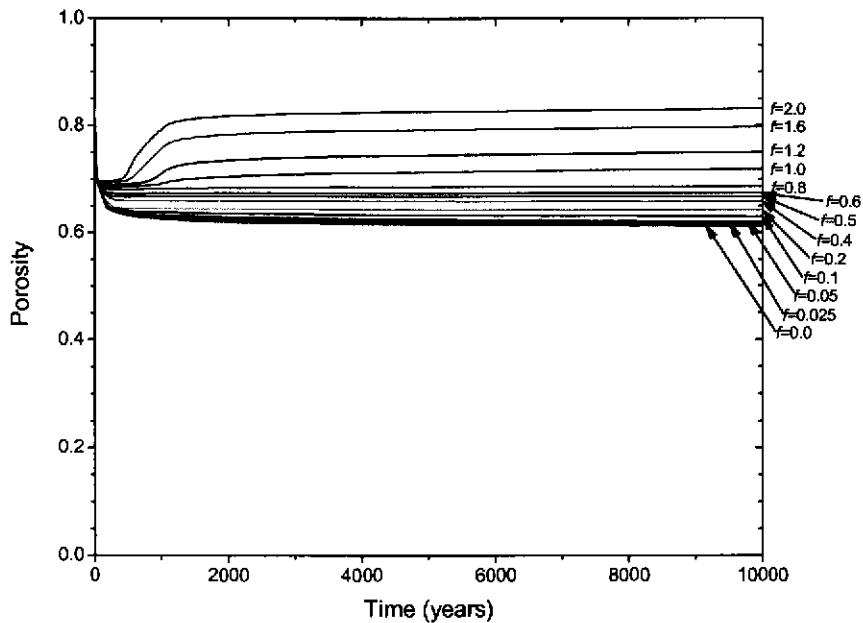


Figure 11. Porosity histories for various waste types,  $f=1.0$ .



**Figure 12. Porosity histories for various waste types,  $f=2.0$ .**

Figures 13 through 15 show the porosity in a room filled with 12-inch pipe overpacks, with the mixed inventory of 2/3 AMWTP and 1/3 standard waste, and with all supercompacted waste, for various gas generation factors  $f$  ranging from 0.0 to 2.0.



**Figure 13. Porosity histories for a room containing the 12-inch POP waste.**

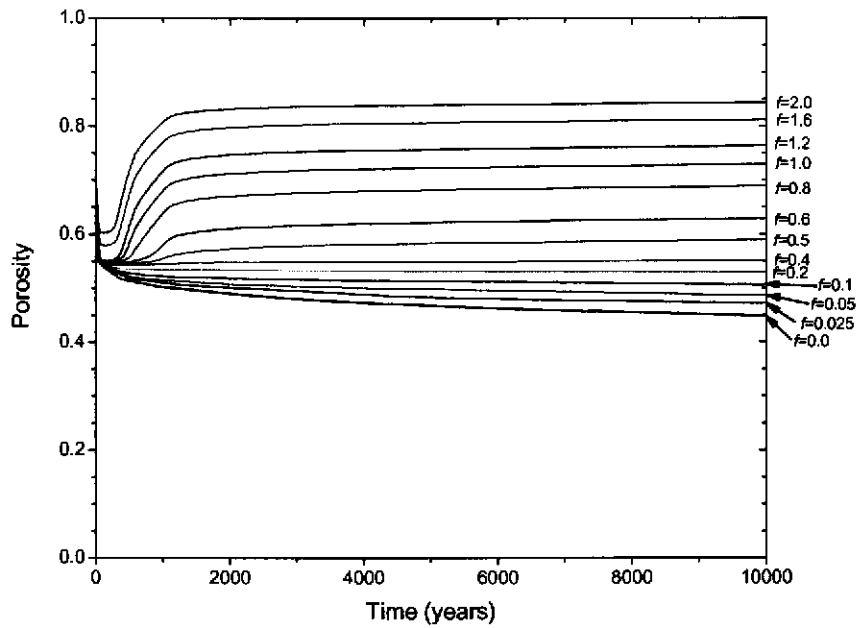


**Figure 14. Porosity histories for a room containing 2/3 supercompacted and 1/3 standard waste.**

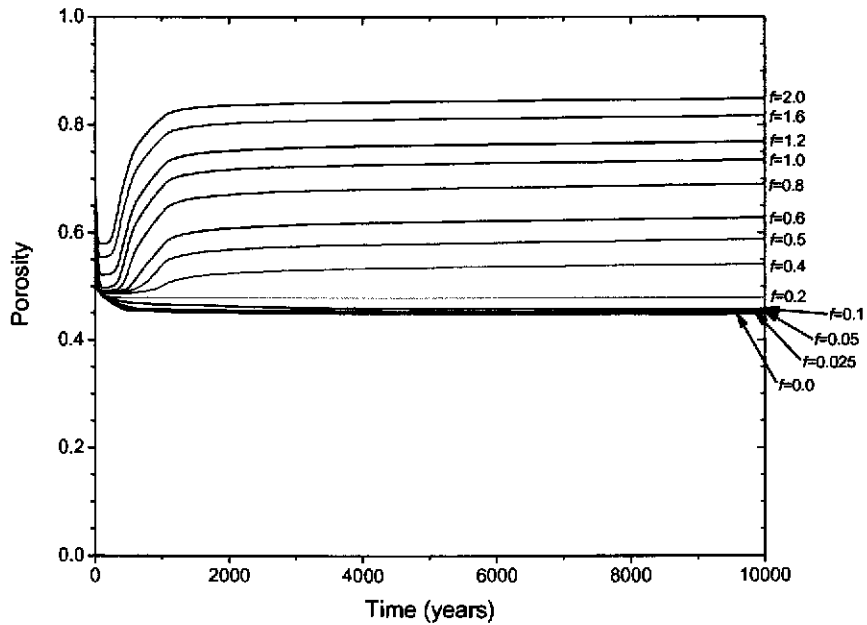


**Figure 15. Porosity histories for a room containing only supercompacted waste.**

### 3.1.7 Implementation in New Performance Assessment

Conceptually, the processes of salt creep, brine flow, gas generation, and room closure are coupled in the performance assessment. The computational model for creep closure is implemented in the BRAGFLO code by means of the porosity surface. The porosity surface is essentially a look-up table that determines the value of room porosity based on pressure, time and gas generation rate. BRAGFLO can use a different porosity surface for each waste material represented in the BRAGFLO grid (shown in Figure 16). In this performance assessment, the BRAGFLO grid includes two waste materials, WAS\_AREA and REPOSIT, having identical hydrologic properties but different porosity surfaces. WAS\_AREA was assigned to the representative waste panel, and REPOSIT was assigned to the two regions for the rest of the repository. Stein (2003) provides more details about the BRAGFLO grid.

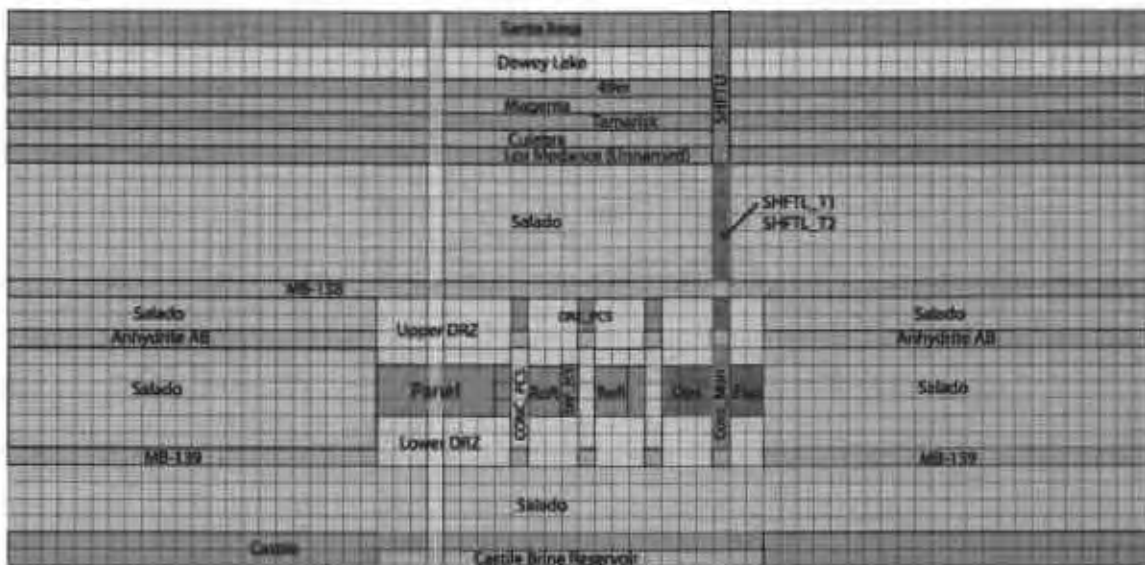


**Figure 16. BRAGFLO grid used in the performance assessment.**

Because the future placement of waste is uncertain, this analysis treats the porosity surface for the waste materials in the BRAGFLO grid as uncertain by sampling from a set of possible porosity surfaces for each waste package configuration. This uncertainty reflects the subjective uncertainty of the spatial arrangement of the waste packages, as well as the subjective uncertainty in the response models for the waste packages. Rather than attempting to represent this uncertainty as a continuous range of surfaces, a set of four porosity surfaces was chosen, three of which represent bounding elements in the set of possible porosity surfaces:

1. **Standard Waste Model.** The standard waste model represents a room filled with a homogeneous mix of waste in 55-gallon drums, identical to the assumptions for the CCA and PAVT. The standard model represents a bounding case of high initial porosity and structurally compliant waste packages.

2. Combined Waste Model. This model assumes that stiff and structurally compliant wastes are mixed within a room. Supercompacted waste is used for the stiff waste, and standard waste is used for the compliant waste. A mix of 2/3 supercompacted waste and 1/3 standard waste (by volume) was selected for this model.
3. Supercompacted Waste Model. This model assumes that all waste is structurally similar to supercompacted waste. This model reflects a bounding case where the initial porosity is low and the waste packages are stiff.
4. Pipe Overpack Model. This model assumes all waste is structurally similar to pipe overpacks. This model represents a bounding case where initial porosity is high and the waste packages are stiff. Results from the porosity surface calculations for 12" pipe overpacks were used for this model.

A new discrete random variable was sampled to select the porosity surface for the representative waste panel in each BRAGFLO realization. The random variable is implemented as the parameter WAS\_AMW/CLOSMOD1, with the distribution indicated in Table 5. The distribution is consistent with the expectation that the waste yet to be shipped to WIPP will not include a significant number of pipe overpacks, and hence only one panel (out of 10 total panels) was modeled with the pipe overpack porosity surface. To preserve the widest range of variability in the selection of porosity surfaces, the other three porosity surfaces are assigned equal probabilities.

**Table 6. Distribution of WAS\_AMW/CLOSMOD1.**

Porosity surface	Probability
1 – Standard Waste Model	0.3
2 – Combined Waste Model (2/3 supercompacted waste & 1/3 standard waste)	0.3
3 – Supercompacted Model	0.3
4 – Pipe Overpack Model	0.1

The rest of repository in BRAGFLO represents the other nine waste panels. The porosity surface for the rest of repository was selected by a discrete random variable, implemented by the parameter WAS\_AMW/CLOSMOD2, with the distribution shown in Table 6. The porosity surfaces for pipe overpacks and for supercompacted waste are not represented in this distribution, because the waste in the rest of repository cannot consist solely of these stiff waste forms (the emplaced volume of supercompacted waste, 19,875 m<sup>3</sup>, is insufficient to fill more than two waste panels). The two remaining porosity surfaces are assigned equal probabilities to preserve the widest range of variability.

**Table 7. Distribution of WAS\_AMW/CLOSMOD2.**

<b>Porosity surface</b>	<b>Probability</b>
1 – Standard Waste Model	0.5
2 – Combined Waste Model (2/3 supercompacted waste & 1/3 standard waste)	0.5

The parameters WAS\_AMW/CLOSMOD1 and WAS\_AMW/CLOSMOD2 are uncorrelated to allow for all combinations of porosity surfaces in the performance assessment calculations. It is possible that some combinations of waste forms may be more or less likely in the inventory than the probability resulting from these distributions. However, there is little basis for assigning probabilities to combinations of porosity surfaces, and the assumption of independence simplifies the sensitivity analysis to determine the significance of the variability in porosity surfaces.

The selection of a discrete distribution using bounding elements captures the range of uncertainty in the various porosity surfaces. The use of bounding elements results from the observation that porosity surfaces created for standard waste, supercompacted waste, and pipe overpack waste do not exhibit monotonic relationships. This means that porosity evolution in the repository does not vary between two hypothetical bounding surfaces as a monotonic function of the concentration of the different waste packages.

In addition to uncertainty in spatial distribution of waste in the repository, there is also uncertainty about the deformational characteristics of the various waste containers, such as the TDOPs. The bounding elements in this assessment capture the uncertainty in waste container characteristics. Therefore, the implementation in this performance assessment accounts for the possibilities that waste containers may range from stiff to compliant.

## **3.2 Chemical Conditions in the Repository**

Chemical conditions in the repository are determined to calculate radionuclide solubilities and to estimate gas generation rates by anoxic corrosion of iron-based metals. This section describes the effects of AMWTP waste on chemical conditions used in the calculation of solubilities, including:

- (1) Analysis of the effects of AMWTP waste on the MgO safety factor. The MgO safety factor is defined as the quantity of MgO to be emplaced in the repository or a panel divided by the quantity of MgO required to consume the CO<sub>2</sub> that could be produced by microbial consumption of the CPR in the waste.
- (2) Analysis of the effects of AMWTP waste on the concentrations of organic ligands that could affect the solubilities of actinides in WIPP brines.

This analysis demonstrates that the assumptions underlying the calculation of solubilities for a homogeneous waste material remain valid with the AMWTP waste included in the inventory. The analysis shows that sufficient MgO will be emplaced to sequester the CO<sub>2</sub> in any panel, regardless of the configuration of waste. The AMWTP waste does not cause factors relevant to calculation of solubilities, such as the fugacity of CO<sub>2</sub> ( $f_{\text{CO}_2}$ ), the pH, the concentrations of organic ligands, to deviate significantly from values for a homogeneous waste material.

In addition, the analysis shows that AMWTP waste does not affect the calculated rates for gas generation by anoxic corrosion of steel. Finally, this section shows that AMWTP waste does not change the treatment of radiolysis effects in the performance assessment.

### **3.2.1 Actinide Solubilities**

In the CCA, actinide solubilities were computed assuming thermodynamic equilibrium conditions and a homogeneous chemical environment throughout the repository. The calculations assumed that all CO<sub>2</sub> produced by biodegradation was sequestered by magnesium oxide (MgO) (DOE, 1996, Appendix BACK). Actinide solubilities included uncertain parameters that varied among realizations; however, for each realization a single solubility was applied to all of the waste material.

#### **3.2.1.1 Cases for Chemical Conditions Analysis**

Four cases were considered: a homogeneous repository (analogous to the CCA waste model); a panel filled with AMWTP waste; and two cases of mixtures of AMWTP waste and other CH-TRU waste. In the homogeneous repository, average concentrations of the relevant constituents (e.g., CPR, ligands) were computed over all CH-TRU waste streams, including the AMWTP waste. In the all AMWTP panel, concentrations were computed for a mix of

supercompacted and uncompacted waste in proportions equal to the ratio of the total volume of the two waste forms in the inventory. The two cases of mixed AMWTP waste and other CH-TRU waste were determined by examining actual waste emplacement patterns in Panel 1 (Leigh, 2003a.)

Leigh (2003a) defined “realistic” and “conservative” cases for combinations of AMWTP and other CH-TRU waste. The realistic case assumes that the fraction of a panel’s volume filled with supercompacted waste is equal to the largest fraction of Panel 1’s filled volume occupied by a single waste stream (waste stream RF 118.01 from the RFETS.) In this case, supercompacted waste occupies about 13.5 percent by volume of the panel; the remaining volume is filled by uncompacted waste from INEEL and other CH-TRU waste from all other sites. The volume of uncompacted waste is derived from the ratio of uncompacted to compacted waste containers at INEEL. The other CH-TRU waste would occupy any remaining available volume in the panel.

The “conservative” case assumes that the fraction of CH-TRU waste packages from INEEL in the panel is equal to the fraction of the waste packages in Panel 1 from all RFETS waste streams. In this case, supercompacted waste would account for 54 percent of the waste packages in a panel, and the remaining waste packages would contain uncompacted waste from INEEL and other CH-TRU waste from all other sites. As in the realistic case, the volume of uncompacted waste is derived from the ratio of uncompacted to compacted waste containers at INEEL.

Table 7 presents volumes and quantities of waste packages for supercompacted waste, uncompacted waste from INEEL and other CH-TRU waste for the homogeneous repository and the two cases of mixed AMWTP and other CH-TRU waste (Leigh, 2003a, 2003b, 2003c.) Using the data in Table 7, quantities of CPR,  $\text{NO}_3^-$  and  $\text{SO}_4^{2-}$ , and ligands were estimated for a realistic panel, the rest of the repository associated with a realistic panel, a conservative panel, and the rest of the repository associated with a conservative panel (Leigh (2003a, 2003b, 2003c).

**Table 8. Waste volumes in the repository and in the realistic and conservative cases.**

Property	Homogeneous Repository	Realistic Panel	Conservative Panel
Total Volume of CH-TRU Waste (m <sup>3</sup> ) <sup>1</sup>	168,500	17,591	17,591
Volume of Supercompacted Waste (m <sup>3</sup> )	19,875	2357	4777
Volume % of Supercompacted Waste (%)	11.8	13.4	27.2
Volume of Uncompacted Waste (m <sup>3</sup> )	40,944	4871	9875
Volume % of Uncompacted Waste (%)	24.3	27.7	56.1
Volume of Non-AMWTP Waste (m <sup>3</sup> )	107,681	10,251	2715
Volume % of Non-AMWTP Waste (%)	63.8	58.3	15.4

1. Volumes of waste in the repository and panel are from Lappin et al., 1989, Table 4-7.

### 3.2.1.2 Effects of Supercompacted Waste on MgO Safety Factors

MgO safety factors were calculated for each of the cases listed in Section 3.2.1.1 (Snider, 2003.) The quantity of MgO in the repository (or in a panel) was adjusted to include only that portion of the emplaced MgO that will actually react with aqueous or gaseous CO<sub>2</sub>, based on experimental studies of the efficacy of Premier MgO, the material being emplaced in the WIPP. Table 8 provides the results of these calculations, which demonstrate that the MgO safety factor exceeds 1.00 for all cases.

In these calculations, the quantity of MgO assumed to be present in a panel is about 9.4 percent greater than the quantity approved by EPA for the repository as a whole (EPA, 2001). The difference in total mass of MgO results from differences in estimating the number of MgO supersacks in each panel. DOE estimates the number of supersacks from the total volume of CH-TRU waste to be disposed at the WIPP, to be consistent with the rest of the performance assessment. EPA's estimate is based on the number of containers actually placed in Panel 1. However, by either method of tabulating the total mass of MgO, the safety factors are well above 1.00, thus the conclusion of this analysis does not depend on the calculation method.

**Table 9. MgO safety factors and other parameters.**

Parameter <sup>1</sup>	Homogeneous Repository with Mini-sacks (CCA) <sup>2</sup>	Homogeneous Repository without Mini-sacks, Jan. 2001 <sup>2</sup>	Homogeneous Repository <sup>3</sup>	Realistic Panel <sup>3</sup>	Conservative Panel <sup>3</sup>	Panel with All AMWTP Waste <sup>3</sup>
CPR Consumed by Denitrification	3%	3%	5%	4%	3%	2%
CPR Consumed by SO <sub>4</sub> <sup>2-</sup> Reduction	2%	2%	1%	1%	0.2%	0.03%
CPR Consumed by Methanogenesis	95%	95%	94%	95%	97%	98%
MgO Safety Factor	3.73	3.23	2.45	2.66	2.02	1.66

<sup>1</sup> The CO<sub>2</sub> yields are 1 mol of CO<sub>2</sub> per mol of organic C consumed from denitrification and SO<sub>4</sub><sup>2-</sup> reduction, and 0.5 mol of CO<sub>2</sub> per mol of C from methanogenesis. This is based on results of Francis and Gillow, 2000, pp. 2, 3, and 10; Gillow and Francis, 2001, pp. 3-4 and 3-5; Gillow and Francis, 2002a, pp. 2.1 - 12 to 2.1 - 14; and Gillow and Francis, 2002b, pp. 3.1 - 5 to 3.1 - 6.

<sup>2</sup> Wang, 2000.

<sup>3</sup> Snider, 2003.

### 3.2.1.3 Effects of Supercompacted Waste on Ligand Concentrations

Organic ligands (acetate, citrate, ethylenediaminetetraacetic acid (EDTA), and oxalate) in TRU waste could dissolve in brines that enter the repository after closure, and increase the solubilities of actinide elements by forming complexes. Concentrations of these ligands were calculated for all four cases listed in Section 3.2.1.1 (Brush and Xiong, 2003c.) Table 9 shows the results of the calculations. The concentrations for a panel filled with supercompacted waste (not shown in Table 7) are zero because supercompacted waste does not contain ligands (Leigh, 2003c). These results (Table 11) demonstrate that any concentration of AMWTP waste in a panel (or panels) will result in lower ligand concentrations and hence lower solubilities than for a homogeneous repository. Hence, the solubilities calculated for a homogeneous repository are conservative for any loading of supercompacted waste in the repository.

**Table 10. Ligand concentrations in WIPP brines (M).**

Ligand <sup>1</sup>	Homogeneous Repository	Realistic Panel	Conservative Panel
Acetate	$3.56 \times 10^{-3}$	$3.46 \times 10^{-3}$	$2.87 \times 10^{-3}$
Citrate	$2.71 \times 10^{-4}$	$2.63 \times 10^{-4}$	$2.20 \times 10^{-4}$
EDTA	$2.73 \times 10^{-6}$	$2.66 \times 10^{-6}$	$2.21 \times 10^{-6}$
Oxalate	$1.53 \times 10^{-2}$	$1.48 \times 10^{-2}$	$1.24 \times 10^{-2}$

<sup>1</sup> From Crawford and Leigh, 2003.

### 3.2.1.4 Effects of Supercompacted Waste on Actinide Solubilities

The results summarized in Section 3.2.1.2 and presented in Snider (2003) demonstrate that the MgO safety factor exceeds 1.00 in each panel, for any configuration of waste in the repository. Therefore, MgO would consume all CO<sub>2</sub> produced by microbial consumption of the CPR in the waste or waste containers. Because MgO would consume the CO<sub>2</sub>,  $f_{\text{CO}_2}$  and pH would not deviate from the values currently predicted for a homogeneous repository. Therefore, this analysis makes no change to the method for calculating solubilities or the conditions assumed for the calculations. Furthermore, these conditions are essentially identical to those used for the PAVT calculations (EPA, 1998b, Tables 4.10-3 and 4.10-4; 1998c, Tables 4-8 and 4-9). A more detailed explanation of the underlying chemical reactions and their relationship to  $f_{\text{CO}_2}$  and pH in the event of significant microbial activity can be found in Brush and Xiong (2003a, 2003b.)

Since ligand concentrations are highest for the homogeneous repository case, the solubilities calculated by Brush and Xiong (2003b) for a homogeneous repository are applied in this analysis. Table 10 compares these solubilities to those used for the CCA and the PAVT.

**Table 11. Comparison of Log( $f_{CO_2}$ ), pH, and solubilities (M).**

Actinide Ox. State, Brine, or Property	CCA, <sup>1</sup> All Vectors (no organics)	PAVT, <sup>2</sup> All Vectors (no organics)	Microbial Vectors (w/organics) <sup>3</sup>	Nonmicrobial Vectors (w/organics) <sup>3</sup>
Log( $f_{CO_2}$ ), Salado Brine	-6.9	-5.50	-5.50	-5.48
Log( $f_{CO_2}$ ), Castile Brine	-6.9	-5.50	-5.50	-6.15
pH, Salado Brine	8.69	8.69	8.69	8.69
pH, Castile Brine	9.24	9.24	9.02	8.99
An(III), Salado Brine	$5.82 \times 10^{-7}$	$1.2 \times 10^{-7}$	$3.07 \times 10^{-7}$	$3.07 \times 10^{-7}$
An(III), Castile Brine	$6.52 \times 10^{-8}$	$1.3 \times 10^{-8}$	$1.69 \times 10^{-7}$	$1.77 \times 10^{-7}$
An(IV), Salado Brine	$4.4 \times 10^{-6}$	$1.3 \times 10^{-8}$	$1.19 \times 10^{-8}$	$1.24 \times 10^{-8}$
An(IV), Castile Brine	$6.0 \times 10^{-9}$	$4.1 \times 10^{-8}$	$2.47 \times 10^{-8}$	$5.84 \times 10^{-9}$
An(V), Salado Brine	$2.3 \times 10^{-6}$	$2.4 \times 10^{-7}$	$1.02 \times 10^{-6}$	$9.72 \times 10^{-7}$
An(V), Castile Brine	$2.2 \times 10^{-6}$	$4.8 \times 10^{-7}$	$5.08 \times 10^{-6}$	$2.13 \times 10^{-5}$
An(VI), Salado Brine <sup>4</sup>	$8.7 \times 10^{-6}$	$8.7 \times 10^{-5}$	$8.7 \times 10^{-6}$	$8.7 \times 10^{-6}$
An(VI), Castile Brine <sup>4</sup>	$8.8 \times 10^{-6}$	$8.8 \times 10^{-6}$	$8.8 \times 10^{-6}$	$8.8 \times 10^{-6}$

1. From Novak, Moore, and Bynum (1996, Table 1, columns entitled "@Mg"); DOE (1996, Appendix SOTERM, Table SOTERM-2), except that Novak, Moore, and Bynum (1996) used molal instead of molar units.
2. From Trovato (1997, Attachment 2), EPA (1998d, Table 5), EPA (1998b, Subsection 4.10.4, Tables 4.10-1, 4.10-3 and 4.10-4; and Subsection 12.4, Table 12.4-1), and EPA (1998c, Subsections 5.26–5.32 and Section 6.0, Table 6.4).
3. From Brush and Xiong (2003b).
4. Estimated for the CCA by Hobart and Moore (1996). See also DOE (1996, Appendix SOTERM, SOTERM-27 - SOTERM-28).

### 3.2.2 Anoxic Corrosion

Supercompacted waste also would have no significant effect on the gas generation rate from anoxic corrosion of steels and other iron-base metals. Supercompacted waste contains relatively high loadings of steel (Lott, 2003a, 2003b) but would not increase the rate of H<sub>2</sub> production from anoxic corrosion. Section 3.2.1.2 shows that MgO would consume CO<sub>2</sub> that could be produced. Consequently,  $f_{CO_2}$  and pH would remain at  $10^{-5.50}$  atm and at about 9, respectively (Brush and Xiong, 2003a, 2003b). These conditions were used to establish the ranges of H<sub>2</sub>-production rates and the probability distributions for the PAVT. Therefore, the H<sub>2</sub>-production rates for any configuration of AMWTP waste would not deviate from those currently used for a homogeneous repository.

### 3.2.3 Radiolysis

Table 9 demonstrates that, even after compaction and packaging in 100-gal containers, supercompacted waste contains significantly lower loadings of 7 of the 10 most important

radionuclides in the WIPP disposal inventory. Table 9 is based on the scaled volumes and activities for selected radionuclides for each CH-TRU waste stream form (Lott, 2003b, Table E-1). The radionuclides  $^{229}\text{Th}$ ,  $^{230}\text{Th}$ ,  $^{233}\text{U}$ ,  $^{234}\text{U}$ ,  $^{238}\text{Pu}$ ,  $^{239}\text{Pu}$ ,  $^{240}\text{Pu}$ ,  $^{241}\text{Pu}$ ,  $^{242}\text{Pu}$ , and  $^{241}\text{Am}$  are the most important from the standpoint of potential effects of radionuclide loading on chemical conditions in the repository because they account for essentially all of the:

- (1)  $\alpha$  decay during the 10,000-year regulatory period, and
- (2) radiolytic effects, if any, on chemical conditions in the repository.

Table 11 also shows that the total loading of these 10 radionuclides in supercompacted waste,  $5.13 \text{ Ci/m}^3$ , is about 15 percent of the loading of these 10 radionuclides in the rest of the CH-TRU inventory,  $34.2 \text{ Ci/m}^3$ . Therefore, any preferential loading of supercompacted waste in a panel would result in lower radionuclide loadings in that panel, and consequently, less  $\alpha$  radiolysis of any brine present in that panel and fewer radiolytic effects (if any) on chemical conditions in that panel.

**Table 12. Radionuclide loadings ( $\text{Ci/m}^3$ ).**

Radionuclide	Average of All CH-TRU Waste <sup>1</sup>	Supercompacted AMWTP Waste <sup>1</sup>	All CH-TRU Without Supercompacted Waste <sup>1</sup>
$^{229}\text{Th}$	$9.23 \times 10^{-6}$	$5.41 \times 10^{-5}$	$3.23 \times 10^{-6}$
$^{230}\text{Th}$	$6.02 \times 10^{-7}$	$5.86 \times 10^{-9}$	$6.81 \times 10^{-7}$
$^{233}\text{U}$	$7.34 \times 10^{-3}$	$4.44 \times 10^{-2}$	$2.38 \times 10^{-3}$
$^{234}\text{U}$	$9.95 \times 10^{-4}$	$9.85 \times 10^{-5}$	$1.12 \times 10^{-3}$
$^{238}\text{Pu}$	$9.56 \times 10^0$	$2.54 \times 10^0$	$1.05 \times 10^1$
$^{239}\text{Pu}$	$3.92 \times 10^0$	$2.00 \times 10^0$	$4.18 \times 10^0$
$^{240}\text{Pu}$	$6.35 \times 10^{-1}$	$1.70 \times 10^{-1}$	$6.98 \times 10^{-1}$
$^{241}\text{Pu}$	$1.43 \times 10^1$	$3.95 \times 10^{-3}$	$1.62 \times 10^1$
$^{242}\text{Pu}$	$1.58 \times 10^{-4}$	$5.66 \times 10^{-4}$	$1.04 \times 10^{-4}$
$^{241}\text{Am}$	$2.38 \times 10^0$	$3.74 \times 10^{-1}$	$2.65 \times 10^0$
All 10 above	$3.07 \times 10^1$	$5.13 \times 10^0$	$3.42 \times 10^1$

1. Decayed to December 31, 2001. Based on Lott (2003b) and Leigh (2003d, Attachment 1).

### 3.3 Implementation of Gas Generation

Two gas generation mechanisms are implemented in performance assessment: microbial degradation of organic compounds in the waste and anoxic corrosion of iron-based metals. Microbial activity in the waste is treated as uncertain, occurring with a 0.5 probability. If microbial activity is present, with a probability of 0.5 only cellulose materials are degraded; otherwise, microbial activity degrades all CPR materials. Iron corrosion is assumed to always occur, although the rate of iron corrosion and resulting gas generation is treated as uncertain.

The homogeneous model for waste assumes that both iron and CPR are distributed uniformly throughout the waste-filled regions of the repository. However, any placement of waste in the repository will result in a spatially variable concentration of CPR, due to differences in CPR content of the various waste streams (see Section 3.3.1). Heterogeneous concentrations of CPR will lead to gas generation that is non-uniform across the repository. The effect of non-uniform gas generation on repository performance is unknown, hence this analysis includes spatially varying CPR concentration. Spatially varying iron concentrations are determined to be unnecessary in this analysis.

### 3.3.1 Heterogeneity in CPR Concentration

The concentrations of CPR materials in the supercompacted AMWTP waste, in the uncompacted AMWTP waste, and in all other CH-TRU waste streams are substantially different. Table 12 presents the numerical values for the densities of CPR materials in the emplaced waste. These densities were computed by dividing the mass of CPR in the waste streams by the volume occupied by the waste as emplaced in the repository (i.e. container volume). The inventory data indicate that the supercompacted AMWTP waste has densities of CPR materials that are almost a factor of 10 greater than the average densities of these materials in CH-TRU waste from all non-AMWTP waste streams. On the other hand, the uncompacted AMWTP waste streams have densities of CPR materials that are almost a factor of 10 smaller than the average densities of these materials in CH-TRU waste from all non-AMWTP waste streams.

**Table 13. Densities of cellulosic, plastic, and rubber materials in CH-TRU waste.**

Waste Type	Density of Cellulose (kg/m <sup>3</sup> )	Density of Plastic (kg/m <sup>3</sup> )	Density of Rubber (kg/m <sup>3</sup> )	Density of Plas. Pckg. (kg/m <sup>3</sup> )
Supercompacted waste <sup>1</sup>	302.67	204.54	79.91	0.0
Uncompacted waste in TDOPs <sup>2</sup>	2.68	3.55	0.01	19.11
Uncompacted waste in SWBs <sup>3</sup>	2.73	3.56	0.01	16
All non-AMWTP waste streams <sup>3</sup>	33.65	26.49	7.12	17.93

1. Leigh and Lott, 2003a

2. Leigh and Lott, 2003b

3. Leigh, 2003a

For this reason, loading a single panel with supercompacted waste could lead to a greater amount of gas being produced in the panel, and may affect releases. Since microbial gas production is treated as a subjectively uncertain process in performance assessment, only half of the possible realizations may be affected by non-uniform distribution of CPR.

To determine how non-uniform loading of CPR within the repository might affect performance, an uncertain parameter (WAS\_AMW/FRACAMW) was defined as the fraction of a single panel's volume that is filled with AMWTP waste (supercompacted and non-compacted.) This parameter was given a uniform distribution between 0.2 and 1.0. This range brackets both the realistic and conservative estimates of the possible amount of

AMWTP waste that could be loaded into a single panel (Leigh, 2003a). As detailed by Hansen (2003), the sampled value of WAS\_AMW/FRACAMW was used to determine a CPR concentration for the representative waste panel and for the rest of repository.

Gas generation by microbial degradation is implemented in the BRAGFLO code. BRAGFLO is limited in its resolution of non-uniform CPR loading by grid-cell spacing, and thus it is assumed that CPR is distributed homogeneously throughout each grid cell. However, the scale of non-uniform loading was set at a single panel; this choice of scale is appropriate because panel closure systems tend to isolate waste panels from one another (Hansen et al., 2002). Thus, the CPR loading is uniform within each of the waste filled regions in the BRAGFLO grid, but may vary between regions. This analysis uses the BRAGFLO grid shown in Figure 16, in which waste is divided into three regions, one labeled PANEL for a single, representative waste panel, and two labeled RoR for the rest of the repository (i.e. the other nine waste panels.)

Biodegradation proceeds only in the presence of brine. Performance assessment conservatively assumes that waste containers do not impede brine flow into the containers, thus allowing brine immediate access to the CPR in the waste. BRAGFLO represents gas generation as a zero-order reaction, meaning that the reaction rate is constant regardless of CPR concentration. If circumstances were such that brine could access all CPR in the waste instantly, a first order reaction would be a more appropriate representation of the chemistry. However, because of the low porosity of the supercompacted waste, brine is not expected to have access to the entire CPR inventory at any one time. Therefore, a zero-order reaction is appropriate for both supercompacted and standard waste. Such a system would be characterized by brine gaining access to successive amounts of CPR in the waste over time as the waste degrades and allows brine to contact more of the CPR. In the zero-order representation of gas generation reaction, greater amounts of CPR will cause gas generation to proceed for a longer period of time at a constant rate, resulting in more total gas generation in areas of the repository with greater CPR concentration.

### **3.3.2 Heterogeneity in Iron Concentration**

Iron is a large component of the waste coming to WIPP. Iron corrosion is important to performance assessment since corrosion is assumed to consume brine and generate gas in all realizations (vectors). The performance assessment assumes that iron is uniformly distributed throughout the repository. There are waste streams that contain higher iron concentrations than the repository average, such as waste streams being packaged in pipe overpacks. However, previous performance assessments have shown that in all vectors, at least 25 percent of the steel remains after 10,000 years, and in most vectors, a larger fraction remains (DOE, 1996; SNL, 1997a). Hence, gas generation due to iron corrosion is limited by the availability of brine rather than the inventory of iron. For this reason, there is little justification for considering scenarios where the iron is distributed non-uniformly. A non-uniform distribution of iron could not increase the total amount of gas produced. Consequently, this analysis does not include a scenario with non-uniform iron distribution.

### **3.4 Waste Permeability**

Waste permeability is an important parameter in the models for brine and gas flow in the repository, and in the models for spillings and direct brine releases. Performance assessment defines waste permeability at the scale of a room or panel, rather than at the scale of an individual waste package. The likely mechanical and physical form of the supercompacted and pipe overpack waste packages over time indicates that the permeability of a room containing these waste forms will be at least as great as that of a room containing standard waste, and may be higher. In addition, previous studies of waste heterogeneity (Hansen et al, 1997) indicate that higher permeability tends to reduce pore pressure gradients near an intruded borehole, therefore reducing spall volumes. Therefore, in the case of human intrusion, a modeling assumption of a homogeneous medium with a constant permeability ( $2.4 \times 10^{-13} \text{ m}^2$ , as used in the PAVT) is conservative with respect to the effects on brine and gas flow, and remains appropriate for this analysis. This section first reviews the waste permeability used in the CCA and PAVT, then provides analysis supporting the conclusions stated above.

#### **3.4.1 Waste Permeability in the CCA and PAVT**

In the CCA the waste permeability was assigned a value of  $1.7 \times 10^{-13} \text{ m}^2$  (Butcher, 1996) based on the value used in the 1991 PA (WIPP PA, 1991). The 1991 PA value was a composite value based on the relative quantities of three different types of materials (combustible, metals/glass, and sludges) each with an inherent range of permeabilities, which had previously been determined for compressed surrogate wastes (Luker et al., 1990). In their review of the data used in the CCA, the EPA recalculated this value as  $2.4 \times 10^{-13} \text{ m}^2$ , although they conceded that the difference was small enough to be inconsequential (EPA, 1998e). This revised value was used in the PAVT calculations.

A constant value for permeability was used in performance assessment even though some variability in this parameter should be expected. A constant value was found to be acceptable (EPA, 1998e) primarily because this permeability value is much higher than the surrounding salt and DRZ, as discussed in WIPP PA (1991). In addition, the coefficient of variation for the uncertainty in measured permeabilities is too small to justify treating waste permeability as an uncertain parameter (Rechard et al, 1991.) Finally, Vaughn et al. (1996) examined whether permeability should be a function of porosity, since porosity was treated as a time-varying quantity in BRAGFLO while permeability was a constant. Their analysis concluded that including a dynamic model for permeability had an insignificant effect on waste room conditions (pressure and saturation), and an insignificant effect on resulting releases.

#### **3.4.2 Waste Permeability of the New Waste Forms**

As noted above, the underlying assumption is that pipe overpacks and supercompacted waste packages will be more durable than the original baseline package of the 55-gallon drum. The rigidity of these packages tends to hold the room open and preserve the structural integrity of the waste stack (see Section 3.1.) The disposal of a more rigid waste package would tend to

maintain the open channels between individual drums and packages. Thus, much of the original porosity inherent in the three-dimensional disposal configuration would be preserved. Permeability of this future state of the waste would tend to be high relative to the values implemented in the CCA and PAVT, with flow taking place through channels preserved between the individual packages. This conceptualization is reinforced by the results of the porosity surface calculations, which show that in the absence of gas generation, the long-term porosity of rooms containing supercompacted and pipe overpack wastes is considerably higher than for room containing standard waste (Figure 9) while with high gas generation rates the porosities are essentially the same (Figures 10 through 12.) Because higher values of permeability have been shown to reduce releases (Hansen et al, 1997, summarized below), this analysis uses the constant permeability value used in the PAVT calculation.

### 3.4.3 Effect of Waste Permeability on Direct Releases

Waste permeability can affect the models for spillings and for direct brine releases. A pertinent study of the effects of spatially variable waste permeability was conducted as part of the spalling model investigations reported in Hansen et al. (1997.) Calculations of gas flow through the porous waste regions were conducted to evaluate the influence of model assumptions on the predicted two-phase pressure response of the disposal rooms during a drilling intrusion. Results of the modeling indicated that waste heterogeneity acts to reduce the flow of gas towards the borehole, and as a consequence, spill volumes are reduced. Therefore, the use of a constant permeability is considered conservative for direct release models.

Hansen et al. (1997) considered two models for heterogeneous waste: 1) layered waste, and 2) a random waste. Waste disposed at WIPP is likely to retain a layered configuration, because gravity would cause any brine present to migrate to the floor. Thus, the material in the lower layers would be more degraded relative to material in the upper layers. In this conceptualization, the waste is divided into four regions, each with a different material porosity, brine saturation, and permeability. Waste in the upper regions consisted largely of compressed, relatively undegraded drums and that the lowest region consisted primarily of degradation products similar in character to the surrogate wastes (See Hansen et al., 1997; Hansen et al., 2003). A schematic of the layered models is shown in Figure 17, and details of the layer properties in Table 13.

**Table 14. Description of waste properties for the layered model.**

Layer	Description	Thickness (m)	Permeability (m <sup>2</sup> )
Waste 1 (Upper)	Crushed, relatively undegraded waste drums	0.1	1 x 10 <sup>-12</sup>
Waste 2	Partially degraded, compressed waste	0.55	5 x 10 <sup>-13</sup>
Waste 3	Partially degraded, compressed waste	0.7	5 x 10 <sup>-16</sup>
Waste 4 (Lower)	Largely degraded waste and by-products	0.65	1 x 10 <sup>-16</sup>

Results from the layered model showed that the geometry and properties of the waste can significantly influence pore pressure gradients during depressurization. The influence of a thin layer consisting of the highest assumed values for permeability and porosity was minimal. However it was found that lower permeability layers significantly slowed the depressurization process.

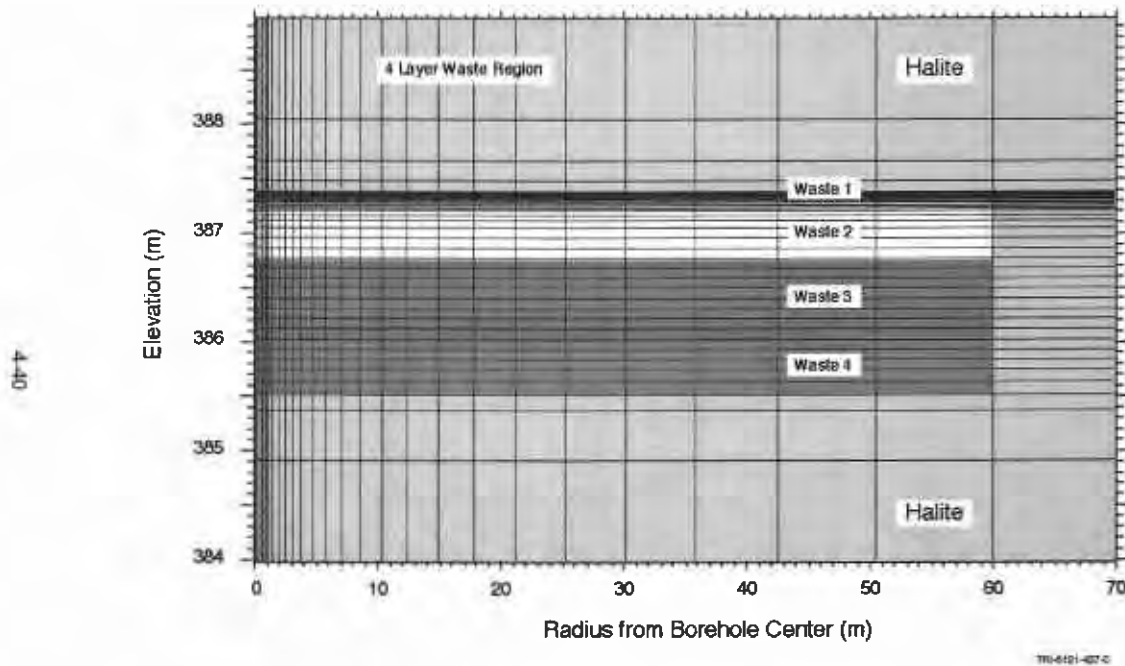


Figure 4-25. Schematic of the layered model.

**Figure 17. Schematic of the layered model (Figure 4-25, Hansen et al., 1997).**

Because of uncertainty with regard to the state of the waste at the time of a drilling intrusion, a random approach also was investigated. Five material types were assumed to exist for the waste, each having a different permeability as shown in Table 14 and Figure 18.

**Table 15. Properties for random waste material types.**

Waste Type	Permeability (m <sup>2</sup> )
Waste 1	1.0E-12
Waste 2	1.0E-13
Waste 3	1.0E-14
Waste 4	1.0E-15
Waste 5	1.0E-16

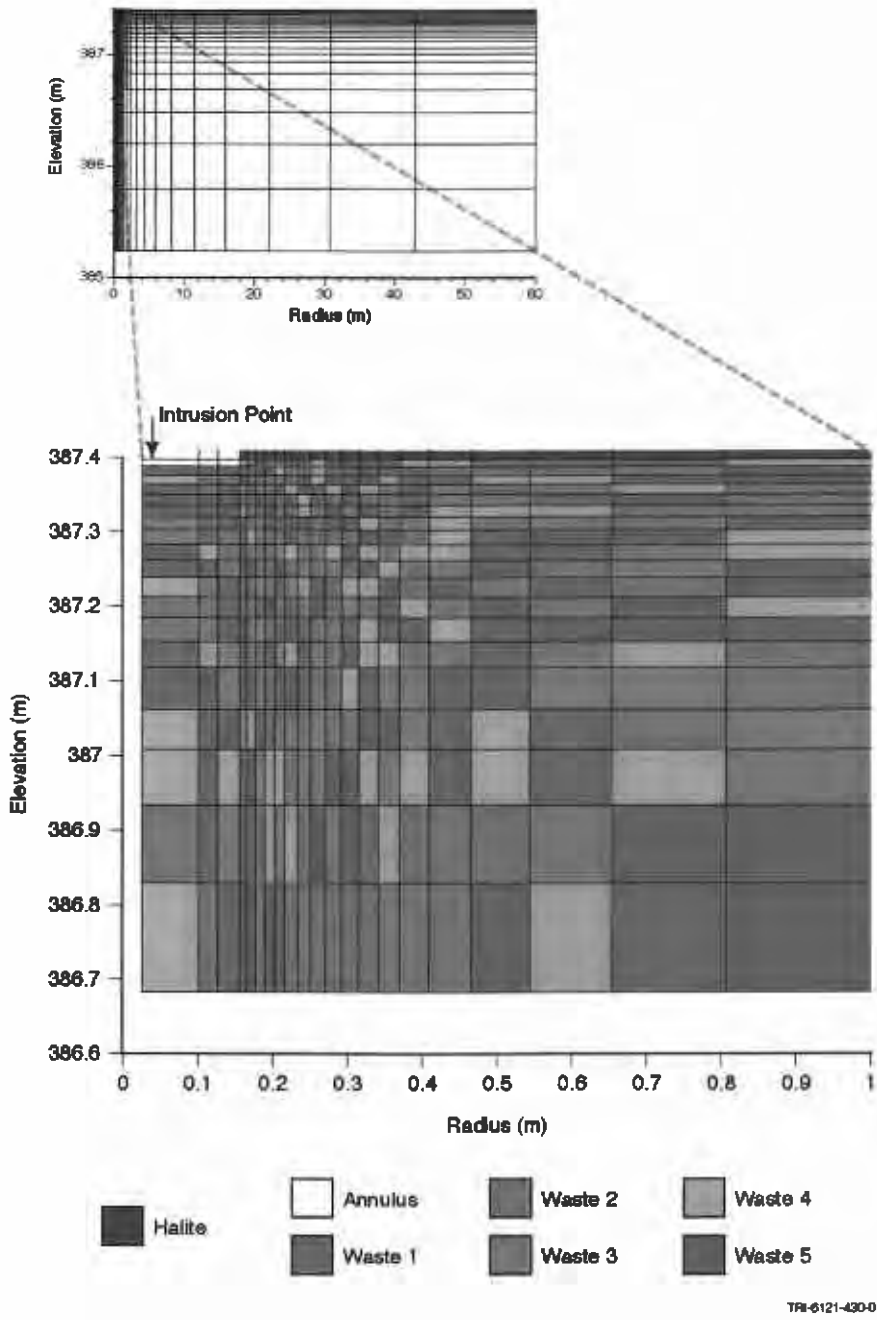


Figure 4-26. Schematic of the random model.

**Figure 18. Schematic of the random model for waste permeability (Figure 4-26, Hansen et al., 1997).**

Gas does not flow readily in the random model because of the absence of large connected zones of high permeability. This result is consistent with results of the layered model. The behavior of the random model is, in fact, similar to that of a homogeneous, low permeability medium (Hansen et al, 1997.)

Results of both the layered and random models therefore indicate that waste heterogeneity will reduce gas flow towards an intrusion borehole, and therefore will reduce estimated spall volumes. In the human intrusion scenario, a modeling assumption of a homogeneous medium is conservative, because the effect of heterogeneous waste permeability is to limit the propagation of high-pressure gradients.

A similar analysis is not available for the effects of heterogeneous waste permeability on direct brine releases. However, the direct brine release model is a single-phase flow model, as is the model used for the calculation of spall volumes outlined above. Therefore, similar conclusions would result from a study of direct brine releases, namely, that using a spatially variable waste permeability would tend to retard flows and thus reduce direct brine release volumes.

### **3.5 Shear and Tensile Strength**

In the performance assessment for the CCA and PAVT, shear and tensile strength were important parameters in the models for cavings and spallings releases, respectively. Supercompacted and pipe overpack waste packages will be less likely to degrade and corrode over time than standard waste forms, and consequently their mechanical shear and tensile strengths may be expected to be equal to or higher than for standard waste. Higher values of shear and tensile strength tend to reduce direct releases by cavings and spallings (Helton et al, Section 9.) Consequently, this analysis makes no changes to these parameters.

#### **3.5.1 Shear Strength**

Shear strength is used in performance assessment to evaluate the volume of cavings released during a human intrusion. In the context of cavings, shear strength is a resistance to shear erosion and is quantified in the laboratory as a critical shear stress. In the CCA, the waste shear strength was sampled from a uniform distribution from 0.05 to 10 Pa, which was conservatively based on properties of marine clays (DOE 1996a, Appendix MASS, Table MASS-1). Sensitivity analyses determined that uncertainty in shear strength was significant in the performance assessment results (Helton et al, 1998, Section 9.)

During review of the CCA, the waste shear strength was estimated by an expert elicitation panel based on particle size distribution (CTAC, 1997), resulting in calculated critical shear strength ranging from 0.64 to 77 Pa. For the PAVT, EPA requested that DOE retain the original lowest value and use a loguniform distribution ranging from 0.05 to 77 Pa. This range of values was conservatively chosen to conform to the extreme case of degradation of waste and waste containers.

Degraded material property estimates were recently summarized for the spallings model peer review (Hansen et al., 2003). The authors assert that degraded waste properties determined for the new spall model represent extreme bounds of the future possible states of the waste. Using 50 percent degraded waste surrogates that represent the extreme possibilities for degradation of the WIPP waste (Hansen et al., 1997, 2003), an average critical shear strength

of 1.4 Pa was determined in laboratory flume experiments (Jepsen et al., 1998.) The minimal critical shear strength could approach this measured value only if degradation of waste occurs without any cementation or compaction during the degradation process. Room closure is almost certain to result in some compaction of degraded waste; however, these strengthening processes are not considered in the range of shear strength determined for surrogate degraded waste. Hansen et al. (2003) conclude that, while a log uniform distribution for this parameter is reasonable, the lower value of 0.05 Pa is overly conservative.

The current minimum value sampled for the waste shear strength is thus at least 30 times smaller than the minimum value supported by empirical data. Therefore, in this analysis shear strength is unchanged from the current values.

### **3.5.2 Tensile Strength**

Tensile strength is used in the calculation of spall volumes following a drilling intrusion. In the CCA, spall volumes were computed by a model of gas flow through fractures. Tensile strength enters the calculation of spall volumes by defining an effective gravity coefficient, which resists particle mobilization in the flowing gas. The CCA calculations used a constant tensile strength of 0.0069 MPa (1 psi) (Helton et al., 1998). In response to EPA's review of the CCA, a mechanistic model for spallings was developed in which gas flow in the waste may induce tensile failure of the waste material, and thus lead to spallings. This mechanistic model (DRSPALL) will serve as the basis for a replacement for the CCA spallings model. DRSPALL is currently undergoing peer review; the spall volumes used in this analysis are based on the CCA model for spall.

In support of DRSPALL, a separate analysis determined a distribution for tensile strength, ranging from 0.12 MPa to 0.17 MPa (Hansen et al., 2003). The range of tensile strength reported assumes that the waste is a weakly consolidated particulate material. The more robust waste forms (supercompacted and pipe overpack waste) would be less susceptible to degradation, so that the tensile strength of masses of these waste forms would certainly be greater than the minimal values proposed for DRSPALL (Hansen et al., 2003), which in turn, is greater than the minimal values used in the CCA model. Hence, any analysis considering tensile strength as a spatially variable property of the waste and accounting for the higher strength of the supercompacted and pipe overpack waste packages would result in smaller spalling releases. Therefore, the current range of tensile strength is conservative, and this analysis proposes no change to this parameter.

### **3.6 Cuttings and Cavings Releases**

Cuttings are solid materials removed from the repository by the drill bit during a drilling intrusion. Cavings are additional solid materials eroded from the sides of the borehole by the circulating drilling mud. The cuttings and cavings model used in the CCA and PAVT treated the waste as a homogeneous material by using a constant value for shear strength for each

realization. As explained in Section 3.5.1, this analysis continues to use the PAVT values for shear strength.

The performance assessment computes releases by cuttings and cavings by combining the volume of material removed from the repository with the radioactivity in the waste. In the CCA and PAVT, each borehole was assumed to intersect three 55-gallon drums. The probability of selecting a drum from a given waste stream was equal to the waste stream's emplaced volume divided by the total volume for CH-TRU waste. The radioactivity in the released material was determined by averaging the (time-dependent) radioactivity of the three randomly selected waste streams at the time of intrusion. In effect, the CCA calculation of cuttings and cavings releases accounted for heterogeneity in waste radioactivity but also assumed random placement of the waste (Helton et al., 1998, Sections 9.1 and 9.2.)

Randomness in waste placement can be measured by the degree to which the location of a drum of waste is correlated with the locations of drums from other waste streams. Correlations can be considered separately in the horizontal plane and among the vertical stacks of waste. Consistent with 40 CFR 194 Section 33(a)(2), performance assessment assumes that drilling events can occur at any location of the repository with equal probability. Therefore, drilling locations are not conditioned on the locations of previous intrusions. As a result, any horizontal correlations in waste location are of no consequence.

This analysis will also compute cuttings and cavings releases by assuming random placement of the waste. Releases will be based on a random sample of three waste streams, representing a completely random vertical arrangement of the waste in the repository. The sensitivity analysis in this report will assess the significance of the assumption of random placement to cuttings and cavings releases. Cuttings and cavings releases will be recalculated based on a random sample of a single waste stream, representing a completely correlated vertical arrangement of the waste in the repository. Comparison of the two release calculations will illustrate the importance of the assumption of random waste placement.

### **3.7 Spallings Releases**

Spallings are solid materials blown into the borehole by gas flow through the waste at the time of a drilling intrusion. Spallings also treat the waste as a mechanically homogeneous material by using parameters such as tensile strength and permeability that are constant for each realization. In the CCA and PAVT, spallings releases were computed by multiplying the volume of material removed by the average radioactivity in the waste at the time of intrusion. Use of the average radioactivity was appropriate, because the maximum spall volume was as large as 4 m<sup>3</sup>, which represents the volume of waste contained in as many as 19 drums. The average radioactivity in 19 randomly selected waste streams would approximate the average radioactivity in all waste streams. Thus, the spallings model for the CCA incorporated the assumption of random placement of waste, albeit on a larger size scale than for cuttings and cavings (Helton et al., 1998, Sections 9.3 and 9.4.)

This analysis will compute spallings releases by using the average radioactivity in the waste. In addition, to evaluate the significance of heterogeneity in waste radioactivity and spatial placement, this analysis will also compute spallings releases by using the radioactivity in waste streams selected for cuttings and cavings releases. Comparison of the two spallings release calculations will illustrate the effect on spallings releases of heterogeneity in waste stream radioactivity, and of random placement in the repository.

### **3.8 Stuck Pipe and Gas Erosion**

This analysis uses the spall model employed in the PAVT, which is a simplification of the spall model used for the CCA. In the CCA model, spall could occur by one of three mechanisms: blowout; stuck pipe; and gas erosion. Only the blowout mechanism was used in the CCA calculations; the other two mechanisms were screened out of the calculations based on the value selected for waste permeability. These models continue to be screened out for this analysis, based on the following justification.

Regarding supercompacted waste, EPA has stated (EPA, 2003a, See Table 1):

*It is unclear from the discussion if the super compacted waste will have porosity and permeability characteristics that may influence the “stuck pipe” and “gas erosion” mechanisms considered in the original certification. Your analysis should clearly demonstrate that, if true, this new waste form does not affect such assumptions in the original certification.*

Gas flow-induced releases from stuck pipe or gas erosion mechanisms can only occur at low permeability, conditions which are less likely for supercompacted and pipe overpack waste forms than for standard waste. As discussed in Sections 3.4 and 3.5, supercompacted and pipe overpack waste packages will have higher permeability and greater strength than will the compacted, degraded standard waste. Stuck pipe and gas erosion, therefore, are less likely to occur for these wastes than for standard wastes.

According to Berglund (1994), stuck pipe occurs when “...low permeability waste ... is pressed against the drill string sufficiently hard to prevent normal drilling. This occurs at high gas pressures.” Gas erosion occurs when “low permeability waste ... is pressed against the drillstring due to stresses from escaping decomposition gas and is eroded by the flowing drilling mud” (DOE, 1996, Appendix CUTTINGS\_S, Appendix A). Both mechanisms are a consequence of movement of the repository material into the wellbore under conditions when the gas flux is too small to displace the drilling mud and loft solid material to the surface in a gas blowout. The conditions under which these mechanisms could occur require a waste permeability less than  $10^{-16}$  m<sup>2</sup> (Berglund, 1994). This permeability threshold is defined as the lower permeability limit for a detectable gas blowout to occur, and is based on simplified calculations of the gas (hydrogen) flow rates adjacent to the repository. Berglund (1994) postulates that stuck pipe will occur at higher gas pressures (>10 MPa), with gas erosion at lower pressures (8 – 10 MPa) when the frictional force of the repository material is too small to be detected as a potential stuck pipe situation. In both cases a prerequisite for the

mechanism is failure of the repository material adjacent to the borehole that will allow the waste to deform sufficiently to impinge on the drill string. Berglund calculates the potential release volumes of these mechanisms from the mud flow rates, and either the drilling time between intersection of the repository and reaching the casing point (for gas erosion), or the cleanout duration (for stuck pipe).

In the CCA neither of these mechanisms was discussed, since the assigned waste permeability of  $1.7 \times 10^{-13} \text{ m}^2$  was 3 orders of magnitude greater than the threshold value. As discussed in Section 3.4.1, this waste permeability is based on the relative quantities of three different types of materials (combustible, metals/glass, and sludges) each with an inherent range of permeabilities, which had previously been determined for compressed surrogate wastes. In responding to comments that questioned the threshold permeability, EPA concluded that

*“...based on information in Hansen, et al. 1997 ... it can be inferred that, since spalling does not occur below about  $10^{-15} \text{ m}^2$ , this permeability represents the upper threshold for stuck pipe/gas erosion.” (EPA, 1998f).*

However, EPA also reviewed the waste permeability under the gas pressure conditions needed for these mechanisms, stating that:

*“(I)t can be seen from Figures PORSURF-3 and -4 that a porosity of about 0.5 is consistent with a gas pressure of 8 MPa – the threshold pressure for gas erosion. At this pressure one can estimate from the Kozeny-Carmen equation above that the permeability for a porosity of 0.5 is about  $7 \times 10^{-14} \text{ m}^2$ . At higher gas pressures the porosity is higher.”*

As a result, they concluded that:

*“EPA believes that the distinction between  $10^{-15}$  and  $10^{-16}$  as the permeability threshold is not important because, as argued above, the contemporaneous occurrence of the pressure and permeability thresholds for stuck pipe/gas erosion is extremely unlikely at either permeability.”*

Similar arguments can be made for the supercompacted waste. In Section 3.1 it was shown that, in the absence of gas generation, porosities for a room containing supercompacted waste would be higher than for a room filled with standard wastes. When gas generation was considered, porosities for a room containing supercompacted waste were similar to or slightly higher than those for standard waste. Thus, for pressure conditions under which stuck pipe or gas erosion might occur, the permeabilities would be high enough to prevent these mechanisms.

In addition, the physical nature of the supercompacted waste will also mitigate releases by the stuck pipe or gas erosion mechanisms. This waste will retain some amount of unfilled void (Figure 5), and some portion of this void may be expected to persist throughout the regulatory period. Under higher gas pressures, a drilling intrusion will lead to flow of gas

predominantly through these channels between and around the pucks, and between drum contact surfaces, and the effective permeability of these channels may be expected to be high (see Section 3.4.2.) The lower permeabilities of the compacted waste pucks will not affect the overall flow of gas, and so will not influence the occurrence of a blowout condition.

It also should be noted that the compacted nature of the pucks might be expected to lead to a reduced potential for degradation and corrosion, and to a somewhat higher tensile strength (Section 3.5.2). This will also make conditions for releases by stuck pipe less likely, since tensile failure, a precondition for stuck pipe releases, will be less likely to occur.

### **3.9 Direct Brine Releases**

Direct brine releases (DBR) are volumes of contaminated brine that may flow from the waste into a borehole during and immediately after a drilling intrusion. Direct brine releases are computed by first calculating a volume of brine that may flow into the borehole, then multiplying by the activity of radionuclides in the brine, either dissolved or sorbed to colloids. The calculation of DBR volumes assumes that the waste is homogeneous by using parameters such as permeability that are constant for each realization. As explained in Section 3.4, this analysis proposes no change to waste permeability.

The concentration of radionuclides in brine is uniform throughout the repository, reflecting an assumption that brine within the waste is well-mixed. This assumption was justified during the review of the CCA (EPA, 1997); the justification (presented below) is not challenged by the presence or properties of the supercompacted or pipe overpack wastes. Therefore, this analysis does not make changes to the DBR calculations.

Radionuclides are mobilized in brine either as dissolved ions or by sorption to colloids. Calculation of mobilized radionuclide concentrations was based on the solubility of radionuclides in the brine present in the repository. For each realization, a constant value for solubility was computed by assuming that the waste was a chemically homogeneous material at thermodynamic equilibrium. As stated in the CCA:

*“Thermodynamic equilibrium is assumed for dissolved actinide concentrations, but oxidation-reduction reactions between the actinides and other waste components are not assumed to proceed to equilibrium. Although materials in the waste will actually dissolve at different rates, the presumption of homogeneity and solubility equilibrium, along with assumed disequilibrium reduction-oxidation conditions, yields the largest reasonable concentration of aqueous actinides in the repository.”* (DOE 1996a Section 6.4.3.4)

The use of a constant solubility was judged as appropriate given that direct brine releases did not occur unless the waste panel was saturated with brine. In the simulation of two-phase flow, brine enters the waste panel by drainage from the overlying disturbed rock zone (DRZ), long-term flow from anhydrite interbeds, and through boreholes from earlier intrusions. In any case, brine must flow through the waste and backfill before it reaches the location of the

intrusion borehole, and thus must have contacted a large volume of waste for a relatively long period of time. It is reasonable to assume that the brine would have achieved chemical conditions representative of brine within a large and well-mixed volume of waste.

### 3.10 Summary of Model and Parameter Changes

In summary, this section presents analyses of the possible changes to waste representation in process models to account for the mechanical and hydrologic properties of supercompacted and pipe overpack wastes, and to represent heterogeneity in the waste materials. Table 15 summarizes the results of the analyses.

**Table 16. Representation of supercompacted waste and waste heterogeneity.**

<b>Model or Parameter</b>	<b>Changes (if any)</b>
Waste Porosity	Implement uncertain parameter for selecting porosity surfaces for waste-filled regions; sample from bounding cases.
Radionuclide Solubility	Chemistry of new waste is consistent with current calculation of solubilities. No changes due to supercompacted waste.
Anoxic Corrosion and Radiolysis	Chemistry of new waste is consistent with current models. No changes due to supercompacted waste.
Gas Generation Models	Implement uncertain parameter representing CPR concentration in waste-filled regions.
Waste Permeability	New waste forms likely have higher permeability on a room scale than the standard waste forms. Performance assessment conservatively uses the PAVT value.
Waste Shear Strength	Current range of shear strength is extremely conservative for all waste forms. Performance assessment conservatively uses the PAVT value.
Waste Tensile Strength	Current range of tensile strength is extremely conservative for all waste forms. Performance assessment conservatively uses the PAVT value.
Cuttings and Cavings	No changes to model are warranted. Sensitivity analysis will examine significance of random placement assumption.
Spallings	No changes to the model are warranted; waste permeabilities remain high enough to rule out stuck pipe and gas erosion mechanisms for the high gas pressures required for these mechanisms. Sensitivity analysis will examine significance of assumption of random placement.
Direct Brine Release	No changes to the model are warranted; assumption of well-mixed brine is still valid.

## 4 Results of Performance Assessment

This section presents the results of the performance assessment (referred to as the AMW calculation) and discusses the effects of heterogeneous waste representation. Results for two-phase flow in and around the repository are summarized for both undisturbed and disturbed scenarios, followed by results for repository performance. The results of the AMW calculation are compared to results from a performance assessment calculation undertaken in support of DOE's Compliance Recertification Application (referred to as the CRA1 calculation.) The CRA1 calculation uses the same models and waste inventory as the AMW calculation, but represents the waste as a homogeneous material as was done in the CCA.

### 4.1 Execution of the Performance Assessment

The AMW calculation was executed with the codes versions and parameter baseline being used in the calculation for the re-certification of the WIPP. All codes were run using the WIPP performance assessment run control system, and the scripts and input and output files are retained in the Code Management System (CMS) libraries for the AMW calculation, class AMW. Long (2003) provides a record of execution of the AMW calculation. Table 16 lists the versions of major codes used and the CMS libraries containing the code results.

**Table 17. Code versions and CMS libraries for this performance assessment.**

Code	Version	Libraries	Class
LHS	2.41	LIBAMW_LHS	AMW
BRAGFLO	5.00	LIBAMW_BF LIBAMW_BFR1Sy	AMW
PANEL	4.02	LIBAMW_PANEL	AMW
NUTS	2.05A	LIBAMW_NUT LIBAMW_NUTR1Sy	AMW
CUTTINGS_S	5.04A	LIBAMW_CUSP LIBAMW_CUSPR1Sy	AMW
SECOTP2D	1.41B	LIBCRA1_ST2D	CRA1A
EPAUNI	1.15A	LIBCRA1_EPU	CRA1A
CCDFGF	5.00A	LIBAMW_CCGF	AMW

The AMW calculation used the same random seed as replicate 1 of the CRA1 calculation. Use of the same seed ensures that subjectively uncertain parameters common to both calculations will have the same sampled values, facilitating comparison of results between the two analyses.

The inventory used for the AMW and the CRA1 calculations is the updated inventory for WIPP (Lott, 2003a, 2003b). This inventory includes the waste streams from the AMWTP and the waste already emplaced in Panel 1.

## **4.2 Results for Two-Phase Flow in and near the Repository**

The BRAGFLO computer code was used to model the flow of brine and gas in and near the repository for the 10,000-year regulatory period. BRAGFLO results are used to determine the initial conditions for the models computing direct releases, and transport through the Salado to the Culebra and to the Land Withdrawal Boundary. The BRAGFLO output variables most important in calculation of releases are pressure and saturation in the waste filled regions, and brine flow up the borehole to the Culebra.

BRAGFLO is run for six scenarios. While all BRAGFLO results are used in the construction of releases, this analysis examines in detail only the undisturbed scenario (S1 scenario) and the disturbed scenario (S2 scenario) in which a drilling intrusion at 350 years also intersects a brine pocket located below the repository. The S1 scenario illustrates long-term, undisturbed flow processes and is useful for identifying sensitivity of model outputs to uncertain inputs. The S2 scenario was chosen because this scenario results in the greatest amount of brine entering the waste panel from the brine pocket and going up the borehole.

BRAGFLO output is often presented as a “horsetail” plot, which shows a single output variable as a function of time for all 100 vectors in a replicate. The horsetail plot demonstrates the qualitative behavior of the output variable and illustrates the range of uncertainty in the output variable over the 10,000-year regulatory period. Horsetail plots for the AMW calculation are presented side-by-side with the comparable plots from the CRA1 calculation. The CRA1 calculation represents waste as a homogeneous material and applies the porosity surface for the standard waste to all waste-filled regions. This comparison thus illustrates the effects of spatially variable CPR concentrations and of the uncertainty in porosity surfaces.

The variables that are plotted include: volume averaged pressure (WAS\_PRES), brine saturation (WAS\_SATB), and porosity (WAS\_POR) in a single waste panel. For the S2 scenario, brine flow up the borehole at the base of the Culebra (BRNBHRCC) is also examined.

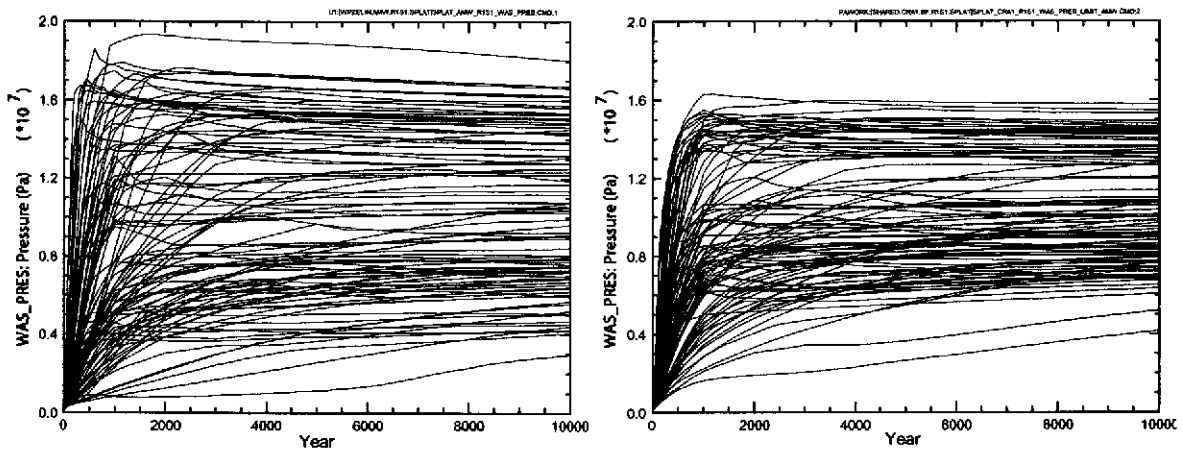
### **4.2.1 Undisturbed Model Results (S1 Scenario)**

Figure 19 compares pressure in a single waste panel for the undisturbed scenario for the AMW and CRA1 calculations. AMW pressures display greater variability over the 100 vectors than CRA1 pressures. That is, the AMW vectors have higher and lower pressures than in the CRA1 calculations. However, Figure 20 demonstrates that the mean pressure as a function of time remains nearly identical for both calculations.

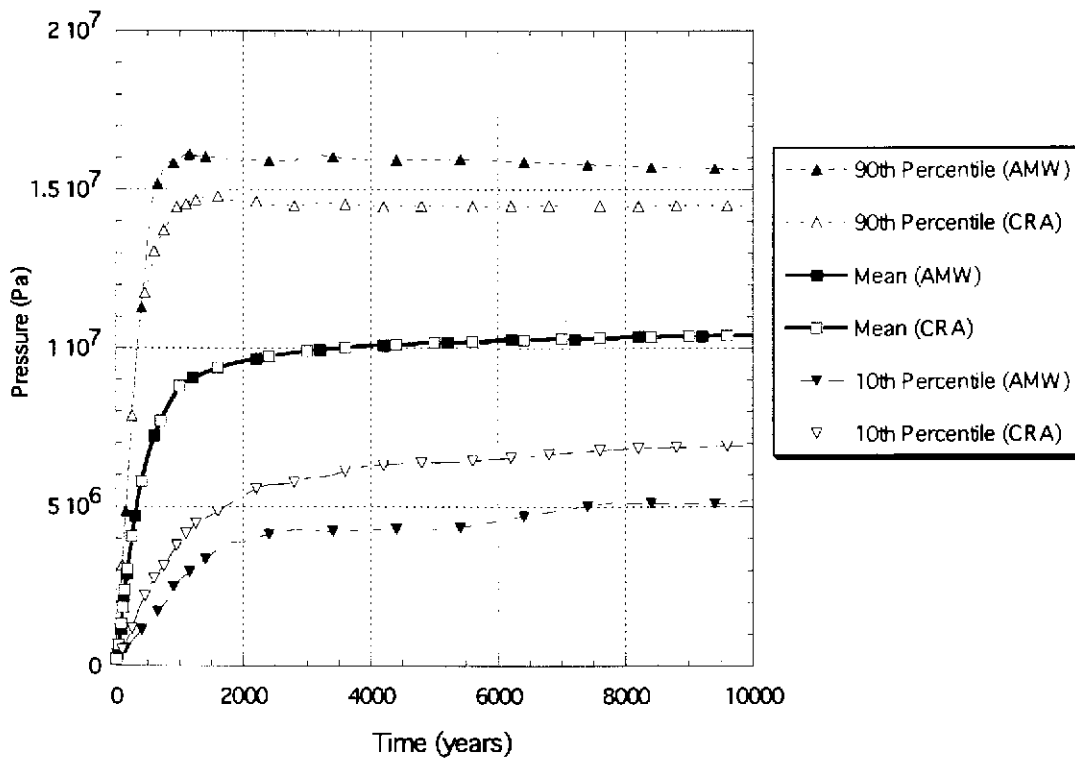
Figure 21 shows brine saturation in the waste panel for both calculations. Although the results vary for individual vectors, the overall range of results is similar.

Figure 22 compares volume-averaged porosity in a waste panel. Porosity in the waste panel in the AMW calculations varies over a greater range than in the CRA1. This difference is expected because of the inclusion of alternate porosity surfaces having greater porosities than

the standard waste model (Section 3.1.6). The highest porosity outlier vector in the AMW calculations is vector 41, which also has the highest pressure (Figure 19.) The pressure in this vector is higher in the AMW calculation than in the CRA1 calculation because the AMW calculation applies the Combined Waste Model (CLOSMOD2 = 2) for porosity to the rest of repository. This closure model results in a significant reduction in the available pore volume in the rest of repository compared to the standard waste model used in the CRA1 calculation; the loss of pore volume tends to increase pressure in all areas of the repository.



**Figure 19. Pressure in the waste panel for the AMW (left) and CRA1 (right) analyses, S1 scenario.**



**Figure 20. Comparison of pressure in the waste panel, S1 scenario.**

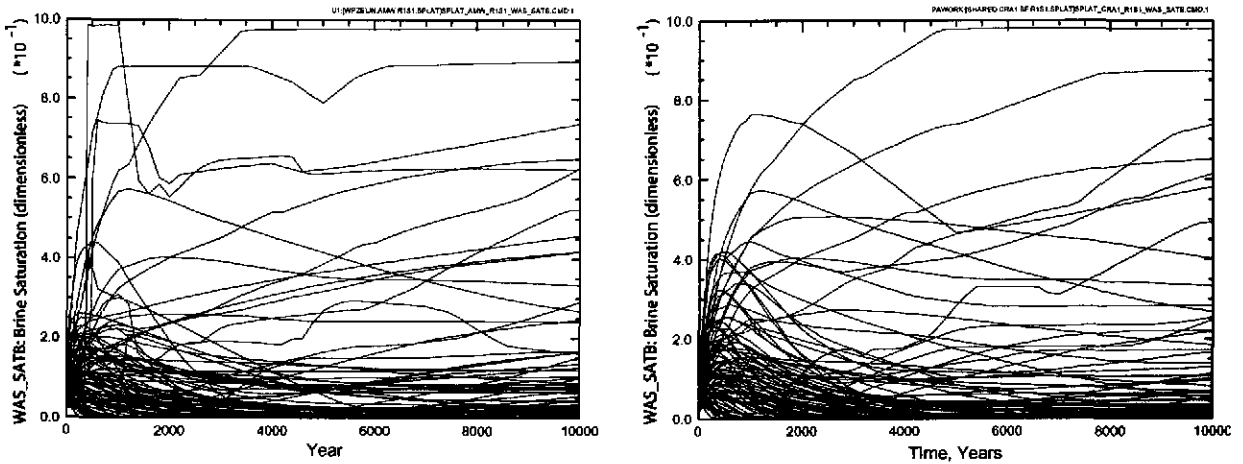


**Figure 21. Brine saturation in the waste panel for the AMW (left) and CRA1 (right) analyses, S1 scenario.**

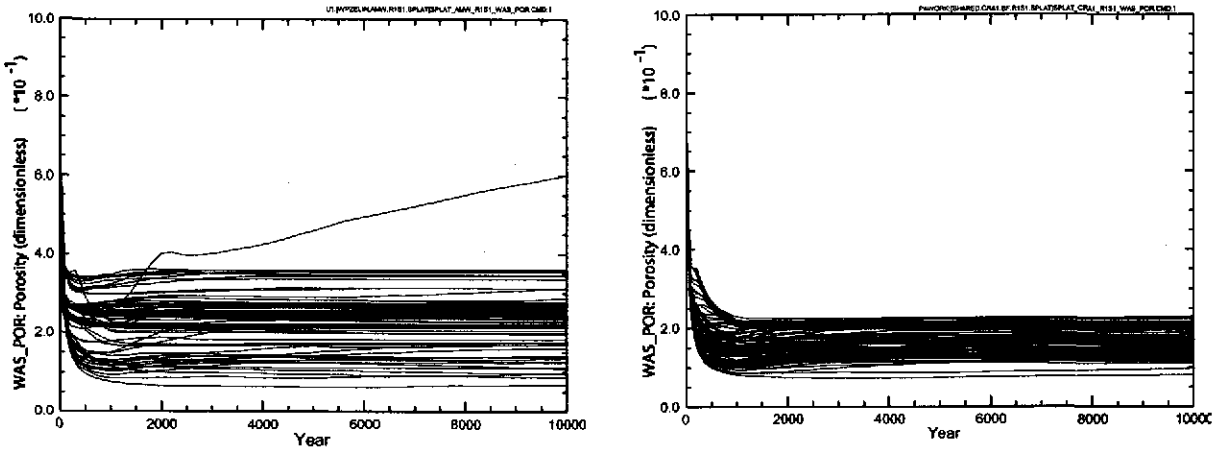
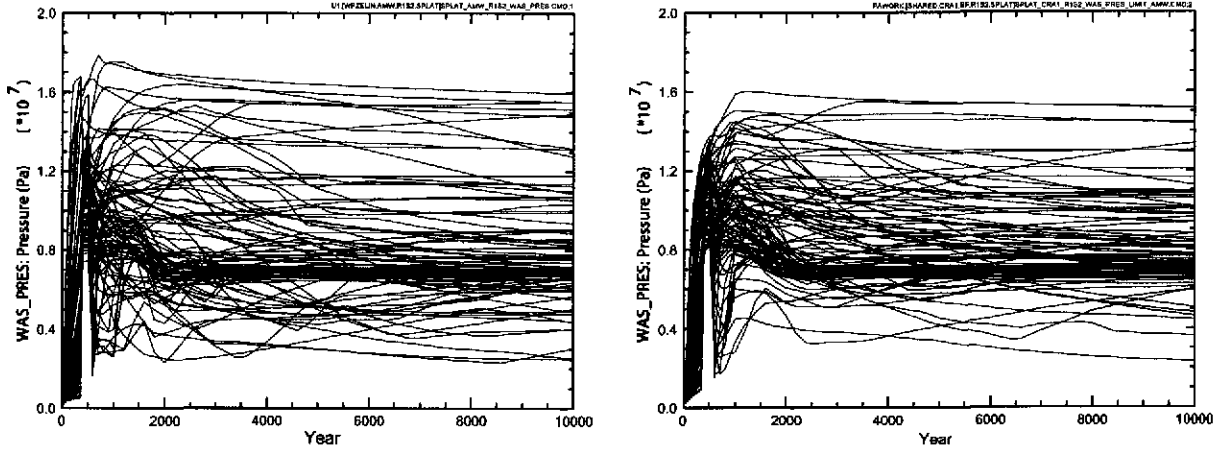


**Figure 22. Porosity in the waste panel for the AMW (left) and CRA1 (right) analyses, S1 scenario.**

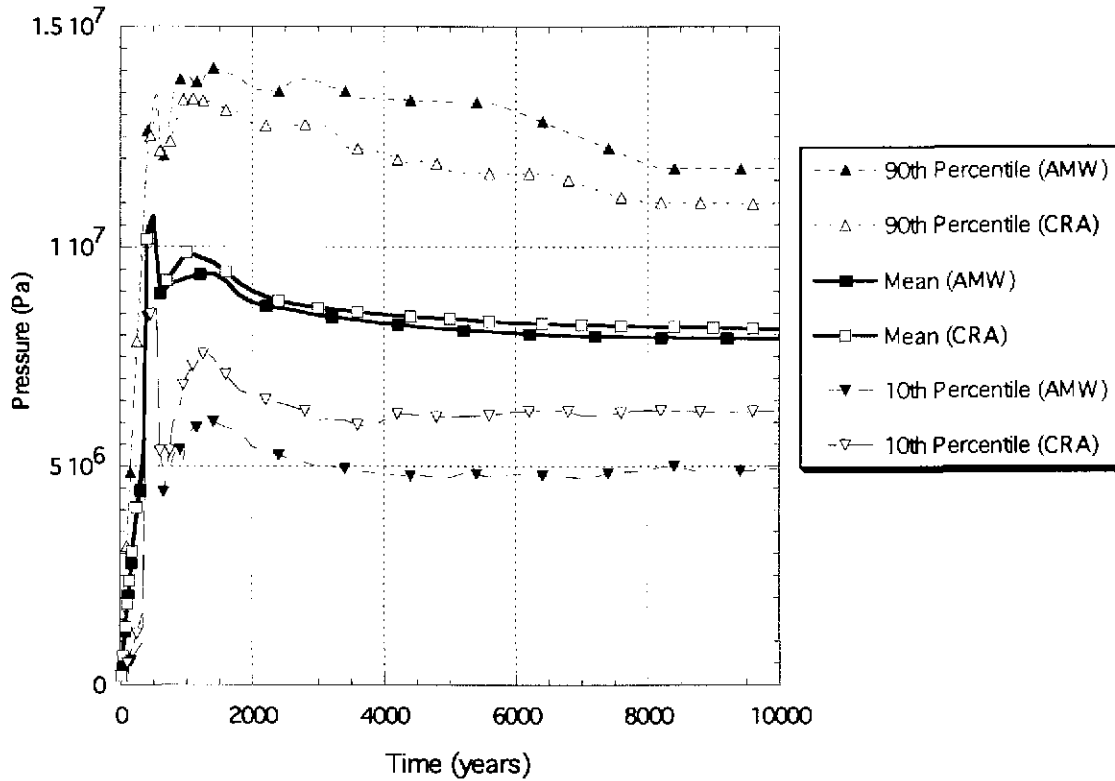
#### 4.2.2 Disturbed Model Results (S2 Scenario)

Figure 23 compares pressure in a single waste panel in the S2 scenario for the AMW and CRA1 calculations. Pressures in the AMW calculation display greater variability than in the CRA1 calculation, although the differences are not as pronounced as in the undisturbed scenario. The mean pressures are very similar for the two calculations (Figure 24).

As in the undisturbed scenario, brine saturation in the waste panel (Figure 25) varies somewhat for each vector between calculations, but the overall range of the results is similar.



**Figure 23. Pressure in the waste panel for the AMW (left) and CRA1 (right) analyses, S2 scenario.**



**Figure 24. Comparison of pressure in the waste panel, S2 scenario.**

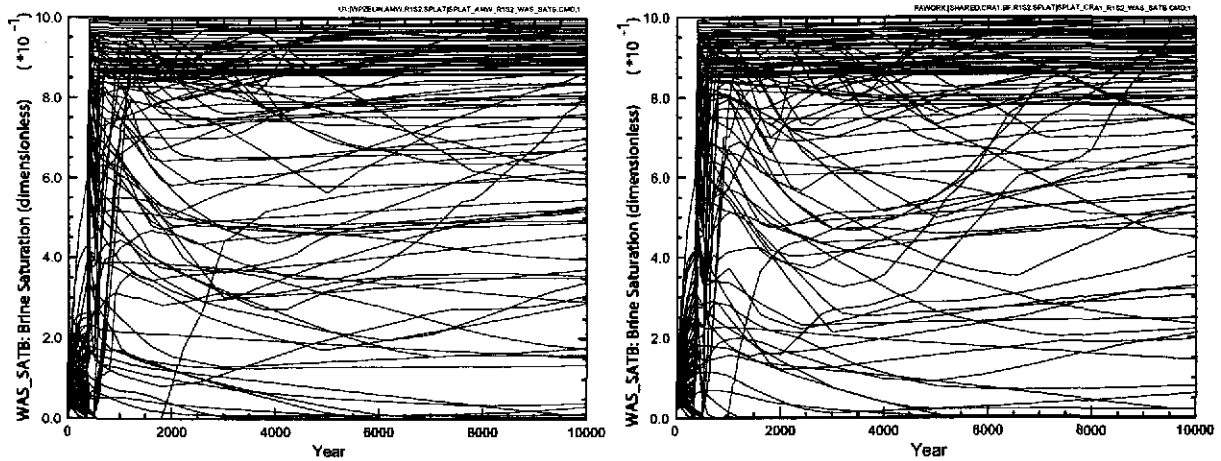


**Figure 25. Brine saturation in the waste panel for the AMW (left) and CRA1 (right) analyses, S2 scenario.**

Figure 26 compares volume-averaged porosity in a waste panel. Porosity in the waste panel for the AMW calculation varies over a greater range than in the CRA1 calculation. The differences in porosity are similar to the undisturbed results.

Cumulative brine flow up the borehole at the base of the Culebra for the S2 scenario is compared in Figure 27. The two plots are similar, with the maximum brine release to the Culebra for the AMW calculation slightly lower than in the CRA1 calculation.

Pressure and brine saturation results have the most direct effect on total releases for the performance assessment. Porosity and brine flow contribute, but are much less important. The differences between the AMW and CRA1 results are minor and are therefore not expected to significantly affect total releases.

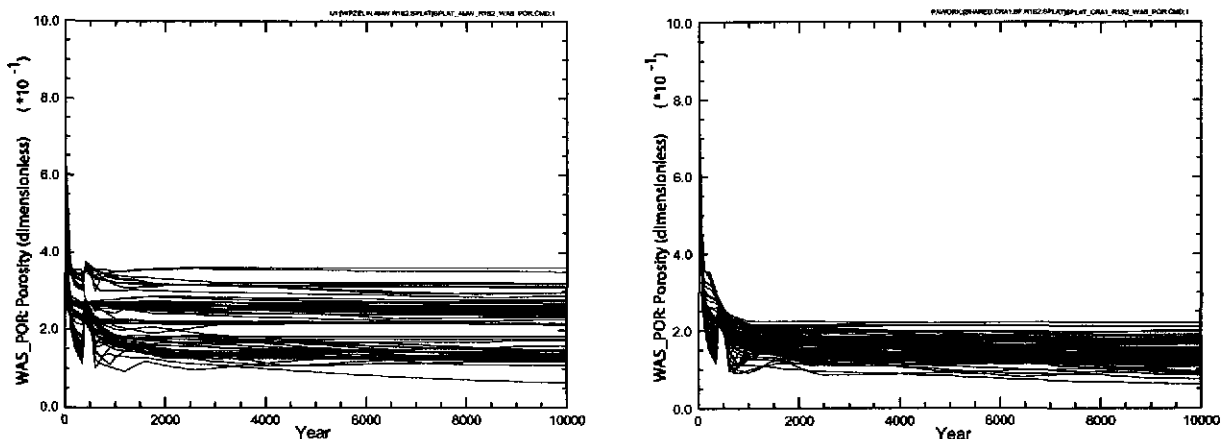


**Figure 26. Porosity in the waste panel for the AMW (left) and CRA1 (right) analyses, S2 scenario.**

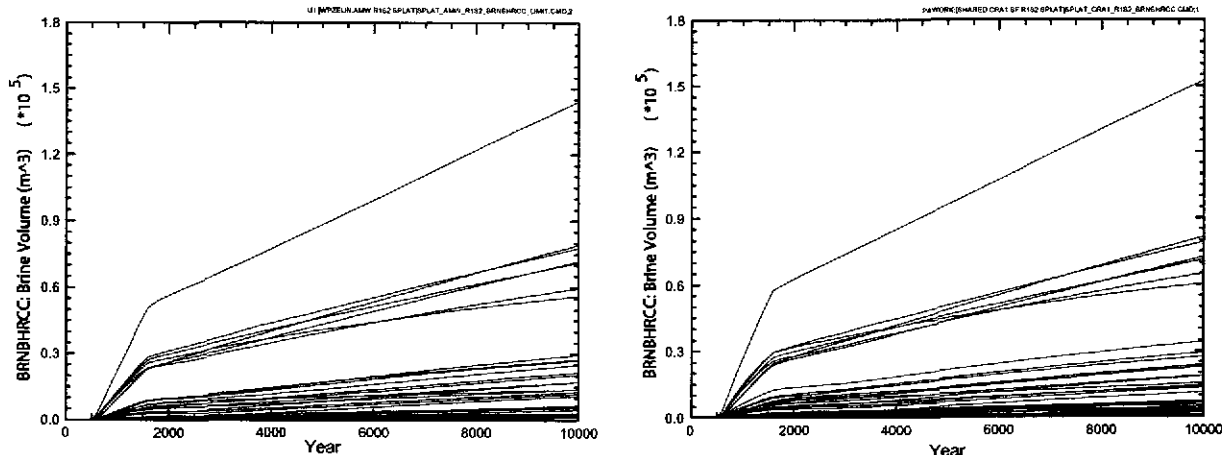


**Figure 27. Brine flow to the Culebra for the AMW (left) and CRA1 (right) analyses, S2 scenario.**

### **4.3 Results for Repository Performance**

Figures 28 and 29 show the CCDFs for total normalized releases from the repository for the AMW and CRA1 calculations. Figure 28 demonstrates compliance with the containment requirements of 40 CFR 191, and answers the first question posed in Section 1.1: what is the expected repository performance when supercompacted waste is explicitly represented in the performance assessment? Comparison of Figures 28 and 29 begins to answer the second question posed in Section 1.1: what is the significance to performance assessment of the representation of supercompacted waste and of waste heterogeneity in general? The similarity between Figures 28 and 29 indicates that the performance assessment results are relatively insensitive to the representation of the supercompacted waste. For all but one realization, total releases in the AMW calculation are very similar to total releases in the CRA1 calculation. In a single realization (vector 22,) direct brine release is different and thus this vector is discussed in greater detail (Section 4.3.2).

Figure 30 compares the mean and 90<sup>th</sup> quantile CCDFs for total releases for both calculations. Figure 30 shows that the total releases are almost statistically identical, reinforcing the conclusion that performance assessment results are not sensitive to the supercompacted waste. Only at very low probabilities ( $\sim 0.001$ ) are the mean releases in the AMW calculation greater by a factor of roughly 2 than those in the CRA1 calculation; the difference in total release is due to the single vector with higher DBR releases in the AMW calculation.

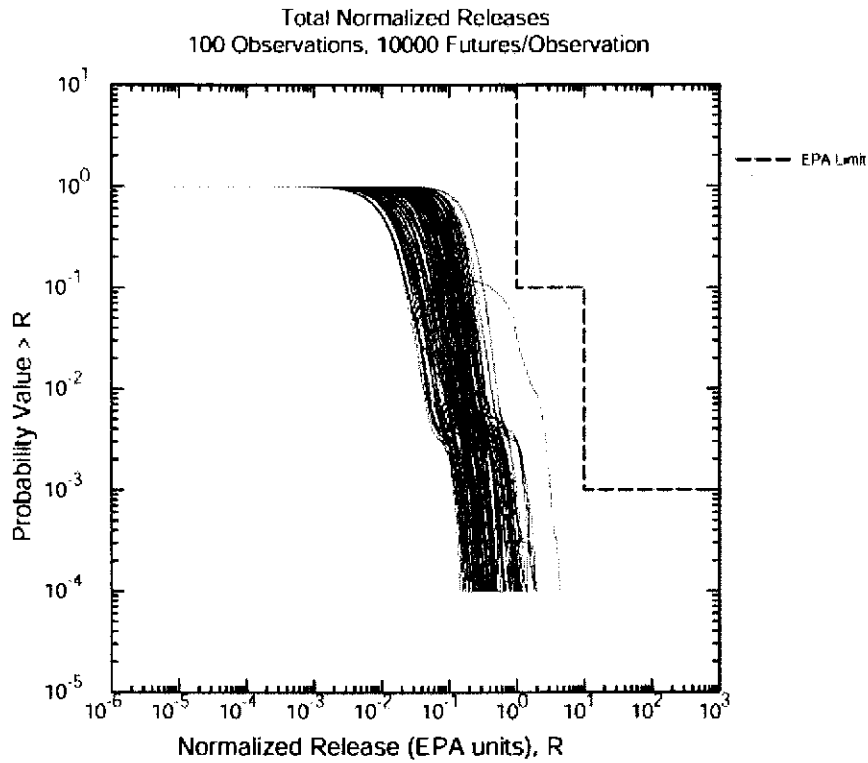


**Figure 28. Total normalized releases, AMW calculation.**

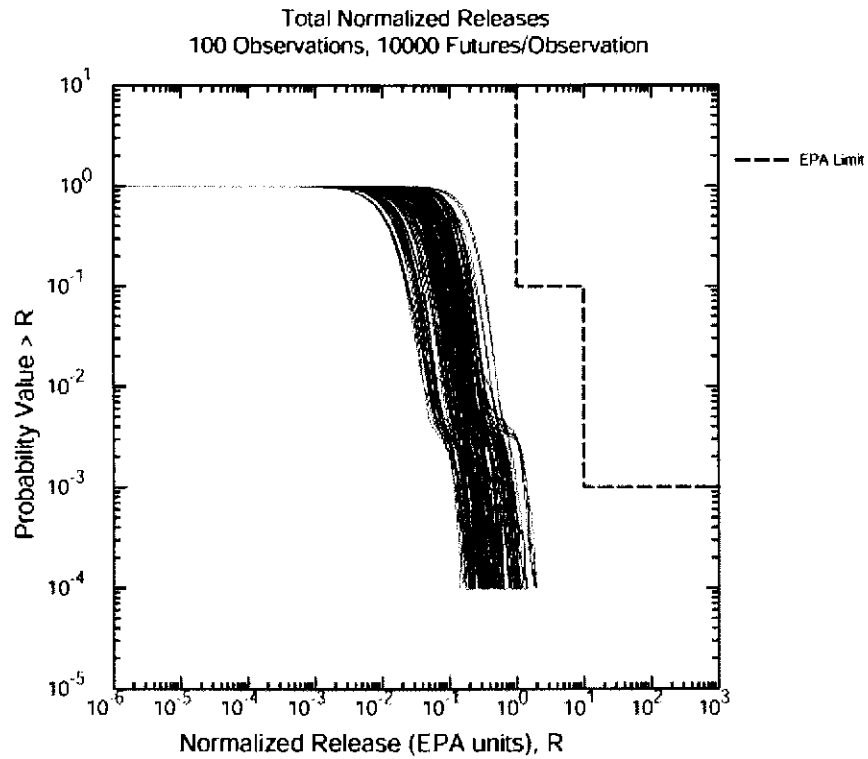


**Figure 29. Total normalized releases, CRA1 calculation.**

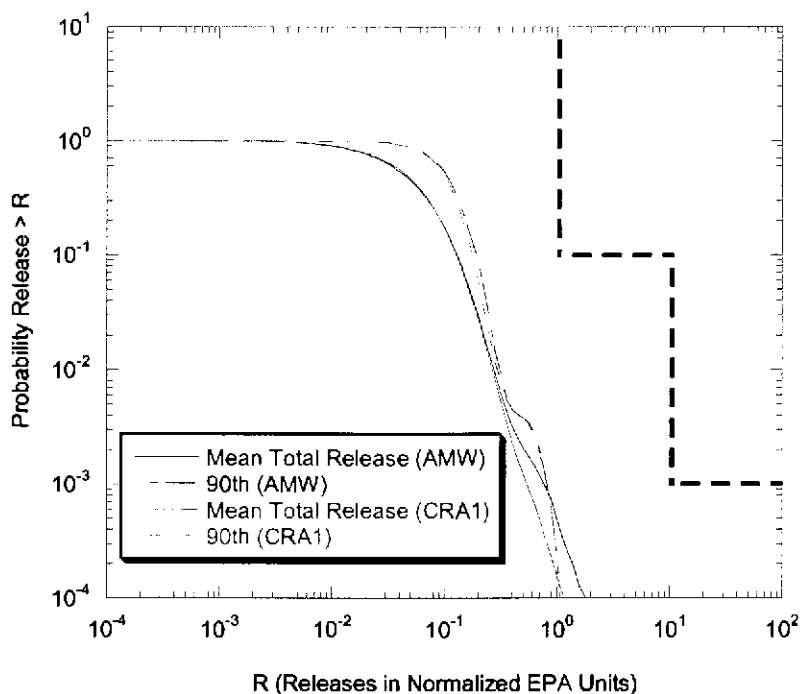


**Figure 30. Comparison of total normalized releases.**

The increase in total releases (in both calculations) at a probability of about 0.003 (Figures 28 and 29) is due to an increase in cuttings and cavings releases (Figure 31), which in turn results from a few waste streams with relatively high radioactivity (Lott, 2003a; 2003b). These waste streams maintain significant radioactivity during the 10,000-year period. For example, a single waste stream (LA-TA-58-48, oil/vermiculate waste from  $^{238}\text{Pu}$  heat source fabrication) has a concentration of radioactivity of 4.05 EPA units/ $\text{m}^3$  at 100 years after repository closure, decaying to 1.95 EPA units/ $\text{m}^3$  after 10,000 years (Fox, 2003.) This waste stream maintains a relatively high activity over time, because it contains higher quantities of longer-lived radioisotopes, principally  $^{239}\text{Pu}$  and  $^{240}\text{Pu}$ . The radioactivity concentrations in this waste stream can lead to cuttings and cavings releases exceeding 1 EPA unit.

The volume of the LA-TA-58-48 waste stream ( $31 \text{ m}^3$ ) implies a probability of  $31/168,500 = 0.00018$  that this waste stream is selected as one of the three waste streams contributing to the cuttings and cavings release for a single intrusion. However, in any future of the repository, roughly six intrusions are expected (Dunagan, 2003), implying that 18 waste streams are selected for cuttings and cavings releases. The mean probability that the LA-TA-58-48 waste stream is selected at least once for cuttings and cavings releases is estimated to be

$$1 - (1 - 0.00018)^{18} = 0.0033$$

thus, the increase in releases at a probability of about 0.003 in Figures 28 and 29.

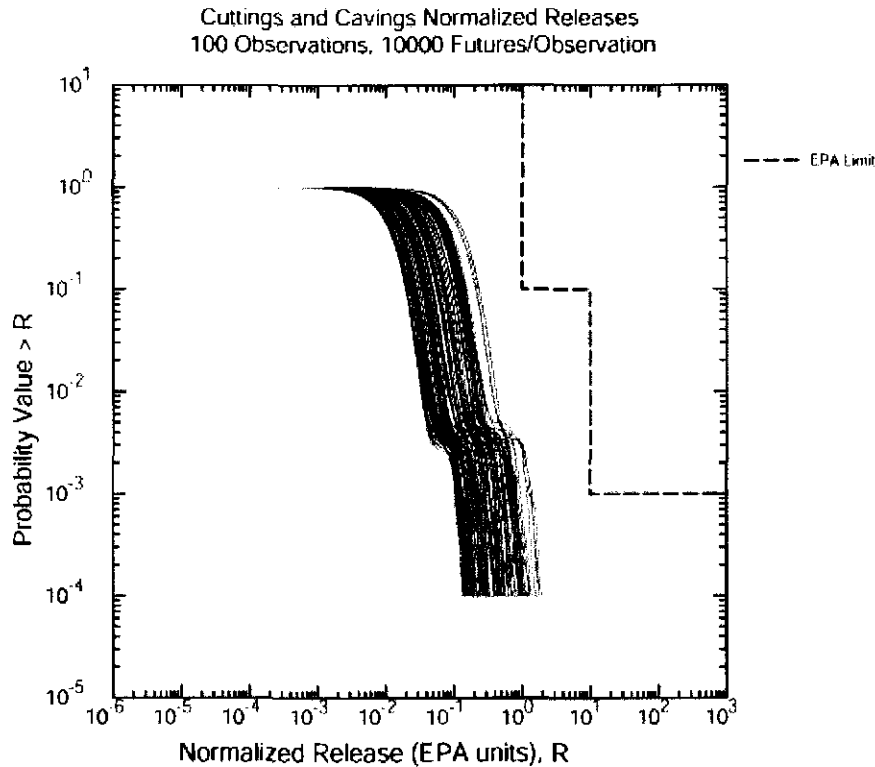


**Figure 31. Cuttings releases for the AMW calculation.**

### 4.3.1 Comparison of Component Releases

Figures 32 and 33 compare mean CCDFs for the components of total releases: cuttings and cavings, spallings, direct brine releases, and releases through the Culebra. In both calculations, cuttings and cavings and spallings combine to account for most of the releases at probabilities above 0.001. The order of importance of the different release mechanisms is similar in both calculations. In the AMW calculation, at a probability of about 0.001, direct brine releases are of the same order of magnitude as cuttings and cavings, due to the single realization (vector 22 as discussed in Section 4.3.2).

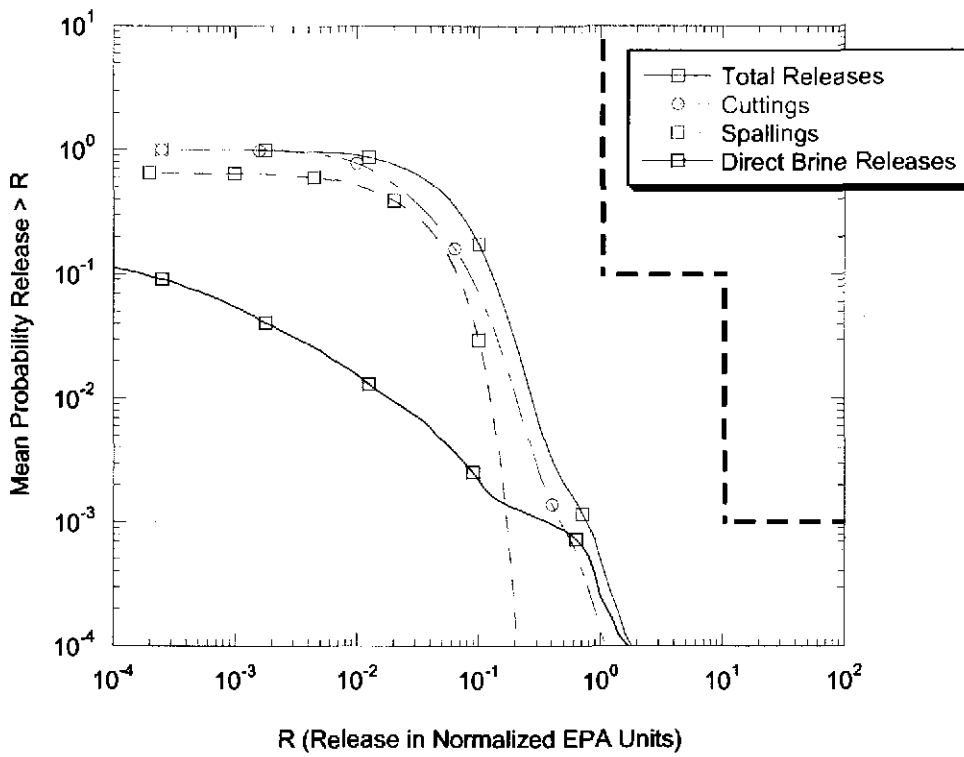


**Figure 32. Mean CCDFs for component releases, AMW calculation.**

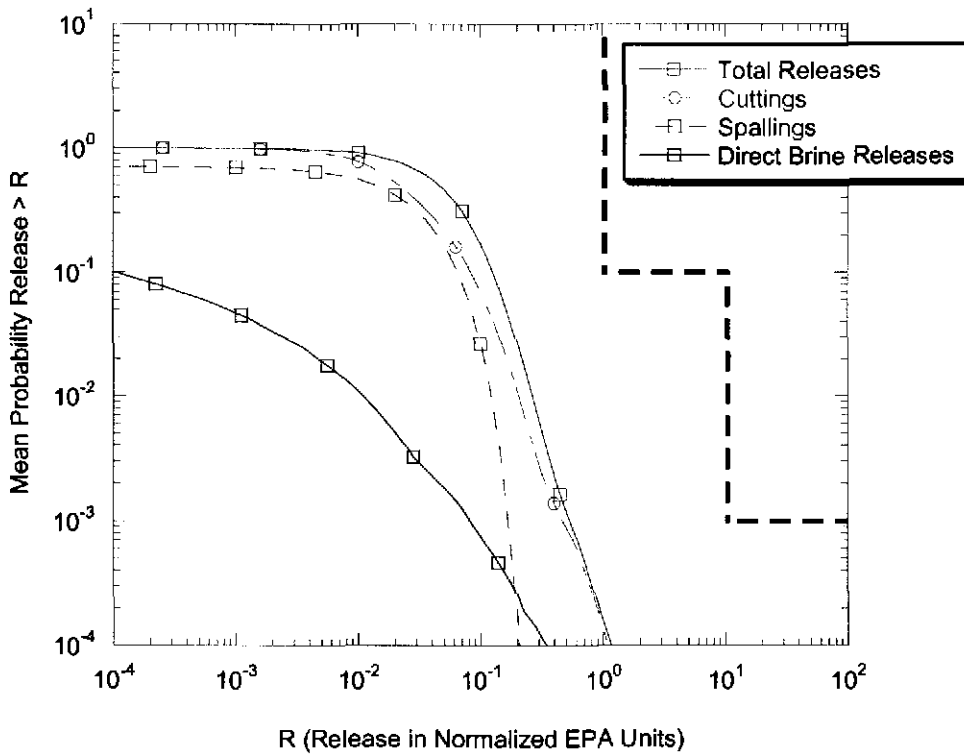
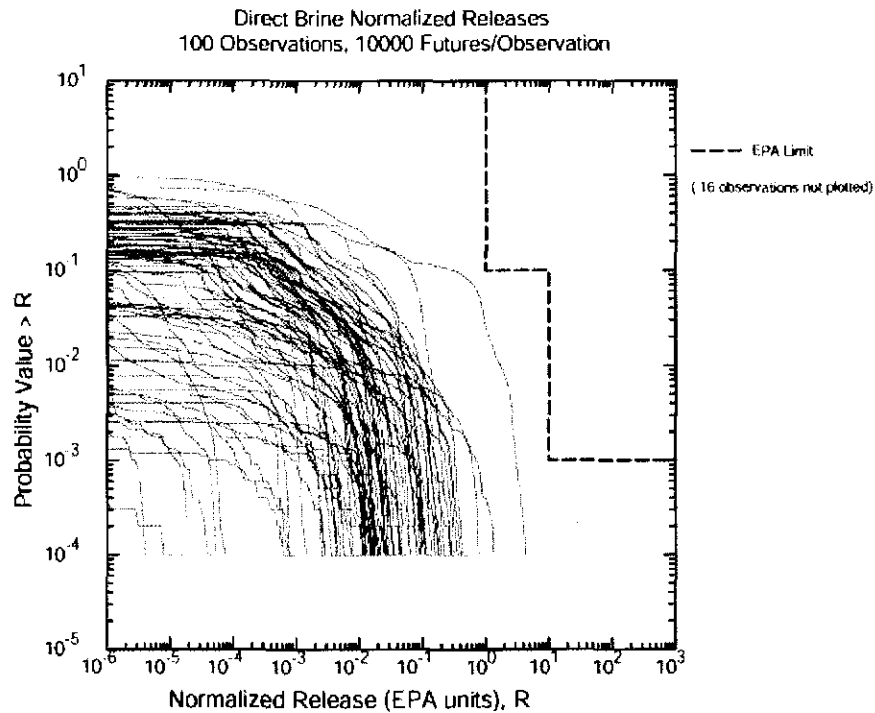


**Figure 33. Mean CCDFs for component releases, CRA1 calculation.**

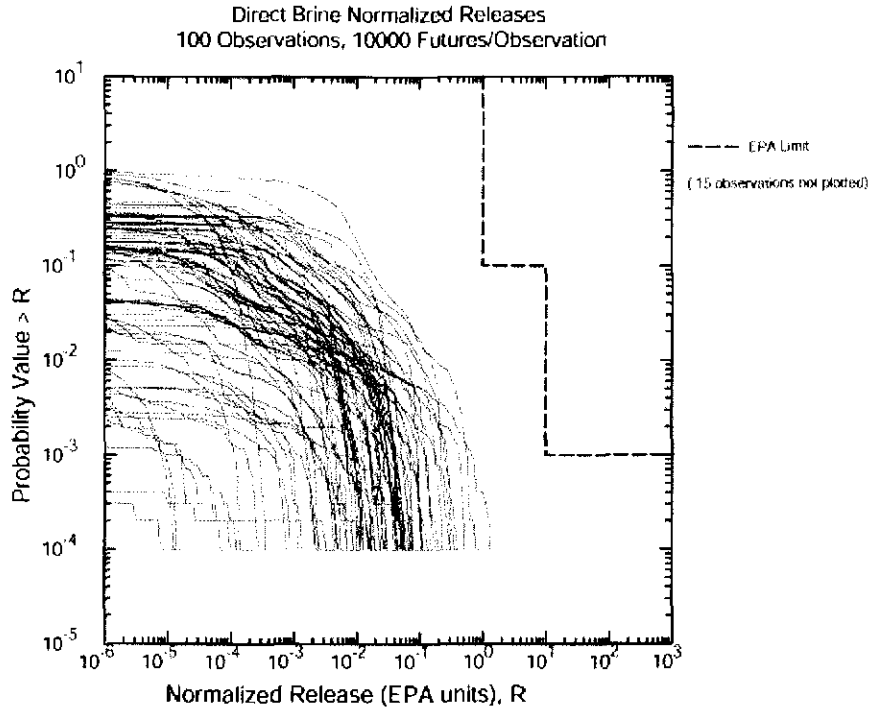
### 4.3.2 Analysis of Direct Brine Releases

Direct brine releases are computed by multiplying the volume of brine released (computed by the code BRAGFLO) by the radioactivity mobilized in brine at the time of the intrusion (computed by the code PANEL). For each realization, direct brine release volumes were computed for 78 separate scenarios varying time of intrusion, drilling location, and times and locations of previous intrusions (see Long, 2003 for details.) The code CCDFGF stochastically generates sequences of drilling intrusions, and uses the BRAGFLO and PANEL results to construct the CCDFs. Figures 34 and 35 show the CCDFs for the AMW and CRA1 calculations of direct brine releases.



09/30/03 06:29:11

Figure 34. DBR releases in the AMW calculation.



06/30/03 18:40:33

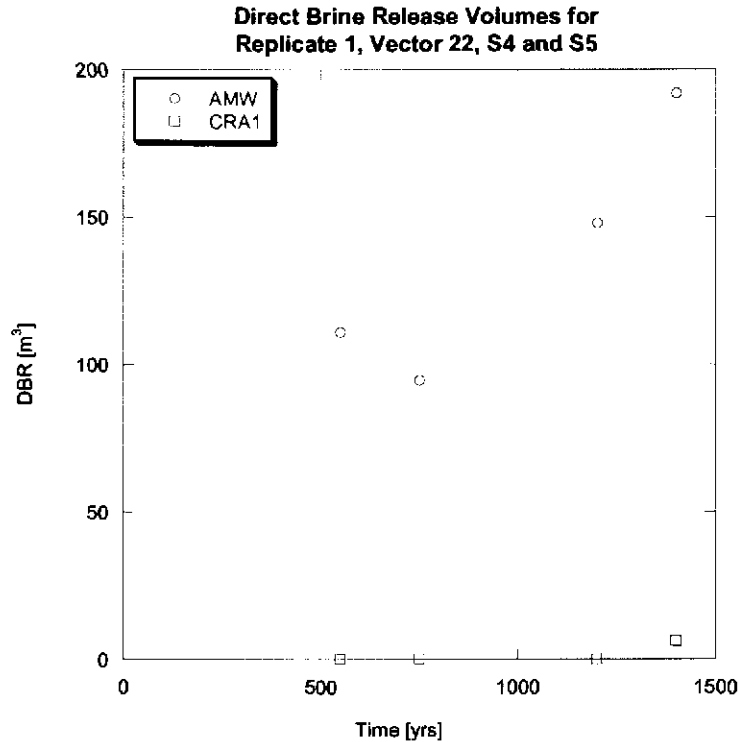
**Figure 35. DBR releases in the CRA1 calculation.**

In Figure 34, the CCDF for vector 22 lies much nearer the EPA limit than the rest of the population of CCDFs. This vector has a larger direct brine release for two reasons:

- (1) Direct brine release volumes for *early* intrusions (before about 1500 years) into the lower waste panel are relatively large due to the combination of porosity surfaces and the values of other hydrological parameters used for this vector.
- (2) The source term for direct releases of Salado brine at *early* times is the greater than that for any other realization.

In vector 22, these two conditions result in significantly larger releases for futures with early intrusions that result in direct releases of Salado brine. This combination of conditions does not occur in other realizations.

Figure 36 shows the direct brine release volumes for vector 22 for the four early intrusions into the lower panel that model the possible release of Salado brine. Direct brine releases volumes are calculated for E2 intrusions at 550 and 750 years (S4 scenario) and for E2 intrusions at 1200 and 1400 years (S5 scenario.) Figure 36 shows that the AMW calculations result in significantly more brine released to the surface than do the CRA1 calculations. Different DBR volumes indicate that pressure and brine saturation in the lower waste panel must be different between the two calculations.



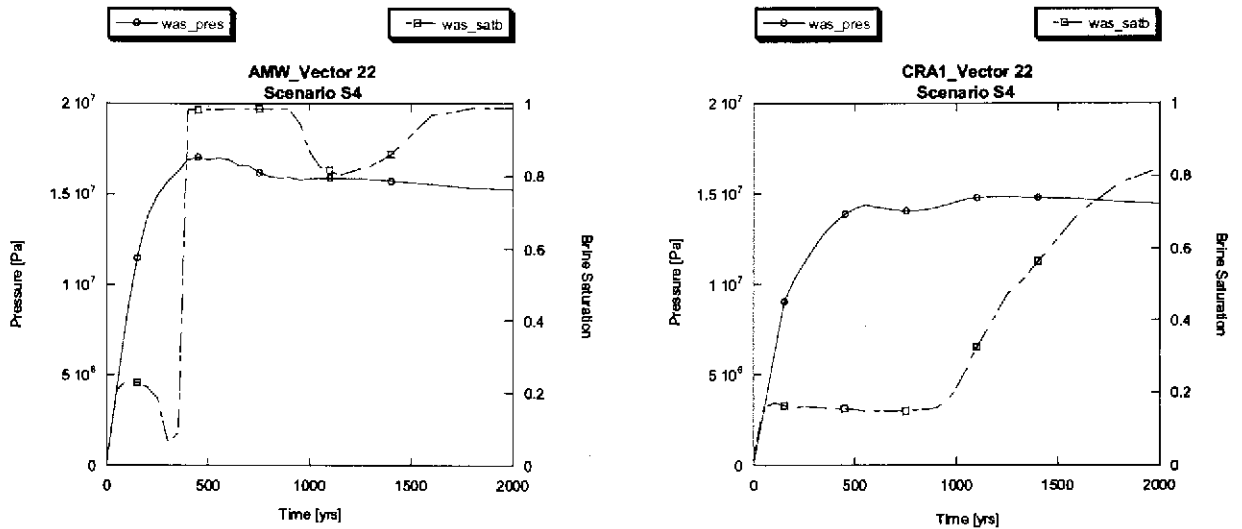
**Figure 36. DBR volumes before 1,500 years for a second intrusion into the lower waste panel (S4 and S5 scenarios.)**

Figure 37 compares the pressure and brine saturation as a function of time between the AMW and CRA1 calculations for the S4 and the S5 scenario. Both pressure and brine saturation are higher at early times in the AMW calculation than in the CRA1 calculation. The only difference between the AMW and CRA1 calculations for this vector is the porosity surface used in the rest of repository. Since FRACAMW is not a significant variable to either pressure or brine saturation (Section 5.1), and since all other uncertain parameters are equal, the differences in pressure and brine saturation are due to this difference in the porosity surface.

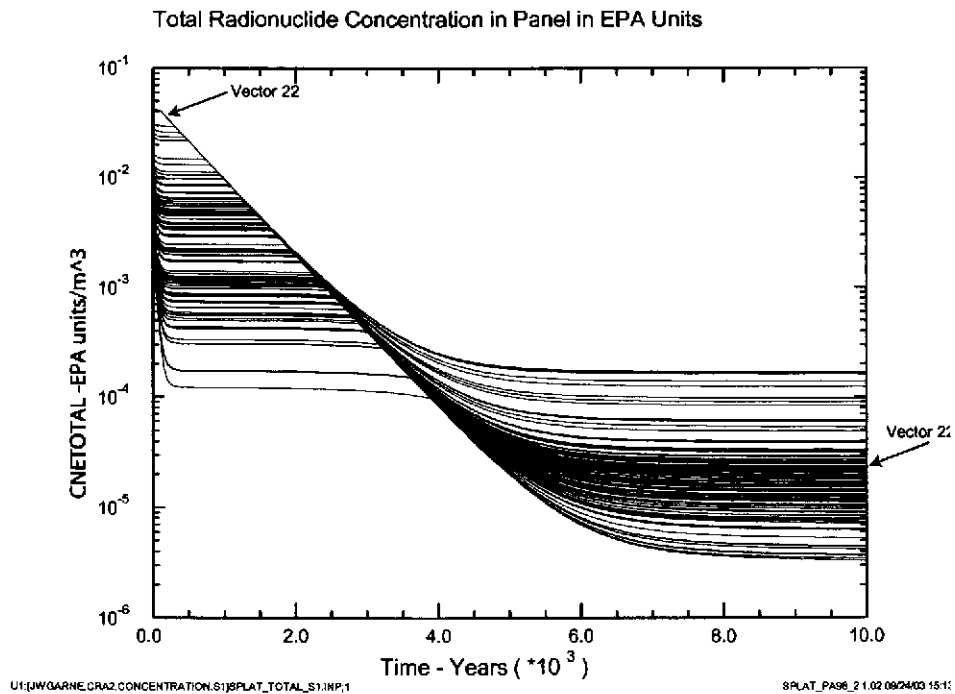
In the AMW calculation, the standard waste model is applied to the waste panel and the combined waste model (2/3 AMWTP waste) to the rest of the repository. The CRA1 calculation uses the standard waste model throughout. In the AMW calculation, the combination of this set of porosity surfaces and the other sampled parameters (e.g., gas generation rate) results in pressures just high enough to fracture the DRZ early in the simulation, increasing DRZ permeability sufficiently to elevate brine inflow rates and thus increase brine saturation. In contrast, the DRZ is not fractured in vector 22 in the CRA1 calculation. The combination of these conditions results in significant direct brine release volumes before 1,500 years.

Figure 38 shows the source term calculations for direct brine release of Salado brine. Note that vector 22 has the highest source term at early times. A single direct brine release volume of 100 m<sup>3</sup> (Figure 36) at a concentration of  $3 \times 10^{-2}$  EPA units/m<sup>3</sup> (Figure 38) results in a

single release of 3 EPA units. Since releases of this magnitude occur for only one out of 100 realizations, and at a probability less than 0.2 (Figure 34), such a release is quite unlikely. The effect of these unlikely high direct brine releases on total performance of the repository is quite minor, as shown by the comparison of the CCDFs in Figure 30.



**Figure 37. Pressure and brine saturation in the waste panel for Vector 22 in the AMW (left) and CRA1 (right) calculations.**



**Figure 38. Mobilized concentrations in Salado brine (Scenarios S4 and S5).**

## 5 Sensitivity Analysis

This section examines the sensitivity of output variables to the three new sampled input variables that were added for the AMW calculation. Three sampled parameters were added for the AMW calculation: *FRACAMW*; *CLOSMOD1*; and *CLOSMOD2*. The variable *FRACAMW* is the fraction of the representative panel's volume that is filled with AMWTP waste, *CLOSMOD1* is the porosity surface model that is applied to the single waste panel, and *CLOSMOD2* is the porosity surface model that is applied to the rest of the repository.

Several methods are used to illustrate sensitivity or lack of sensitivity to these new variables. Correlation analysis is used to identify which uncertain input parameters are most important to the uncertainty in the output variables. Scatter plots are employed to illustrate and identify relationships between input and output variables. Comparison of statistics (mean, maximum, and minimum) for output variables as a function of time are also used to demonstrate the effect of sampled input parameters on output results.

### 5.1 Sensitivity to Fraction of AMWTP Waste in a Single Waste Panel

In the AMW analysis, the fraction of a single panel's volume filled with AMWTP waste (*FRACAMW*) was sampled from a uniform distribution between 0.2 and 1.0. A correlation analysis was performed using the code *PCCSRC* to determine the standard correlation coefficients between *FRACAMW* and the *BRAGFLO* output variables for scenarios S1 and S2 discussed in Section 4.2. The largest value of the standard correlation coefficient for *FRACAMW* was -0.11 for brine saturation in the waste panel (*WAS\_SATB*) and for brine flow up the borehole (*BRNBHRCC*). This indicates that no significant correlation exists between *FRACAMW* and any of the *BRAGFLO* output variables.

To determine if the variable *FRACAMW* is responsible for the observed differences between the AMW and CRA1 calculations, Figure 39 shows scatter plots of *FRACAMW* against the difference in pressure in the waste panel for the realizations in which microbial action produces gas. The lack of any observable correlation between *FRACAMW* and the differences in pressure indicates that the variability in *FRACAMW* is not responsible for the differences in pressure between the two calculations.

The scatter plots, the correlation analysis, and the discussion in Section 4.2 demonstrate that non-homogeneous loading of CPR in the repository will have little or no effect on performance assessment results. Thus, this report concludes that, although total CPR content of the repository is significant to performance, variations in CPR content of individual waste panels is not a significant feature for repository performance, and thus heterogeneity in CPR resulting from waste placement can be excluded from performance assessment.

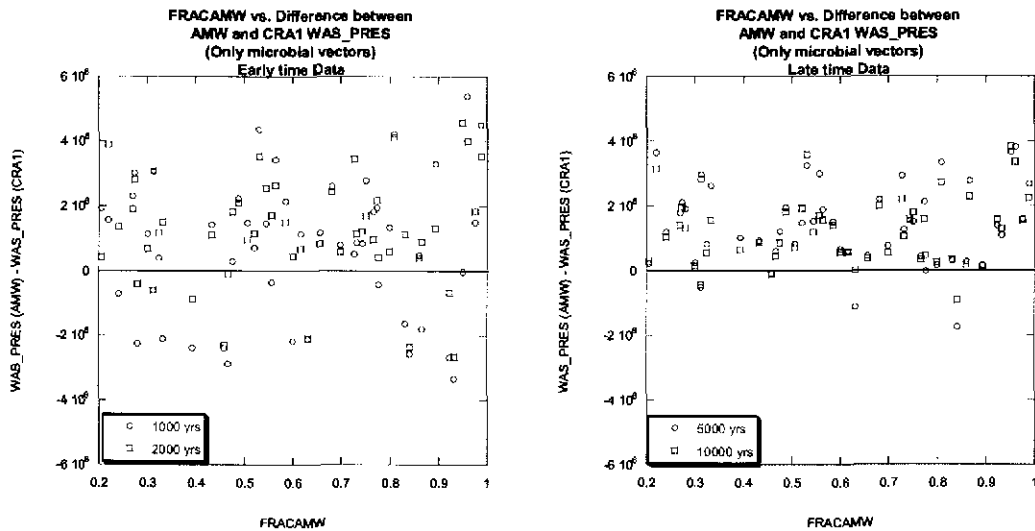
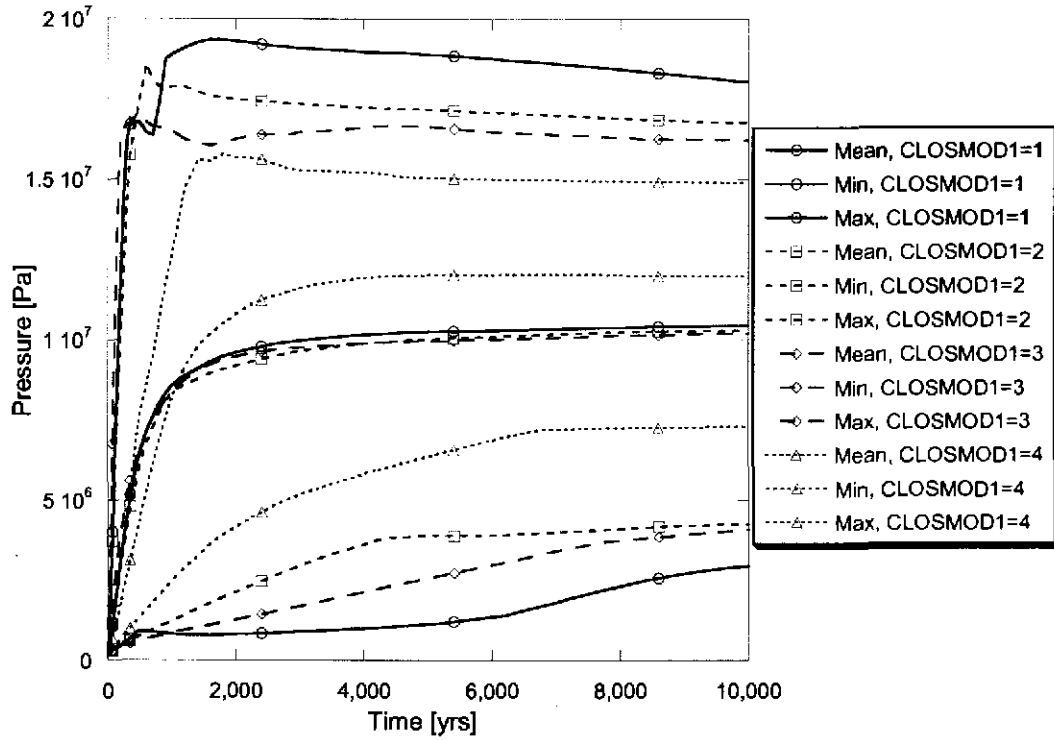


Figure 39. Sensitivity of pressure to FRACAMW, S1 scenario.

## 5.2 Sensitivity to Porosity Surface

In the AMW calculation, the porosity surface that represents creep closure of a single waste panel (CLOSMOD1) was sampled from a discrete distribution of four different porosity surfaces (see Section 3.1.6). The porosity surface that is applied to the rest of the repository (CLOSMOD2) was sampled from a discrete distribution of two of these surfaces. Because the sampling was independent, there are eight possible combinations of porosity surfaces that occur in the AMW calculation. Details regarding the SANTOS calculations used to develop these closure models are described in Section 3.1. The sensitivity of model output to the uncertainty represented by the selection of a porosity surface is determined by comparing model output for subsets of realizations that use a common porosity surface or combination of surfaces.

Figures 40, 41, and 42 compare the mean, minimum, and maximum pressure in the waste panel as a function of time for different subsets of realizations with common porosity surfaces. The statistics in Figure 40 are computed for groups of vectors with equal values of CLOSMOD1. Figure 40 shows that the standard waste model results in the widest distribution of pressures in the waste panel. Figure 40 also indicates that the mean pressure is nearly equivalent for three of the porosity surfaces (1 = standard waste model, 2 = combined waste model, and 3 = supercompacted waste model), which together account for 90 percent of the realizations. Given that the overall range of pressure in the AMW calculation is greater than in the CRA1 calculation (see Figures 21 and 22), and since mean pressures are insensitive to the porosity surface applied to the waste panel, the wider range of pressures in the AMW calculation is a consequence of the sampled values for CLOSMOD2.



**Figure 40. Sensitivity of pressure in the waste panel to CLOSMOD1 (AMW calculation.)**

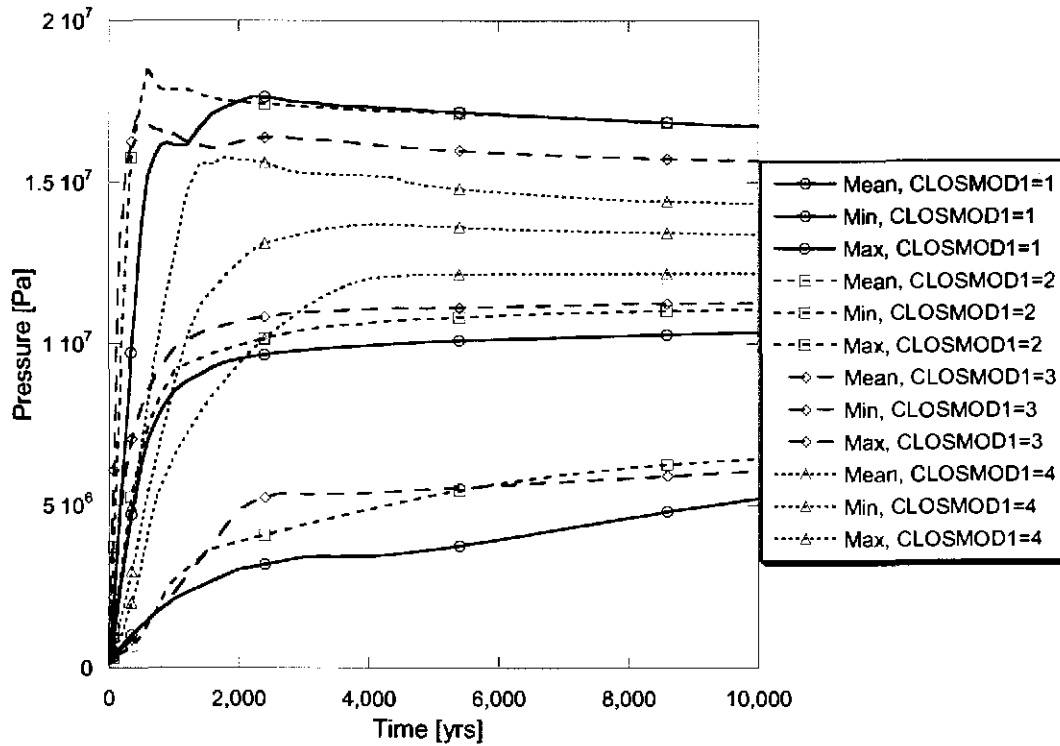


**Figure 41. Pressure in the waste panel for vectors where the Standard Waste Model applies to the rest of repository (AMW calculation.)**

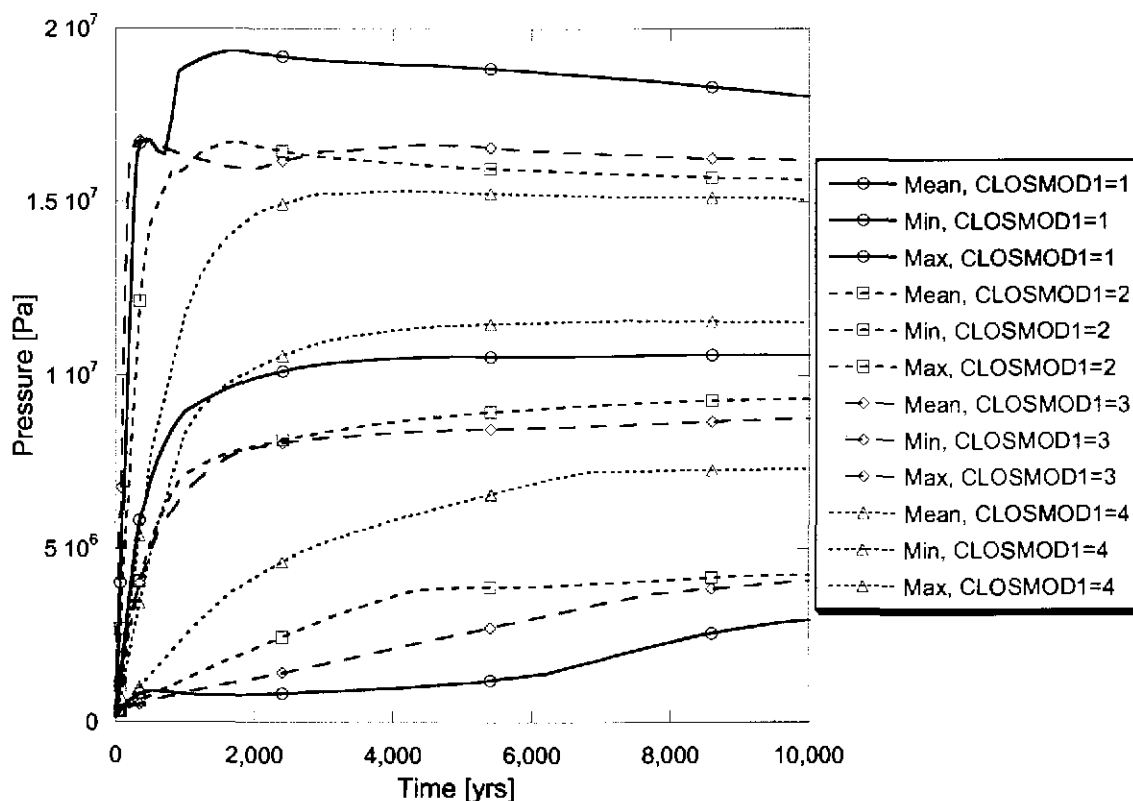


**Figure 42. Pressure in the waste panel for vectors where the Combined Waste Model applies to the rest of repository (AMW calculation.)**

Figure 41 shows pressure in the waste panel for those vectors where the standard waste model is applied to the rest of repository (CLOSMOD2 = 1, 50% of realizations). Figure 42 presents similar statistics where the combined waste model is applied to the rest of repository (CLOSMOD2 = 2). Figure 42 indicates that the largest range of pressures, shown in Figure 40, results from applying the combined waste model to the rest of the repository (CLOSMOD2 = 2). Figure 41 displays a narrower range of pressures that is more similar to the range seen in the CRA1 calculation (see Figure 21.)

Figure 43 illustrates the relationship between porosity and pressure in the waste panel, for each porosity surface used the AMW calculation and the single surface used in the CRA1 calculation. Porosity in the waste regions is determined from a lookup table listing porosity as a function of pressure and time for each porosity surface. Each closure model follows a distinct trend. The porosity surface for the standard waste model (CLOSMOD1 = 1) results in the lowest porosity and also the greatest range of porosity values. The porosity surface for the pipe overpack model (CLOSMOD1 = 4) results in the highest porosity (except for the high pressure vector 41). Figure 43 shows that the porosity-pressure relationship is relatively linear for most pressures, however at more extreme pressures, porosity increases consistent with reversal of creep closure.

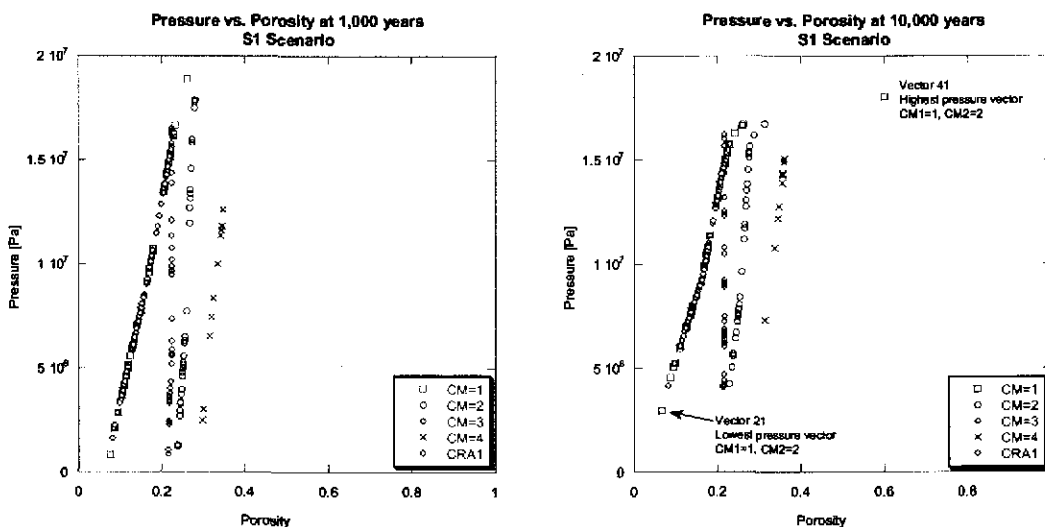


**Figure 43. Pressure vs. porosity in the waste panel at 1,000 years (left) and at 10,000 years (right) for the S1 scenario (AMW calculation.)**

The analysis shows that repository conditions are not greatly affected by the uncertainty in waste structural properties and spatial arrangement, as characterized by the uncertainty in the porosity surface. Moreover, the total releases at probabilities above 0.001 are relatively unchanged by the use of different porosity surfaces (Figure 30.) Thus, the uncertainty in waste structural properties and spatial arrangement, as represented by the uncertain porosity surfaces, is not significant in the performance assessment. Consequently, the use of a single porosity surface is appropriate for performance assessment. Because the porosity surface for the standard waste model preserves the greatest range of porosity and the widest range of pressure, this report recommends that this porosity surface be retained for performance assessment.

### **5.3 Sensitivity of Cuttings and Cavings to Random Placement of Waste**

The CCDFs presented in Section 4.3 computed cuttings and cavings releases with the assumption that wastes were randomly placed in the repository. As explained in Section 3.6, this assumption is implemented by randomly selecting three waste streams for each intrusion, and using the radioactivity in these waste streams to calculate cuttings and cavings releases. Selecting three waste streams for cuttings and cavings releases represents the bounding case of zero correlation in the spatial distribution of the waste. The other bounding case, that of complete correlation in the spatial distribution of the waste, is implemented by selecting a single waste stream for cuttings and cavings releases. The complete correlation case

represents the unlikely configuration in which every waste stream is placed as a contiguous mass.

Figure 44 compares the mean and 90<sup>th</sup> percentile of the distributions of CCDFs for cuttings and cavings releases for the AMW calculation, for the two extreme cases for waste placement. The mean CCDFs are nearly identical for all meaningful probabilities. The similarity in the 90<sup>th</sup> quantiles indicates that changing the assumption from random placement to a correlated placement does not significantly affect the distribution of cuttings releases. The actual placement of waste in the repository will fall somewhere between these two extreme cases. However, this analysis shows that the effects on performance of the spatial correlations are not significant, and thus the spatial correlations can be omitted from calculation of cuttings and cavings releases.

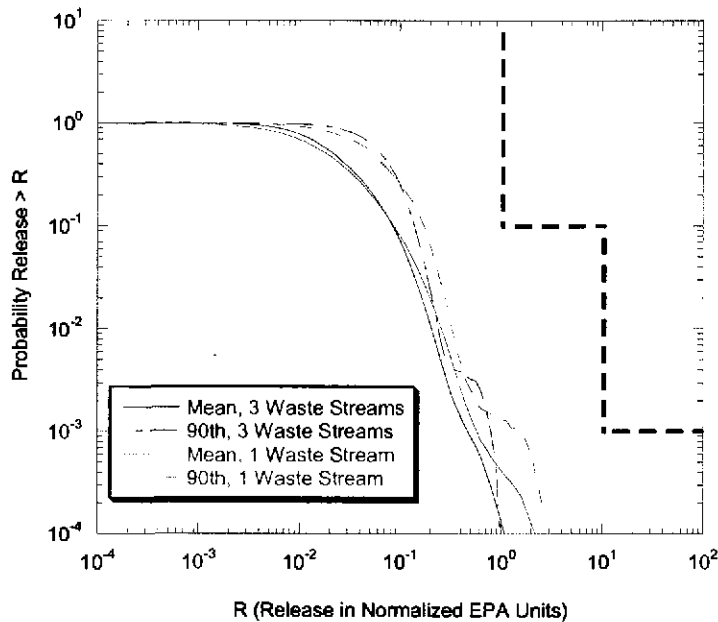
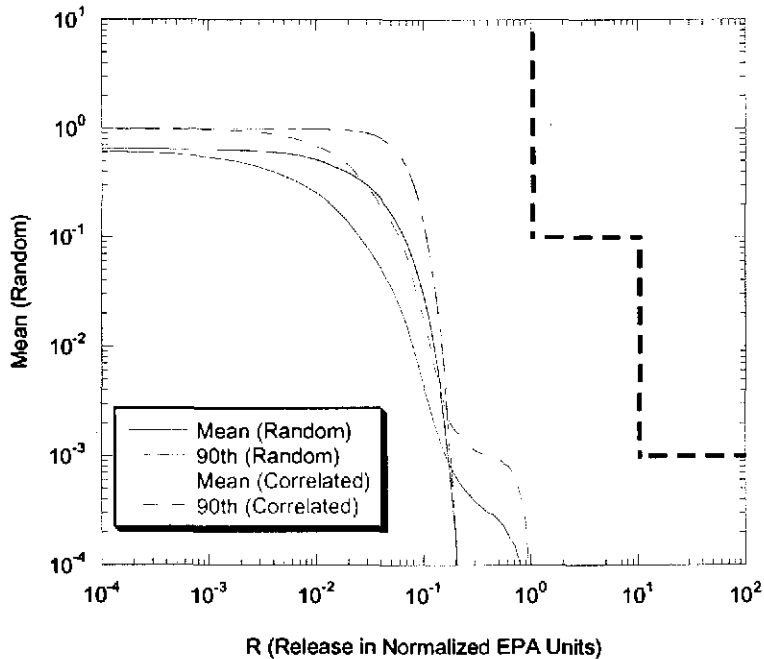


Figure 44. Sensitivity of cuttings and cavings releases to random placement of waste.

#### 5.4 Sensitivity of Spallings to Waste Heterogeneity and Random Placement of Waste

The CCDFs presented in Section 4.3 computed spallings releases by using the average radioactivity in all CH-TRU waste streams. As explained in Section 3.7, the use of the average radioactivity is consistent with the assumption that waste is placed randomly in the repository. To evaluate the significance of heterogeneity in waste activity and spatial placement of the waste in the calculation of spallings releases, spallings releases were calculated for a case of spatial correlation in the waste (i.e., each waste stream is placed as a contiguous mass).

Figure 45 shows that the mean CCDF for spillings shows higher releases at almost all probabilities when average radioactivity is used to compute releases. Only at very low probabilities do the releases for heterogeneous radioactivities and correlated spatial placement exceed the releases for average activity and random placement. Therefore, this analysis concludes that calculation of spillings is not significantly affected by heterogeneity in radioactivity or in spatial placement. In fact, use of the average activity and the assumption of random placement are shown to be conservative for spillings releases.



**Figure 45. Sensitivity of spillings releases to assumptions about waste placement.**

## 6 Summary and Conclusions

Performance assessment is the primary tool used by DOE to demonstrate compliance with the long-term disposal regulations in 40 CFR 191 (Subparts B and C) and the compliance criteria in 40 CFR 194. Previous performance assessments have used the simplifying assumption that the waste would be randomly placed in the repository, and could be represented as a homogeneous material. Section 2.1 of this report explains how this assumption was implemented in models for the performance assessment conducted for the CCA.

In response to DOE's submittal seeking approval to accept supercompacted waste, EPA requested more information about the possible effects of supercompacted waste on repository performance. EPA's questions are summarized in Table 1. EPA's questions stem from the wide disparities between the characteristics of supercompacted waste and the characteristics of other waste streams; these disparities, and the actual placement of waste in Panel 1, suggest more general questions about the representation of waste as a homogeneous material and the importance of the assumptions of random waste placement. Thus, DOE framed a PA that sought to address EPA's specific concerns and also to provide insight about these more general questions.

As stated in the Introduction, this report answers the specific questions asked by EPA and also addresses the following more general questions:

1. What is the expected repository performance when supercompacted waste is explicitly represented in the performance assessment?
2. What is the significance to performance assessment of the representation of supercompacted waste and of waste heterogeneity in general?

The specific approach used in this analysis involved four steps. First, the FEPs on which performance assessment is based were examined to determine specific components of performance assessment that may be affected by the presence of supercompacted waste. Second, the representation in performance assessment of supercompacted waste and of waste heterogeneity was determined. Third, the performance assessment was executed using the parameters and model changes identified by the analyses in steps one and two. Finally, the performance assessment results were examined in a sensitivity study to determine the effects of the supercompacted waste and the importance of heterogeneous waste representation.

The FEPs evaluation determined that no changes to the waste-related FEPs in the baseline are warranted.

Analysis of creep closure of waste-filled rooms showed that a wide range of long-term porosity could be achieved, given the uncertainty about the rigidity of waste containers, and about the spatial arrangement of the waste. Thus, the performance assessment in this analysis treats the creep closure of waste-filled regions as an uncertain variable.

Chemical conditions within the repository were examined to determine if the presence of supercompacted waste would alter assumptions, parameters or models used in the performance assessment. The analysis determined that, under a wide range of possible arrangements of waste, sufficient MgO backfill is present in each panel to maintain the desired chemical conditions. In addition, the analysis found that the constituents of the supercompacted waste do not alter the reactions that determine equilibrium conditions. Consequently, no changes to the calculation of actinide solubilities or to the models for gas generation are warranted.

Since the supercompacted waste contains a much higher concentration of CPR materials than is found in other waste streams, and the future arrangement of the waste is uncertain, this analysis treats the concentration of CPR in the waste materials as uncertain. However, the analysis found that differences in concentration of iron-based metals could not be significant to performance assessment, thus no change was made to the model for anoxic corrosion.

Analysis of the mechanical properties of the supercompacted waste and waste in pipe overpacks concluded that no change in the permeability of the waste materials should be made. In addition, the analysis found that the current values for waste tensile and shear strengths are extremely conservative. In fact, the mechanical properties of the supercompacted waste and of pipe overpack containers may serve to reduce direct releases by cavings and spallings. Finally, the analysis concluded that inclusion of the stuck pipe and gas erosion mechanisms for spallings in performance assessment calculations is not warranted.

The performance assessment was thus run with three new, uncertain variables, accounting for the uncertainty in long-term porosity of the waste and in the distribution of CPR materials in the repository. The performance assessment used the same codes and sampling of parameter values as were used in a performance assessment that represents the waste as a homogeneous material. Comparison of results between the two calculations identified the effects of the additional uncertain variables.

Analysis of performance assessment results showed that total normalized releases from the repository fall below the regulatory limits specified in 40 CFR 194, thus demonstrating compliance with the regulations. Comparison of total releases showed that the two calculations are statistically quite similar, exhibiting similar ranges of uncertainty in repository performance. The only differences in releases between the two calculations occur at very low probabilities. Thus, repository performance is not significantly affected by the explicit representation of supercompacted waste.

In addition, a sensitivity analysis showed that performance assessment results were quite insensitive to the uncertainty in CPR distribution. Performance assessment results were also insensitive to the uncertainty in the selection of the porosity surface. The sensitivity analysis showed that, among the four porosity surfaces considered, the porosity surface used for the CCA resulted in the greatest variability in porosity. Thus, the sensitivity analysis concludes that CPR materials can continue to be represented as homogeneously distributed, and that performance assessment should continue to use the CCA model for waste porosity.

Finally, the sensitivity analysis considered the importance of the assumption of random waste placement in the calculation of direct releases. The analysis found that the mean and 90<sup>th</sup> percentile CCDFs for cuttings, cavings and spillings releases are not significantly different when waste is placed randomly or when waste is placed as contiguous blocks comprising single waste streams. Thus, this analysis concludes that direct releases are insensitive to uncertainty in the spatial arrangement of the waste.

This analysis concludes that repository performance with supercompacted wastes included in the inventory complies with the regulations specified in 40 CFR 194. Moreover, explicit representation of the specific features of supercompacted waste, such as structural rigidity and high CPR concentration, is not warranted, since the performance assessment results are insensitive to the effects of these specific features. Finally, this analysis concludes that performance assessment results are not significantly different when waste heterogeneity is included in the direct release models; thus, the assumption of random waste placement and the representation of waste as a homogeneous material remain appropriate.

## 7 References

Berglund, J.W. 1994. *The Direct Removal of Waste Caused by a Drilling Intrusion Into a WIPP Panel --- A Position Paper*. Memorandum of Record. NMERI. August 31, 1994. ERMS 209882.

BNFL, Inc. 2003. *Physical Information on AMWTP Supercompacted Wastes: Questions and Responses*. BNFL, Inc. May 22, 2003.

Brush, L.H., and Y. Xiong. 2003a. *Calculation of Actinide Solubilities for the WIPP Compliance Recertification Application, Analysis Plan AP-098, Rev 1*. Sandia National Laboratories. Carlsbad, NM. ERMS 527714.

Brush, L.H., and Y. Xiong. 2003b. *Calculation of Actinide Solubilities for the WIPP Compliance Recertification Application*. Sandia National Laboratories. Carlsbad, NM. May 8, 2003. ERMS 529131.

Brush, L.H., and Y. Xiong. 2003c. *Calculation of Organic Ligand Concentrations for the WIPP Compliance Recertification Application and for Evaluating Assumptions of Homogeneity in WIPP PA*. Sandia National Laboratories. Carlsbad, NM. September 11, 2003. ERMS 531488.

Butcher, B.M., T.W. Thompson, R.G., VanBuskirk, and N.C., Patti. 1991. *Mechanical Compaction of Waste Isolation Pilot Plant Simulated Waste*. SAND90-1206. Sandia National Laboratories, Albuquerque, NM.

Butcher, B.M. 1996. *QAP 9-2 Documentation of the Overall Waste Permeability and Flow Property Values for the CCA*. Memorandum to M. Tierney. Sandia National Laboratories. Carlsbad, NM. ERMS 30921.

Crawford, B.A., and C.D. Leigh. 2003. *Estimate of Complexing Agents in TRU Waste for the Compliance Recertification Application*. Los Alamos National Laboratory. Carlsbad, NM. August 28, 2003. ERMS 531107.

CTAC. 1997. *Expert Elicitation on WIPP Waste Particle Diameter Size Distribution(s) during the 10,000-Year Regulatory Post-closure Period: Final Report* U.S. Department of Energy Carlsbad Area Office. Carlsbad, NM.

DOE (U.S. Department of Energy.) 1996. *Title 40 CFR Part 191 Compliance Certification Application for the Waste Isolation Pilot Plant*. DOE/CAO-1996-2184. October 1996.

DOE. 2000. *TRUPACT-II Authorized Methods for Payload Control (TRAMPAC), Revision 19*. US Department of Energy Carlsbad Area Office. Carlsbad, NM. April 2000.

DOE. 2002. *Assessment Of Impacts On Long-Term Performance From Supercompacted Wastes Produced By The Advanced Mixed Waste Treatment Project*. US Department of Energy Carlsbad Area Office. Carlsbad, NM. December 6, 2002.

Dunagan, S.D. 2003. *Estimated Number of Boreholes Into CH-Waste in 10,000 years*. Memorandum to C. Hansen. Sandia National Laboratories. Carlsbad, NM. October 3, 2003.

EPA (U.S.Environmental Protection Agency). 1997. Letter from G. Dials, Manager, Department of Energy Carlsbad Area Office, to R. Travato, Manager, EPA Office of Indoor Air, Second Response to EPA's letter of March 19, 1997 requesting additional information. EPA Docket A-93-02, II-I-28, Comment #18. U.S. Environmental Protection Agency Office of Radiation and Indoor Air. Washington D.C. May 2,1997

EPA. 1998a. *40 CFR Part 194. Criteria for the Certification and Recertification of the Waste Isolation Pilot Plant's Compliance With the 40 CFR Part 191 Disposal Regulations: Certification Decision; Final Rule*. FR Vol. 63 No. 95, pp. 27354 – 27406. U.S. Environmental Protection Agency Office of Radiation and Indoor Air. Washington, D.C. May 18, 1998.

EPA. 1998b. *Technical Support Document for Section 194.23 - Models and Computer Codes*. EPA Docket A93-02-V-B-6. U.S. Environmental Protection Agency Office of Radiation and Indoor Air. Washington, DC.

EPA. 1998c. *Technical Support Document for Section 194.23: Parameter Justification Report*. EPA Docket A-93-02-V-B-14. U.S. Environmental Protection Agency Office of Radiation and Indoor Air. Washington, DC.

EPA. 1998d. *Compliance Application Review Documents for the Criteria for the Certification and Recertification of the Waste Isolation Pilot Plant's Compliance with the 40 CFR Part 191 Disposal Regulations: Final Certification Decision. CARD 23: Models and Computer Codes*. EPA Air Docket A93-02-V-B-2. U.S. Environmental Protection Agency Office of Radiation and Indoor Air. Washington, DC.

EPA. 1998e. *Criteria for the Certification and Recertification of the Waste Isolation Pilot Plant's Compliance with 40 CFR Part 191 Disposal Regulations: Certification Decision*. , Response to Comments, Section 5 Models and Codes – Section 194.23; Issue L: CCA parameters and PAVT parameter selection, Response to Comments 5.L.4 and 5.L.5. EPA Docket A-98-02, V-C-1. U.S. Environmental Protection Agency Office of Radiation and Indoor Air, Washington D.C.

EPA. 1998f. *Criteria for the Certification and Recertification of the Waste Isolation Pilot Plant's Compliance with 40 CFR Part 191 Disposal Regulations: Certification Decision*. , Response to Comments, Section 5 Models and Codes – Section 194.23; Issue E: Stuck Pipe, Gas Erosion and Related Waste Permeability, Threshold Permeability. EPA Docket A-98-02, V-C-1. U.S. Environmental Protection Agency Office of Radiation and Indoor Air, Washington D.C.

EPA. 2001. Letter from F. Marcinowski, Director, Radiation Protection Division, to Dr. I. Triay, Manager, Carlsbad Field Office. EPA Docket A-98-49, II-B-3-15. U.S. Environmental Protection Agency Office of Radiation and Indoor Air, Washington D.C. 11 January 2001. ERMS 519362.

EPA. 2003a. Letter from F. Marcinowski, Director, Radiation Protection Division, to Dr. I. Triay, Manager, Carlsbad Field Office. U.S. Environmental Protection Agency Office of Radiation and Indoor Air, Washington D.C. 21 March 2003.

EPA. 2003b. Letter from F. Marcinowski, Director, Radiation Protection Division, to Dr. I. Triay, Manager, Carlsbad Field Office. U.S. Environmental Protection Agency Office of Radiation and Indoor Air, Washington D.C. 12 June 2003.

EPA. 2003c. Letter from F. Marcinowski, Director, Radiation Protection Division, to Dr. I. Triay, Manager, Carlsbad Field Office. EPA Docket A98-49, II-B-3-51. U.S. Environmental Protection Agency Office of Radiation and Indoor Air, Washington D.C. 15 May 2003.

Fox, B.L. 2003. *Analysis Package for EPA Unit Loading Calculations: Compliance Recertification Application, Revision 1*. Sandia National Laboratories. Carlsbad, NM. September 18, 2003. ERMS 531582.

Francis, A.J., and J.B. Gillow. 2000. *Progress Report: Microbial Gas Generation Program*. Memorandum to Y. Wang. Brookhaven National Laboratory. Upton, NY. January 6, 2000. ERMS 509352.

Gillow J.B., and A.J. Francis. 2001. *Re-evaluation of Microbial Gas Generation under Expected Waste Isolation Pilot Plant Conditions: Data Summary and Progress Report (February 1 – July 13, 2001)*. Appears in Sandia National Laboratories Technical Baseline Reports, WBS 1.3.5.4, Repository Investigations Milestone RI020, pp. 3-1 to 3-21. Sandia National Laboratories. Carlsbad, NM. July 31, 2001. ERMS 518970.

Gillow J.B., and A.J. Francis. 2002a. *Re-evaluation of Microbial Gas Generation under Expected Waste Isolation Pilot Plant Conditions: Data Summary and Progress Report (July 14, 2001 – January 31, 2002), January 22, 2002*. Appears in Sandia National Laboratories Technical Baseline Reports, WBS 1.3.5.3, Compliance Monitoring; WBS 1.3.5.4, Repository Investigations, Milestone RI110, pp. 2.1 - 1 to 2.1 - 26. Sandia National Laboratories. Carlsbad, NM. January 31, 2002. ERMS 520467.

Gillow J.B., and A.J. Francis. 2002b. *Re-evaluation of Microbial Gas Generation under Expected Waste Isolation Pilot Plant Conditions: Data Summary and Progress Report (February 1 – July 15, 2002), July 18, 2002*. Appears in Sandia National Laboratories Technical Baseline Reports, WBS 1.3.5.3, Compliance Monitoring; WBS 1.3.5.4, Repository Investigations, Milestone RI130, pp. 3.1 - 1 to 3.1 - A10. Sandia National Laboratories. Carlsbad, NM. July 31, 2002. ERMS 523189.

Hansen, C.W., C.D. Leigh, D.L. Lord, and J.S. Stein. 2002. *BRAGFLO Results for the Technical Baseline Migration*. Sandia National Laboratories. Carlsbad, NM. ERMS 523209.

Hansen, C.W. 2003. *Waste Parameters for AP-107 Analysis*. Memorandum to Records. Sandia National Laboratories. Carlsbad, NM. August 27, 2003. ERMS 531073.

Hansen, F.D., M.K. Knowles, T.W. Thompson, M. Gross, J.D. McLennan and J.F. Schatz. 1997. *Description and Evaluation of a Mechanistically Based Conceptual Model for Spall*. SAND97-1369. Sandia National Laboratories. Albuquerque, NM.

Hansen, F.D., T.W. Pfeifle, and D.L. Lord. 2003. *Parameters Justification Report for DRSPALL*. Sandia National Laboratories. Albuquerque, NM. ERMS 531057.

Helton, J.C., Bean, J.E., Berglund, J.W., Davis, F.J., Economy, K., Garner, J.W., Johnson, J.D., MacKinnon, R.J., Miller, J., O'Brien, D.G., Ramsey, J.L., Schreiber, J.D., Shinta, A., Smith, L.N., Stoelzel, D.M., Stockman, C., and P. Vaughn. 1998. *Uncertainty and Sensitivity Analysis Results Obtained in the 1996 Performance Assessment for the Waste Isolation Pilot Plant*. SAND98-0365. Sandia National Laboratories. Albuquerque, N.M.

Hobart, D.E., and R.C. Moore. 1996. "Analysis of Uranium(VI) Solubility Data for WIPP Performance Assessment." Sandia National Laboratories. Albuquerque, NM. ERMS 239856.

Jepsen, R., J. Roberts, and W. Lick. 1998. *Development and Testing of Waste Surrogate Materials for Critical Shear Stress*. Sandia National Laboratories. Albuquerque, NM. WPO #52647.

Lappin, A.R., R.L. Hunter, D.R. Garber, and P.B. Davies, eds. 1989. *Systems Analysis, Long-Term Radionuclide Transport, and Dose Assessments, Waste Isolation Pilot Plant (WIPP), Southeastern New Mexico; March 1989*. SAND89-0462. Sandia National Laboratories. Albuquerque, NM.

Leigh, C.D. 2003a. *Estimate of Cellulosics, Plastics, and Rubbers in a Single Panel in the WIPP Repository in Support of AP-107, Supercedes ERMS #530959*. Sandia National Laboratories. Carlsbad, NM. September 4, 2003. ERMS 531324.

Leigh, C.D. 2003b. *Estimate of Oxyanion Masses in a Single Panel in the WIPP Repository in Support of AP-107, supercedes ERMS #530988*. Sandia National Laboratories. Carlsbad, NM. September 4, 2003. ERMS 531332.

Leigh, C.D. 2003c. *Estimate of Complexing Agent Masses in a Single Panel in the WIPP Repository in Support of AP-107, Supercedes ERMS 531113*. Sandia National Laboratories. Carlsbad, NM. September 4, 2003. ERMS 531328.

Leigh, C.D. 2003d. *Radionuclide Densities in CH Waste Streams from TWBID Revision 2.1 Version 3.12 Data Version 4.09*. Letter to L.H. Brush. Sandia National Laboratories. Carlsbad, NM. September 19, 2003. ERMS 531586.

Leigh, C.D. and S. Lott. 2003a. *Calculation of Waste Stream Volume, Waste and Container Material Densities, and Radionuclide Concentrations for INEEL Waste Stream IN-BN-510 for the Compliance Recertification Application*. Los Alamos National Laboratories. Carlsbad, NM. ERMS #530666.

Leigh, C.D. and S. Lott. 2003b. *Calculation of Waste Stream Volumes, Waste and Container Material Densities, and Radionuclide Concentrations for Nondebris AMWTF Waste Streams at INEEL for the Compliance Recertification Application*. Los Alamos National Laboratories. Carlsbad, NM. ERMS #530688.

Long, J. 2003. *Execution of Performance Assessment for the Advanced Mixed Waste Calculations*. Sandia National Laboratories. Carlsbad, NM.

Lott, S. 2003a. *Response to the Request for Waste Material and Container Material Densities from TWBID Revision 2.1, Version 3.12, Data Version D.4.08*. Letter to C.D. Leigh. Los Alamos National Laboratory. Carlsbad, NM. August 15, 2003. ERMS 530767.

Lott, S. 2003b. *Response to the Request for Radionuclide Activities in TRU Waste Streams from TWBID Revision 2.1 Version 3.12, Data Version D.4.09*. Letter to C.D. Leigh. Los Alamos National Laboratory. Carlsbad, NM. September 19, 2003. ERMS 531566.

Ludwigsen, J.S., D.J. Ammerman and H.D. Radloff. 1998. *Analysis in Support of Storage of Residues in the Pipe Overpack Container*. SAND98-1003. Sandia National Laboratories. Albuquerque, NM.

Luker, R.S., T.W. Thompson and B.M. Butcher. 1990. *Compaction and permeability of simulated waste,* Proc. 32<sup>nd</sup> U.S. Symposium on Rock Mechanics. Norman OK. 1990.

National Research Council. (NRC). 1996 *The Waste Isolation Pilot Plant A Potential Solution for the Disposal of Transuranic Waste*. National Academy Press. Washington, D.C.

Novak, C.F., R.C. Moore, and R.V. Bynum. 1996. *Prediction of Dissolved Actinide Concentrations in Concentrated Electrolyte Solutions: A Conceptual Model and Model Results for the Waste Isolation Pilot Plant (WIPP)*. SAND96-2695C. Sandia National Laboratories. Albuquerque, NM.

Park, B.Y. and J.F. Holland. 2003. *Structural Evaluation of WIPP Disposal Room Raised to Clay Seam G*. Sandia National Laboratories. Albuquerque, NM.

Park, B.Y. and F.D. Hansen. 2003. *Determination of the Porosity Surfaces of the Disposal Room Containing Various Waste Inventories for the WIPP PA*. Sandia National Laboratories. Albuquerque, NM.

Rechard, R.P., A.C. Peterson, J.D. Schreiber, H.J. Iuzzolino, M.S. Tierney, J.S. Sandha. 1991. *Preliminary comparison with 40 CFR Part 191, Subpart B for the Waste Isolation Pilot Plant, Vol 3: Reference Data*. SAND91-0893/3. Sandia National Laboratories. Albuquerque, NM.

SNL (Sandia National Laboratories.) 1997a. *Summary of EPA-Mandated Performance Assessment Verification Test (Replicate 1) and Comparison with the Compliance Certification Application Calculations (Rev 1)*. Sandia National Laboratories. Carlsbad, NM. September, 1997. WPO 46674. See also EPA Docket A-93-02-II-G-26.

SNL. 1997b. *Supplemental Summary of EPA-Mandated Performance Assessment Verification Test (All Replicates) and Comparison with the Compliance Certification Application Calculations*. Sandia National Laboratories. Carlsbad, NM. August, 1997. WPO 46702. See also EPA Docket A-93-02-II-G-28.

Snider, A.C. 2003. *Calculation of MgO Safety Factors for the WIPP Compliance Recertification Application and for Evaluating Assumptions of Homogeneity in WIPP PA*. Sandia National Laboratories. Carlsbad, NM. September 11, 2003. ERMS 531508.

Stein, J. 2003. *Analysis Plan for Calculations of Salado Flow and Transport: Compliance Recertification Application*. AP-099. Sandia National Laboratories. Carlsbad, NM. ERMS 526891.

Stone, C.M. 1997. *Final Disposal Room Structural Response Calculations*. SAND97-0795. Sandia National Laboratories. Albuquerque, NM.

Trovato, E.R. 1997. Untitled letter from E.R. Trovato to G. Dials. U.S. Environmental Protection Agency Office of Radiation and Indoor Air. Washington, DC. April 25, 1997.

Vaughn, P., and J. Bean, J. Garner, M. Lord, R. MacKinnon, D. McArthur, J. Schreiber, A. Shinta. 1996. *FEPs Screening Analysis DR2, DR3, DR6, DR7, and S6*. Record Package SWCF-A:1.1.6.3:PA:QA:TSK:DR2, DR3, DR6, DR7, and S6. Sandia National Laboratories. Carlsbad, NM. WPO 38152.

Wang, Y. 2000. *Methanogenesis and Carbon Dioxide Generation in the Waste Isolation Pilot Plant (WIPP)*. Memorandum to B.A. Howard. Sandia National Laboratories. Carlsbad, NM. January 5, 2000. ERMS 519362.

WIPP PA. 1991. *Preliminary Comparison with 40 CFR Part 191, Subpart B for the Waste Isolation Pilot Plant, Volume 3: Reference Data*. SAND91-0893/3. Sandia National Laboratories. Albuquerque, NM.

WIPP PA. 2002. *Sandia National Laboratories FEPS Assessment for Advanced Mixed Waste Treatment Facility Wastes at the WIPP*. Sandia National Laboratories. Carlsbad, NM. November 2002.

WIPP PA. 2003a. *Analysis Plan for Evaluating Assumptions of Waste Homogeneity in WIPP Performance Assessment*. AP-107, Rev. 1. Sandia National Laboratories. Albuquerque, NM. August 25, 2003. ERMS 531067.

WIPP PA. 2003b. *Verification and Validation Plan/Validation Document for SANTOS Version 2.1.7, Document Version 1.20BOC*. Sandia National Laboratories. Carlsbad, NM. July, 2003. ERMS 530421.